

**MICROCALORIMETRY OF CYCLODEXTRIN
INTERACTIONS WITH AMINO ACIDS AND PROTEINS**

Michelle Lovatt

Thesis presented for the degree of Doctor of Philosophy

Department of Chemistry, University of Glasgow

September, 1997

ProQuest Number: 11007767

All rights reserved

INFORMATION TO ALL USERS

The quality of this reproduction is dependent upon the quality of the copy submitted.

In the unlikely event that the author did not send a complete manuscript and there are missing pages, these will be noted. Also, if material had to be removed, a note will indicate the deletion.



ProQuest 11007767

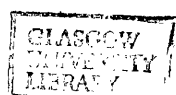
Published by ProQuest LLC (2018). Copyright of the Dissertation is held by the Author.

All rights reserved.

This work is protected against unauthorized copying under Title 17, United States Code
Microform Edition © ProQuest LLC.

ProQuest LLC.
789 East Eisenhower Parkway
P.O. Box 1346
Ann Arbor, MI 48106 – 1346

Thesis 10980
Copy 1



ACKNOWLEDGEMENTS

A special thanks to Alan Cooper for his supervision and guidance throughout all of this work. I would also like to thank Patrick Camilleri for his interest and help over the past few years. Thanks also to Steve Ford, Lindsay McDermott, Deborah McPhail, Margaret Nutley, Stephen Robertson and Abdul Wadood for their help, friendship and interest. I thank EPSRC and SmithKline Beecham for my stipend and conference funding. Thanks also to Andrew Dyke for proof reading this thesis. My extra special thanks goes to my parents not only for their support and encouragement over the years but for everything they have done to get me this far. A final thanks goes to my brother Paul for his patience and advice in a number of situations.

ABBREVIATIONS

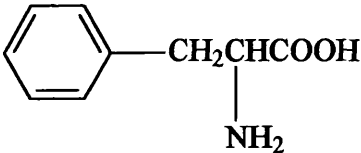
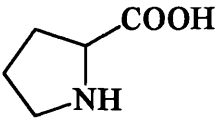
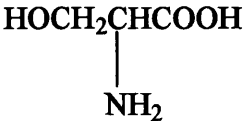
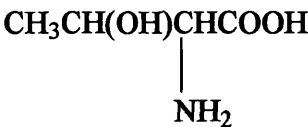
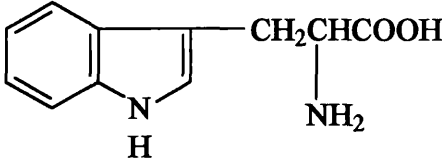
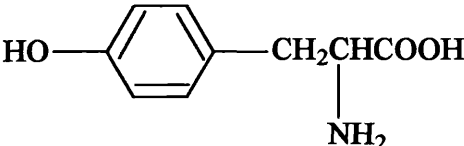
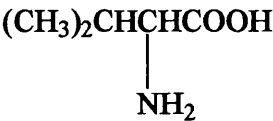
ATP	Adenosine 5'-triphosphate
CD	Cyclodextrin
DSC	Differential scanning calorimetry
ITC	Isothermal titration calorimetry
DTT	Dithiothreitol
EDTA	Ethlenediaminetetracetic acid
NADH	β -nicotinamide adenine dinucleotide
NMA	N-methylacetamide
PGK	Phosphoglycerate kinase
TEA	Triethanolamine
GAPDH	Glyceraldehyde-3-phosphate

ENERGY UNITS

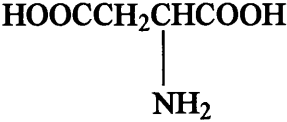
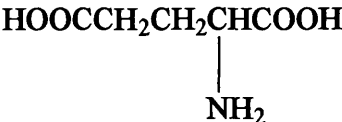
In some sections of this thesis *calorie* is used instead of the accepted SI energy unit, the *joule*. In order to convert from *calorie* to *joule*, the conversion factor $1 \text{ cal} = 4.184 \text{ J}$ is used.

AMINO ACIDS

Name	Abbreviations	Structure
<i>Neutral amino acids</i>		
Alanine	Ala	A
		$\begin{array}{c} \text{CH}_3\text{CHCOOH} \\ \\ \text{NH}_2 \end{array}$
Asparagine	Asn	N
		$\begin{array}{c} \text{O} \\ \\ \text{H}_2\text{N}-\text{C}-\text{CH}_2\text{CHCOOH} \\ \\ \text{NH}_2 \end{array}$
Cysteine	Cys	C
		$\begin{array}{c} \text{HSCH}_2\text{CHCOOH} \\ \\ \text{NH}_2 \end{array}$
Glutamine	Gln	Q
		$\begin{array}{c} \text{O} \\ \\ \text{H}_2\text{N}-\text{C}-\text{CH}_2\text{CH}_2\text{CHCOOH} \\ \\ \text{NH}_2 \end{array}$
Glycine	Gly	G
		$\begin{array}{c} \text{CH}_2\text{COOH} \\ \\ \text{NH}_2 \end{array}$
Isoleucine	Ile	I
		$\begin{array}{c} \text{CH}_3\text{CH}_2\text{CH}(\text{CH}_3)\text{CHCOOH} \\ \\ \text{NH}_2 \end{array}$
Leucine	Leu	L
		$\begin{array}{c} (\text{CH}_3)_2\text{CHCH}_2\text{CHCOOH} \\ \\ \text{NH}_2 \end{array}$
Methionine	Met	M
		$\begin{array}{c} \text{CH}_3\text{SCH}_2\text{CH}_2\text{CHCOOH} \\ \\ \text{NH}_2 \end{array}$

Phenylalanine	Phe	F	
Proline	Pro	P	
Serine	Ser	S	
Threonine	Thr	T	
Tryptophan	Trp	W	
Tyrosine	Tyr	Y	
Valine	Val	V	

Acidic amino acids

Aspartic acid	Asp	D	
Glutamic acid	Glu	E	

Basic amino acids

Arginine	Arg	R	$\begin{array}{c} \text{H}_2\text{N}-\text{C}-\text{NHCH}_2\text{CH}_2\text{CH}_2\text{CHCOOH} \\ \parallel \qquad \qquad \qquad \\ \text{NH} \qquad \qquad \qquad \text{NH}_2 \end{array}$
Histidine	His	H	$\begin{array}{c} \text{N} \\ \diagup \quad \diagdown \\ \text{C}=\text{C} \\ \diagdown \quad \diagup \\ \text{N}-\text{H} \end{array} \text{---CH}_2\text{CHCOOH} \\ \qquad \qquad \qquad \\ \qquad \qquad \qquad \text{NH}_2$
Lysine	Lys	K	$\begin{array}{c} \text{H}_2\text{NCH}_2\text{CH}_2\text{CH}_2\text{CH}_2\text{CHCOOH} \\ \qquad \qquad \qquad \\ \qquad \qquad \qquad \text{NH}_2 \end{array}$

ABSTRACT

Microcalorimetry of Cyclodextrin Interactions with Amino Acids and Proteins

The interaction of a range of cyclodextrins with amino acids, both free and in proteins has been investigated using sensitive microcalorimetry and spectroscopic techniques. With a view towards possible applications in chiral separation technologies, isothermal titration calorimetry (ITC) was used to study the complexation of cyclodextrins with the enantiomers of α -amino acids by competition with *p*-nitrophenolate or *p*-aminobenzoic acid under various pH conditions. It was found the majority of amino acids showed no complexation. However, complexes of α -cyclodextrin with phenylalanine, and tryptophan demonstrated small, but distinct, differences in dissociation constants for their separate enantiomers. Thermodynamic parameters (K_d , ΔH° , ΔG° and ΔS°) were obtained for all amino acids which showed complexation. Isothermal titration (dilution) microcalorimetry was also used to study the effect of cyclodextrins on the dissociation of bovine insulin in aqueous solution under various conditions. Thermodynamic data indicate that cyclodextrins increased dissociation of insulin oligomers in a manner consistent with their interaction with protein side chains. For example, the addition of methyl- β -cyclodextrin makes dissociation significantly more endothermic and reduced the apparent dimer dissociation constant by more than two orders of magnitude. Differential scanning calorimetry (DSC) was used to examine the effects of cyclodextrins on thermal unfolding of proteins. It was found that the mean unfolding temperature (T_m) of cytochrome c and lysozyme was reduced in the presence of cyclodextrins. Such observations indicate that the weak interaction of cyclodextrins with exposed amino acid residues promotes unfolding and dissociation of proteins. The possibility that such interactions may facilitate the use of cyclodextrins as “chaperone-mimics” in the refolding of denatured protein has been explored with the enzyme phosphoglycerate kinase (PGK). It was found that the presence of cyclodextrins or N-methylacetamide during thermal denaturation significantly enhanced the regain of enzyme activity of PGK by up to forty percent.

CONTENTS

Acknowledgements	ii
Abbreviations/Energy Units	iii
Amino Acids	iv
Abstract	vii
Contents	viii

<u>Chapter 1</u>	Introduction	1
1.1	The Aims of Thesis	2
1.2	Cyclodextrins	
1.2.1	Structure and Physical Properties	3
1.2.2	Inclusion Complex Formation	6
1.2.3	Cyclodextrin Derivatives	8
1.2.4	Applications of Cyclodextrins	9
1.3	Amino Acids	14
1.4	Protein Folding and Stability	18
1.4.1	Thermodynamics of Folding	18
1.4.2	Effects of Ligand Binding on Folding	
	Thermodynamics	26
1.5	Microcalorimetry	30
1.5.1	Isothermal Calorimetry	42
1.5.2	Differential Scanning Calorimetry	46

<u>Chapter 2</u>	Materials and Methods	49
2.1	Reagents	50
2.2	Isothermal Calorimetry	51
2.2.1	Competitive Inhibition Experiments	52
2.2.2	Insulin Dissociation Experiments	56
2.2.3	Calibration	58
2.3	Differential Scanning Calorimetry	58
2.3.1	Thermal Stability Studies	58
2.3.2	Analysis of Data	60
2.3.3	Calibration: Temperature	63
2.3.4	Calibration: Excess Heat Capacity	64
2.4	Spectral Titration Experiment	64
2.5	UV Absorption of Amino Acids	65
2.6	UV Absorption of Proteins	65
2.7	Measurement of <i>p</i> -Nitrophenolate and <i>p</i> -Aminobenzoic Acid Concentrations	66
2.8	PGK Assay	66
<u>Chapter 3</u>	Interaction of Cyclodextrins with Amino Acid Enantiomers	68
3.1	Introduction	69
3.2	Results	70
3.2.1	α -Cyclodextrin	75
3.2.2	β -Cyclodextrin	83
3.2.3	Methyl- β -Cyclodextrin	84
3.2.4	Hydroxypropyl- β -Cyclodextrin	85
3.3	Discussion	86

<u>Chapter 4</u>	Energetics of Protein-Cyclodextrin Interactions	89
4.1	Introduction	90
4.2	Cyclodextrin-Induced Dissociation of Insulin	91
4.2.1	Introduction	91
4.2.2	Results and Discussion	94
4.3	Effect of Cyclodextrins on the Thermal Stability of Cytochrome c and Lysozyme	108
4.3.1	Introduction	108
4.3.2	Results	110
4.3.3	Discussion	118
 <u>Chapter 5</u>	 Cyclodextrins as Chaperone Mimics	 120
5.1	Introduction	121
5.2	Phosphoglycerate Kinase	123
5.3	Thermal Denaturation of PGK	126
5.4	Discussion	129
 <u>Chapter 6</u>	 Conclusions	 131
 References		 134

CHAPTER 1

INTRODUCTION

1.1 The Aims of Thesis

The primary aim of the work presented in this thesis was to investigate the interaction of cyclodextrins with amino acids, both free and in proteins, with a view to establishing the following: (a) the thermodynamics of cyclodextrin-amino acid interactions in solution and potential for chiral discrimination and enantiomer separation; (b) the possible effects of cyclodextrins on protein-protein interactions and stability; and (c) the possibility of an important role for cyclodextrins as chaperone mimics in assisting the folding or refolding of complex polypeptides. All these topics were examined using a range of biophysical techniques centred mainly on the use of sensitive microcalorimetry (both ITC and DSC) for analytical and direct thermochemical observations. The introductory background on cyclodextrins, amino acids, proteins and calorimetric techniques is presented in this chapter, with more detailed explanations where necessary in subsequent methods and results sections.

1.2 Cyclodextrins

Cyclodextrins, also known as Schardinger dextrins, cycloamyloses and cycloglucoamyloses, were first discovered in 1891 by Villiers (Villiers, 1891). The first detailed description of their preparation and isolation was made in 1903 by Schardinger (Schardinger, 1903). Cyclodextrins are a series of cyclic oligosaccharides obtained from starch by enzymatic degradation, in this process the starch is treated with the amylase of *Bacillus macerans*. The starch helix is hydrolysed, and its ends are joined together through α -1,4 linkages. The site of hydrolysis is not specific, therefore the product contains α -, β -, and γ -cyclodextrins together with small amounts of higher cyclodextrins. Up to now, α -, β -, γ -, and δ -cyclodextrins, which are comprised of six, seven, eight and nine glucose units, respectively, have been isolated by selective precipitation with appropriate organic compounds. Cyclodextrins, having fewer than six glucose residues, are not known to exist and are probably prohibited due to steric hindrance (Bender & Komiyama, 1978).

1.2.1 Structure and Physical Properties

Cyclodextrins are all in classical C_1 chair conformation and are composed of α -1,4 linked D-glucopyranose units (Figure 1.1). A cyclodextrin molecule can be envisaged as an empty cone-shaped capsule with the wider side formed by the secondary 2- and 3-hydroxyl groups and the narrower side by the primary 6-hydroxyl (Figure 1.2). The dimension and size of the internal cavity is determined by the number of glucose units. The cavity is lined by hydrogen atoms and glycosidic oxygen bridges. The non-bonding electron pairs of the glycosidic oxygen bridges are directed towards the inside of the cavity, producing a high electron density and lending it some Lewis base character. The outer surfaces of these molecules are hydrophilic, while the internal cavity is of apolar character.

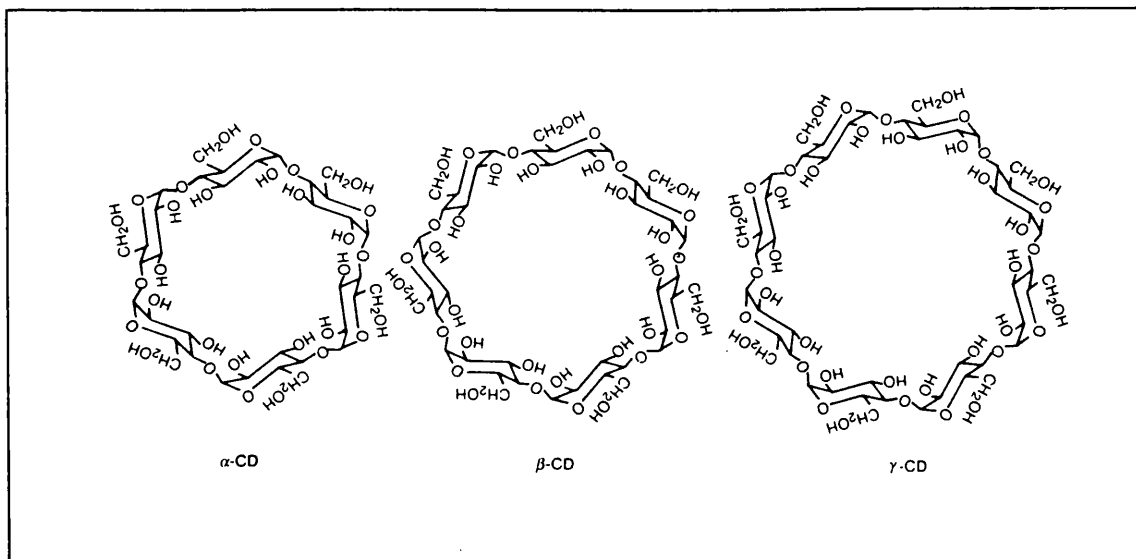


Figure 1.1 Structure of α , β , and γ -cyclodextrin.

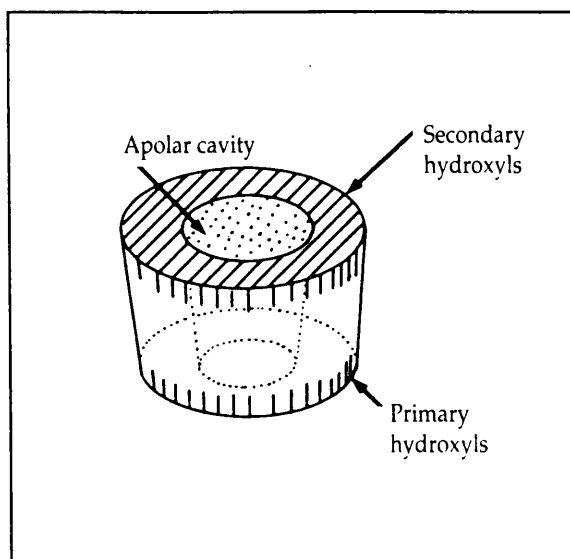


Figure 1.2 Functional structural scheme of a cyclodextrin.

In the cyclodextrin molecule, a ring of hydrogen bonds is formed intramolecularly between the 2-hydroxyl and the 3-hydroxyl groups of adjacent glucose units. This hydrogen bonding ring gives the cyclodextrin a highly rigid structure (Szejtli, 1982).

Cyclodextrin physical properties and characteristics are displayed in Table 1.1. As a direct result of their hydrophilic outside edge, cyclodextrins are water soluble, with solubilities of 14.5, 1.85 and 23.2 g/100 ml for α , β , and γ -cyclodextrin, respectively. Cyclodextrin molecules are stable in alkaline solutions, but are however susceptible to acid hydrolysis. The stability of cyclodextrins towards acid hydrolysis depends on the acidity and temperature. For example, the rate constants of hydrolysis of β -cyclodextrin in solutions of 0.0115 M HCl and 1.15 M HCl at 100 °C are 1.3×10^{-4} and $4.8 \times 10^{-2} \text{ min}^{-1}$, respectively. In the presence of 1.15 M HCl, the rate constants at 40 °C, 60 °C and 80 °C are 1.0×10^{-5} , 2.7×10^{-4} and $3.7 \times 10^{-3} \text{ min}^{-1}$, respectively (Bender and Komiyama, 1978; Szejtli, 1982).

Characteristics	α -cyclodextrin	β -cyclodextrin	γ -cyclodextrin
No. of glucose units	6	7	8
Molecular weight	972	1135	1297
Solubility in water (g/100 ml)	14.5	1.85	23.2
Cavity diameter (Å)	4.7 - 5.3	6.0 - 6.5	7.5 - 8.3
Height of torus (Å)	7.9 ± 0.1	7.9 ± 0.1	7.9 ± 0.1
pK _a values	12.3	12.2	12.1

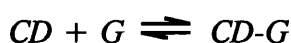
Table 1.1 Characteristics of α , β , and γ -cyclodextrins (Li and Purdy, 1992).

The conformations of cyclodextrins in solutions are quite pertinent, since most of the reactions by cyclodextrins are performed in solution, mostly in water. In general, they are nearly identical with those in the crystalline state. Optical rotatory dispersion spectroscopy, infrared spectroscopy and proton nuclear magnetic resonance (^1H -NMR), showed that the D-glucopyranose units in cyclodextrins are in the C1 chair

conformation in D₂O and dimethyl sulfoxide. These data necessarily require that the primary and secondary hydroxyl groups have similar conformation to those in the crystalline state (Bender and Komiyama, 1978).

1.2.2 Inclusion Complex Formation

One of the most remarkable characteristics of cyclodextrins is their ability to form inclusion complexes with a wide variety of compounds (guests), in which the guest compounds are included in the cavity of cyclodextrins (host). Guests can range from inorganic or organic compounds of neutral or ionic nature to noble gases. Complex formation in solution is a dynamic equilibrium process, which can be described by:



where CD is the cyclodextrin, G is the guest molecule and CD-G is the inclusion complex. The inclusion complex stability can be described in terms of a formation constant (K_f) or a dissociation constant (K_d) as determined in following equations:

$$K_f = \frac{[CD-G]}{[CD][G]}$$

$$K_d = \frac{1}{K_f} = \frac{[CD][G]}{[CD-G]}$$

The binding forces involved in the complex formation have been generally accepted to be; (i) van der Waals interactions and hydrophobic interactions between the guest molecules and the cyclodextrin cavity; (ii) hydrogen bonding between the polar functional groups of the guest molecules and the hydroxyl groups of the cyclodextrin; (iii) release of high energy water molecules from the cavity in the complex formation process; and (iv) release of strain energy in the ring frame system

of the cyclodextrin. These factors are all operative, however the relative contribution of each factor is still unknown (Bender and Komiyama, 1978). Importantly, no covalent bonds are formed, so the complexes are easily dissociated under physiological conditions (Dalla Bella and Szejtli, 1983).

The most important factors determining the stability of the inclusion complex are the polarity and the geometric capability of the guest molecules. Geometric rather than chemical factors are decisive in determining the type of guest molecules which can penetrate into the cavity. If the guest is too small it will easily pass in and out of the cavity with little or no bonding. Complex formation with guest molecules significantly larger than the cavity, may also be possible, however the complex is formed in such a way that only certain side chains or groups penetrate into the cyclodextrin cavity. The stability of an inclusion complex also depends on the hydrophobic nature of the guest molecule. Guests that are less polar than water can form inclusion complexes with cyclodextrins. Highly hydrophilic molecules complex weakly or not at all.

Inclusion complexes can be formed either in crystalline state or in solution. However, complexation is normally carried out with water as the solvent. The type of medium used for complexation also contributes to the stability of the inclusion complex. Even though inclusion complex formation takes place in an organic solvent, the guest molecules are generally only weakly complexed (Li and Purdy, 1992).

As a result of complex formation, the properties of the included guest can be altered in a number of ways for example, solubility (Pitha et al., 1986; Brewster et al., 1991; Loftsson et al., 1991; Pitha et al., 1992; Szejtli, 1994), diffusion (Szejtli, 1982; Rymden et al., 1984), chemical reactivity (VanEtten et al., 1967), pK_a values (Gelb, et al., 1981), electrochemical properties (Osa et al., 1977; Matsue et al., 1984) and spectral properties (Fujita et al., 1982; Inoue et al., 1985). Due to cyclodextrins having this unique property, it has led to their growing use in pharmaceutical, chemical, food and other industrial areas.

Inclusion complex formation in aqueous solution can be studied by various spectroscopic methods for example; UV-visible spectrophotometry (Cramer et al., 1967; Cooper and MacNicol, 1978; Buvari and Barcza, 1988; Horksy and Pitha, 1994) luminescence spectrometry (Baeyens, et al., 1990), and NMR spectroscopy (Thakkar and Demarco, 1971; Wood et al., 1977; Rekharsky, et al., 1995). Cyclodextrin complexes can also be studied by electrochemical methods, such as conductometry, polarography and voltametry (Bersier et al., 1991). An important method for directly measuring the thermodynamic properties of complex formation is calorimetry (Cooper and MacNicol, 1978; Inoue et al., 1993; Rekharsky et al., 1995).

1.2.3 Cyclodextrin Derivatives

The name “cyclodextrin derivatives” denotes compounds which contain only one or two cyclodextrin rings; those containing three or more units are termed “cyclodextrin polymers”, as their molecular weights exceed 3000.

For a number of reasons, such as price, availability and cavity dimensions, the β -cyclodextrin is the most widely used, and represents at least 95% of all produced and consumed cyclodextrins. However, its exceptional low aqueous solubility is a serious barrier in its wider utilization. Nevertheless, the solubility of all cyclodextrins can be sufficiently improved by chemical or enzymatic modifications, for example partial methylation increases solubility, possibly due to the disruption of the hydrogen bond system in the solid phase. The solubility of a partially methylated β -cyclodextrin containing 7 methyl groups increases e.g., from 18 g/L to 67 g/L.

In the cyclodextrins every glucopyranose unit has three free hydroxyl groups which differ in their functions, and reactivity. The relative reactivities of C(2) and C(3) secondary, and the C(6) primary hydroxyls depend on the reaction conditions

i.e. pH, temperature, reagents. Cyclodextrins can be modified by; (i) substituting for the H atom of the primary or secondary hydroxyl groups; (ii) substituting for one or more primary and/or secondary hydroxyl groups; (iii) eliminating the hydrogen atoms of the $-\text{CH}_2\text{OH}$ groups (e.g. by conversion to $-\text{COOH}$); or (iv) splitting one or more $\text{C}_2\text{-C}_3$ bonds through a periodate oxidation (Li and Purdy, 1992). The aim of such derivatizations may be to improve the solubility of the cyclodextrin derivative (and its complexes), to improve the fitting between the cyclodextrin and its guest, to attach specific groups to the binding site (e.g. in enzyme modelling) and lastly to form insoluble, immobilized cyclodextrin-containing structures (Szejtli, 1994). In this thesis, the only cyclodextrin derivatives used were hydroxypropyl- β -cyclodextrin and methyl- β -cyclodextrin.

1.2.4 Applications of Cyclodextrins

Although cyclodextrins were initially very expensive to produce, these compounds can now be produced in large quantities and at reasonable prices. This has led to a wide variety of applications for cyclodextrin complexes in a number of industries. The use of cyclodextrins in chiral discrimination, as well as some other applications are presented next.

Cyclodextrins in Chiral Discrimination

Since cyclodextrins are known to form diastereomeric complexes with optically active molecules, which can result in possible enantiomeric discrimination, they have been extensively used for the separation of enantiomers in various areas of science. Before giving some examples, it is important to understand why such separations are necessary.

The separation of enantiomers is of great interest and importance particularly to the pharmaceutical industry and regulatory authorities, for the reason that many drugs

are available in only racemic mixtures for clinical use. This can present problems because even though enantiomers have identical physical and chemical properties, except for directing plane polarized light in opposite directions, in a chiral environment they can often act as two different molecules with different biological activities. This was initially observed in the 1960's where pregnant women gave birth to children with malformed limbs after being given the sedative thalidomide, which had been contaminated with the wrong enantiomer. Although new evidence such as the rapid racemization of thalidomide enantiomers (Eriksson et al., 1995) has suggested that the use of the pure enantiomer may not have prevented such a tragedy, the need for testing pharmaceutical products for the effects of left- and right-handed molecules is still extremely important. Numerous examples exist where the undesired effects of one isomer limit the overall effectiveness of the active species because of host toxicities, biodistribution problems, altered mechanisms and unwanted drug interactions. For example, in the case of prototype β -blocker propranolol, D-propranolol is about 40 times more potent than L-propranolol and appears to mediate the antiarrhythmic and antihypertensive activity of the racemic mixture, whereas only L-propranolol appears to be beneficial in treating angina pectoris (Wilson et al., 1969). A similar case occurs with synthetic opiates such as methadone, in which there may be about 3-5 stereoselective opiate receptors, each of which triggers a different physiological response (Wuster et al., 1981). It is clear from these examples that the use of specific enantiomers would allow more exact therapeutic effects.

For many years now, cyclodextrins have been used in separation chromatography as a separation medium. The partitioning and binding of many hydrophobic and hydrophilic molecules to the cyclodextrin cavity can be much more selective than partitioning and binding to a single traditional stationary phase or to a single solvent. Consequently, cyclodextrins are increasingly being used in typically difficult separations of enantiomers, diastereomers, structural isomers and geometric isomers, in all current types of chromatography. For instance, enantiomers of agricultural chemicals were separated via gas chromatography using modified beta cyclodextrin chiral stationary phases (Konig et al, 1991). Such chiral phases were also successful in the

separation of phenoxypropionic acid herbicides, polychlorinated polycyclic pesticides, organophosphorous pesticides, and components of chlordane, an environmental toxin (Buser et al., 1992). Additionally, cyclodextrins have been used in high performance liquid chromatography to obtain excellent separations for a range of drugs such as prostaglandins, vitamin D₂ and sterols, as well as for general chemicals (Armstrong et al., 1985a), quinones and heterocyclic compounds (Armstrong et al., 1985b), barbiturates, dansyl amino acids (Thuaud et al., 1991; Hinze et al, 1984; Armstrong and DeMond, 1984), and isomers of disubstituted benzene derivatives (Tanaka et al., 1984). In addition, cyclodextrins have also been utilized in capillary electrophoresis for the separation of enantiomers of amino acid derivatives (Copper et al., 1994; Okafo and Camilleri, 1993) and of drugs such as ibuprofen and leucovorin (Sun et al., 1993 and 1994).

Other Applications

In the pharmaceutical industry, following complexation the physical and chemical properties of a guest drug molecule can be altered, so as to impart beneficial characteristics. Some of the major advantages of forming a cyclodextrin complex with drug molecules are as follows; (a) increased water solubility and increased rate of dissolution of poorly soluble substances; (b) transformation of liquid drugs into solids; (c) stabilization of unstable drugs (e.g. volatile compounds); (d) protection from oxidation of easily oxidizable substances; (e) masking of an unpleasant taste or smell; (f) enabling formulation of incompatible compounds through protection of one component by formation of a cyclodextrin complex; and (g) reduction or elimination of adverse effects (Saenger, 1980). Most important among these advantages are stabilization of unstable compounds and enhancement of solubility. For example, by complexation with cyclodextrin, a poorly water soluble drug is molecularly dispersed in a hydrophilic matrix and becomes completely soluble. This improved solubility results in faster dissolution, which can potentially lead to a faster onset of activity and, in some instances, higher blood levels of the drug. Thus, the same dosage of a

drug may have a greater biological effect when included in a cyclodextrin (Dalla Bella and Szejtli, 1983).

As with pharmaceuticals, cyclodextrins are being utilized in a number of applications in food systems. Cyclodextrins can form inclusion compounds with a variety of molecules, including fats, flavours and colours. Cyclodextrins may be utilized for removal and masking of undesirable components or controlled release of desired food constituents (Eastburn and Tao, 1994). For example, cyclodextrins were most effective in debittering grapefruit juice by removing a bitter component naringin (Su and Yang, 1991). A more recent application of cyclodextrins is the removal of cholesterol from eggs and whole milk (Haggin, 1992).

Applications in the chemical industry include the use of cyclodextrins as catalysts (Tabushi, 1984) or as enzymes mimics (Breslow, 1991). In the field of analytical chemistry cyclodextrins have extensive applications, which are based upon the properties of increased solubility, higher melting point, inclusion compound formation and molecular recognition. In addition to chromatography, cyclodextrins can also be used in other separation techniques. For example, Du et al. (1991) developed a molecular device for photochemical charge separation with both mono-6-deoxy-6-[4-(1-ethyl-4-pyridinio)-1-pyridinio]-beta cyclodextrin and C-6-mono-pyridinio-beta cyclodextrin. Electrostatic interactions between the modified cyclodextrin and the guest molecule were the basis for the separation, and the differences between the binding ability of the two cyclodextrins were due to molecular charge.

Other analytical applications also exist for cyclodextrins. For instance, Ueno et al. (1992) found that 6-deoxy-6-amino-beta cyclodextrin, when reacted with methyl red, produced a colour change indicator. The colour change will occur upon host-guest interaction with organic species, which will displace the methyl red from the interior of the cyclodextrin, making it available to protonation. Minato et al. (1991) determined that bis(2-naphthyl-sulfonyl) derivatives of gamma and beta cyclodextrin were capable of molecular recognition. They concluded that these substances could

be use as host-guest sensors for detection of organic species, such as cholic acid, cyclohexanol and L-borneol, through excimer fluorescence. Frankewich et al. (1991) studied the effects of hydroxyethyl beta cyclodextrin, 2-hydroxypropyl beta cyclodextrin and heptakis (2,6-di-O-methyl)-beta cyclodextrin on fluorescence properties. They determined that the cyclodextrin derivatives increased the stability of fluorescent systems of dansyl amino acids and organic/pharmaceutical compounds. The increased stability of the solute-cyclodextrin complex resulted in the increase in fluorescence.

In addition to these general uses, specific applications of cyclodextrins that will be discussed in this thesis are the possibility of cyclodextrins affecting the aggregation state of protein solution. Also, the effect of cyclodextrins in reducing the thermal stability of various proteins. Combining both these effects, the use of cyclodextrins as possible chaperone mimics is also discussed.

1.3 Amino Acids

α -Amino acids are small molecules which are the building blocks of polypeptides and proteins. They consist of a tetravalent asymmetric carbon atom to which are attached four different groups (R-, H-, NH_2 - and CO_2H). The pK_a 's of the carboxyl and amino groups of the α -amino acids are about two and ten, respectively. Therefore, in the vicinity of neutral pH the carboxylate group will have lost a proton, and the amino group will have picked up a proton, to yield the zwitterion form (this is the form we customarily write amino acid structures).

There are twenty different kinds of natural amino acids which are coded for in the genes and incorporated into proteins. The twenty amino acids contain, in their 20 different side chains, a remarkable collection of diverse chemical groups; these form the vocabulary that allows proteins to exhibit such a great variety of structures and properties.

Stereochemistry of the α -Amino Acids

Whenever a carbon atom has four different substituents attached to it, forming an asymmetric molecule, the carbon is said to be chiral, a center of chirality, or a stereocenter. In such cases, two distinguishable stereoisomers exist, as shown in Figure 1.3. The forms of alanine shown here are called L and D enantiomers. These enantiomers can be distinguished from one another experimentally by the fact that their solutions rotate the plane of polarized light in opposite directions. Thus, they are sometimes called optical isomers. All amino acids except glycine can exist in L and D forms, since in each case the α -carbon is chiral. Glycine is the exception since two of the groups on the α -carbon are the same (H).

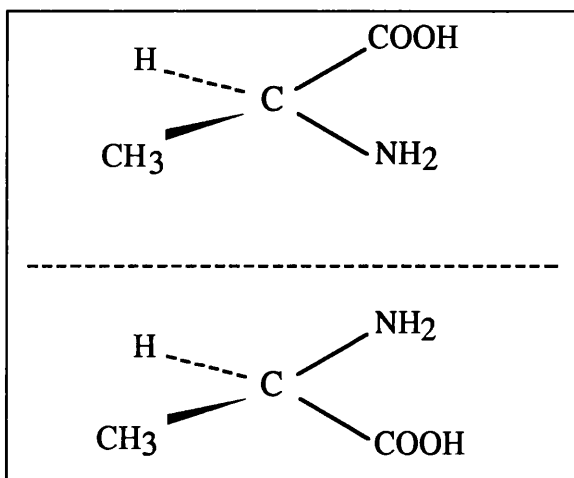


Figure 1.3 Enantiomers of alanine.

An important fact is that almost all amino acids incorporated by organisms into proteins are of the L form. It is not clear why this should be so, for L-amino acids have no obvious inherent superiority over their D isomer for biological function. Indeed, D-amino acids do exist in nature, and some play important biochemical roles for example, D-alanine and D-glutamic acid exist in the polypeptides of some bacterial cell walls. It is assumed that very early in the evolution of life the L isomers were ‘chosen’ by chance, or had some small advantage, and that the mechanism for synthesizing and utilizing proteins became fixated on these forms. However, we really do not know the answer to this enigma.

Properties of Amino Acid Side Chains

Amino acids have several different side chains, distinguished by their dominant chemical features. These features include hydrophobic or hydrophilic character, polar or non-polar nature, and presence or absence of ionizable groups. The groups of amino acids will be discussed in an order from the simplest to the more complex.

First, are the amino acids with aliphatic side chains, which are glycine, alanine, valine, leucine and isoleucine. Progressing from glycine to isoleucine, the R group

becomes more extended and more hydrophobic. Isoleucine, for example, has a much greater preference to transfer from water to a hydrocarbon solvent than does glycine. The more hydrophobic amino acids usually prefer an environment within a protein molecule, where they are shielded from water. The side chain of proline is aliphatic like those above, with no functional groups. It is unique, however, in that it is bonded covalently to the nitrogen atom of the peptide backbone. Although it is a cyclic amino acid, its side chain has primarily aliphatic character.

Amino acids with hydroxyl or sulphur containing side chains are serine, cysteine, threonine and methionine. These amino acids are generally more hydrophilic than their aliphatic analogs due to their weakly polar side chains, although methionine is fairly hydrophobic. Cysteine is noteworthy in two respects, the side chain can ionize at high pH, and oxidation can occur between pairs of cysteine side chains to form a disulphide bond.

The three amino acids, phenylalanine, tyrosine and tryptophan, carry aromatic side chains. Phenylalanine, together with valine, leucine and isoleucine, is one of the most hydrophobic amino acids. Tyrosine and tryptophan have some hydrophobic character as well, but it is tempered by the polar groups in their side chains. In addition, tyrosine can ionize at high pH. The aromatic amino acids, like most compounds carrying conjugated rings, exhibit strong absorption of light in the near-ultraviolet region of the spectrum.

Histidine, lysine and arginine carry basic groups in their side chains. The pK_a of the imidazole side chain of histidine is in the physiological range, allowing it to exist in both the ionized and non-ionized states. While, lysine and arginine are more basic amino acids, with their side chains being positively charged under physiological conditions. The basic amino acids are strongly polar and are usually found on the exterior surfaces of proteins, where they can be hydrated by the surrounding aqueous environment.

Chapter 1

Finally, the acidic amino acids aspartic acid and glutamic acid are the only amino acids that carry negative charges at neutral pH. Companions to aspartic and glutamic acids are their amides, asparagine and glutamine. Unlike their acidic analogs, asparagine and glutamine have uncharged side chains, though they are decidedly polar. Similar to the basic and acidic amino acids, they are definitely hydrophilic and tend to be on the surface of a protein molecule, in contact with the surrounding water.

1.4 Protein Folding and Stability

Proteins are linear macromolecules composed of a variety of combinations of 20 different amino acids linked together by peptide bonds in a specific order, using genetic information, to form polypeptide chains. The amino acid sequence is known as the primary structure of a protein. Proteins may be classified into three types: fibrous, membrane and globular, of which the latter type will be discussed in this thesis.

In globular proteins, the native or folded state is extremely compact and unique. The native state depends on its primary sequence, which means a protein usually folds to only one native state (the native states of different proteins can be quite similar, despite differences in their primary structure). The secondary structure of a globular protein includes hydrogen bonded α -helices and β -sheets, these are linked together by specific loops and turns to form the tertiary structure which gives monomeric proteins their overall shape. In some proteins, the association of monomers into larger aggregates is known as the quaternary structure.

Proteins are normally in their native state in aqueous solvents near to neutral pH at 20-40 °C. The native state is only marginally more stable than the unfolded state. Under some nonphysiological conditions such as minor changes in temperature, pH, pressure, ligand concentration, the addition of denaturing agents or other solvent changes, the unique folded structure of a protein can become unfolded or denatured.

1.4.1 Thermodynamics of Folding

The folding of a globular protein is a thermodynamically favoured process under physiological conditions. Therefore, the overall free energy change on folding must be negative, but it is clear that the folding process, which involves going from a

multitude of random coil conformations to a single folded structure, must involve a decrease in randomness and thus a decrease in entropy. The free energy equation,

$$\Delta G = \Delta H - T\Delta S \quad (1.1)$$

shows that this negative ΔS will yield a positive contribution to ΔG . Therefore, to explain the overall negative ΔG in protein folding, it is understood that this entropy effect is compensated by the free energy gained as a result of a redistribution of various intramolecular interactions between the protein groups and the environment.

The non-covalent interactions identified as possibly playing a part in stabilizing the native fold are hydrogen bonding, electrostatic interactions, van der Waals interactions and the hydrophobic effect. In addition, one type of covalent interaction that may have a strong influence on protein structure and stability is the disulphide bridge.

For information on many of these forces the following references are extremely useful: Kauzmann, 1959; Dill, 1990; Creighton, 1991; Rose and Wolfenden, 1993; Cooper, 1997.

Hydrogen Bonding

A hydrogen bond occurs when a hydrogen atom is shared between two electronegative atoms (usually in proteins between groups such as -NH and -C=O or -OH). A hydrogen bond is primarily a linear arrangement of donor, hydrogen and acceptor. The strength of a hydrogen bond depends on the electronegativity and orientation of the binding atoms, and the more the three atoms deviate from co-linearity the weaker the bond.

Mirsky and Pauling (1936) were the first to suggest the importance of hydrogen bonds in protein folding (Pauling, 1939) and it has been long thought that hydrogen bonding is the principal stabilizing force in folded proteins (Privalov and Gill, 1988). In proteins, the inherent strengths of individual intramolecular hydrogen bonds are modulated by direct competition with water molecules that supply alternative binding partners and by other polar groups in the surroundings. The breaking of a hydrogen bond between two groups in vacuum requires a significant amount of energy, for example a peptide hydrogen bond requires approximately 25 kJ mol^{-1} (Rose and Wolfenden, 1993). However, in water such exposed groups would probably form new hydrogen bonds to surrounding water molecules to cancel the effect, and the true effect of a hydrogen bond between groups in an aqueous environment might be closer to zero. The overall interaction will also include significant entropy contributions due to solvent involvement. The usually excellent solubility of polar compounds in water reflects this, and model compound studies generally lead to a picture in which hydrogen bonds contribute little if anything to the free energy of folding of a polypeptide chain. Nevertheless, they will certainly determine the specific conformation adopted by the polypeptide when folded (Dill, 1990).

Electrostatic Interactions

The electrostatic interaction between two point charges is determined by Coulomb's law:

$$F = \frac{q_1 q_2 k}{\epsilon r}$$

where q_1 and q_2 are the charges of the two points, k is a constant, ϵ is the dielectric constant and r is the distance between the two points. Electrostatic interactions are very simple and well understood in model systems, but they become remarkably complex in non-homogeneous environment, such as folded proteins in water.

The pH dependence of protein unfolding indicates that electrostatic interactions between charged groups are important for stability (Goto et al., 1990). At neutral pH, electrostatic interactions can occur in proteins between positively and negatively charged side chain groups, for example a lysine side chain amino group may be placed close to the carboxyl group of some glutamic acid residue. This particularly close, direct electrostatic interaction is called a salt bridge, and in the 1930's it was believed to be responsible for stabilising the native state (Cohn et al., 1933; Mirsky and Pauling, 1936). The situation can most readily be envisaged by considering two charged groups which are separated in water. The water molecules have a significant, permanent dipole which results in the charged groups becoming surrounded by water molecules. Water molecules in the proximity therefore become compressed and oriented in particular ways. When the two charges come together their electric fields no longer have a strong influence on the water molecules' behaviour, which leads to the solvent becoming much less compressed and structured, hence a large increase in entropy accompanies the association of the charged groups. This can also be shown by the temperature dependence of the dielectric constant of water. Reducing the temperature of water forces the molecules into a more structured arrangement resulting in a smaller entropy difference and therefore a smaller force.

Water is an extremely polar solvent, and has a large dielectric constant of 80, while the interior of the protein has a smaller dielectric constant. When the charged groups of proteins are interacting in conditions from which water is excluded the magnitude of the electrostatic force is increased. Therefore, the influence of charged groups depends on where they are situated and the polarity of the environment.

The addition of salt weakens electrostatic interactions by shielding the charge, whereas pH directly changes the charge on acidic or basic groups. The variation of pH and addition of salt, close to the isoelectric point has little effect on the stability of the protein (Tanford, 1968; Hermans and Scheraga, 1961). This may imply that ion pairing is not the dominant force in protein folding.

Van der Waals

Van der Waals or London dispersion forces are a specific type of electrostatic interaction between all atoms and molecules that arise from quantum mechanical fluctuations in the electronic distribution. Transient fluctuations in electron density distribution in one group will produce changes in the surrounding electrostatic field that will affect adjacent groups. Simply, a transient electric dipole will polarise or induce a similar but opposite dipole in an adjacent group such that the two transient dipoles attract. The dipole-dipole interaction is extremely short range varying as the inverse of distance to the power six, and such interactions are usually only of significance for groups in close contact. The interior of proteins is extremely close packed which allows van der Waals forces to exist within their structure. In fact, it is packed as well as crystals of small organic molecules (Richards, 1977).

The strength of the interaction also depends on properties such as high-frequency polarizability of the groups involved, but apart from this, such interactions involve very little specificity. All atoms or groups will show van der Waals attractions for each other. Also sometimes included in van der Waals interactions is the steep repulsive potential between atoms in close contact. This arises from repulsions between overlapping electronic orbitals in atoms on non-covalent contact, which make atoms behave almost like hard, impenetrable spheres at sufficiently short range. Thermodynamically, van der Waals interactions would normally be considered to contribute to the enthalpy, with no significant entropy component.

Hydrophobic Effect

The hydrophobic effect is defined as the process by which non-polar groups are removed from contact with water. When a hydrophobic molecule is introduced into bulk water, it is unable to form hydrogen bonds to the water. To compensate for this, neighbouring water molecules of the non-polar molecule form as many hydrogen bonds possible with each other, to form a cagelike structure around them. This

results in a more ordered structure (Frank and Evans, 1945) and a loss of randomness in the system, therefore the entropy is decreased. The entropy is further decreased as the non-polar molecule itself loses much of its original rotational and translational entropy (Aronow and Witten, 1960; Howarth, 1975).

It has been generally accepted that the hydrophobic effect makes a major contribution to the thermodynamic stability of proteins (Kauzmann, 1959). Suppose a protein contains, in its amino acid sequence, a substantial number of residues with hydrophobic side chains (for example, leucine, isoleucine, and phenylalanine). When the polypeptide chain is in an unfolded form, these residues will be in contact with water and cause ordering of the surrounding water structure. However, when the chain folds into its native structure, these hydrophobic residues can be buried within the molecule. The water molecules that they have ordered will be then be released. Consequently, internalizing hydrophobic groups can increase the randomness and therefore yield an entropy increase on folding. This will make a negative contribution to the free energy of folding and increase the stability of the protein structure.

There is considerable evidence for the involvement of the hydrophobic effect. The transfer of a hydrocarbon into a polar environment is accompanied by large positive changes in heat capacity, which has been explained in terms of gradual melting of the structured water layers formed around the solute. These large changes are similarly observed upon unfolding of protein molecules. Furthermore, the stability of proteins can be affected by the addition of cyclodextrins, by which the hydrophobic side chains on the unfolded protein are buried in the cyclodextrin cavity (Cooper, 1992), removing it from contact with water, therefore reducing the magnitude of the hydrophobic effect.

Disulphide Bonds

A disulphide bond is formed when oxidation occurs between pairs of cysteine side chains, and differs from the other types of interactions within folded proteins, such as hydrogen bonds, electrostatic and van der Waals interactions, in being covalent. Being a covalent bond, there are stereochemical requirements for the relative positions and orientation of the two cysteine residues. The sulphur atoms must be 2.05 ± 0.03 Å apart, the angle between the disulphide and the β -carbon of each cysteine residue must be near to 103° , and the two β -carbons atoms must be oriented so that they correspond to a rotation of close to either $+ 90^\circ$ or $- 90^\circ$ about the disulphide bond (Creighton, 1988).

The presence of disulphide bonds and other crosslinks connecting regions of the polypeptide is generally believed to increase the stability of the folded protein. The introduction of such crosslinks can be an extremely effective way to improving stability. The effect is mainly entropic, arising from topological constraints leading to a reduction in the number of configurations available to the unfolded chain (Schellman, 1955; Flory, 1956; Poland and Scheraga, 1965; Pace et al., 1988).

In the absence of disulphide crosslinks, the distance between any two groups in the unfolded protein varies, with a probability determined by the statistics of the polymer chain and a range dependent only on the length of the chain. A disulphide crosslink between two distant groups forms a loop, resulting in a restricted set of possible chain configurations. For any one loop, the reduction in conformational entropy (ΔS_{conf}) of the unfolded chain estimated by considering the relative probability that the ends of a polymer chain will be found within the same volume element (v_s) is given by:

$$\Delta S_{\text{conf}} = -R \ln \left(\frac{3}{(2\pi l^2 n)^{3/2}} \right) v_s$$

where R is the constant, n is the number of residues in the loop, and l is the length of a statistical segment of the chain (i.e. 3.8 Å). There are various estimates of v_s , for example 2.83 Å³ (Schellman, 1955), 5.17 Å³ (Poland and Scheraga, 1965) and 57.9 Å³ (Pace et al., 1988).

It is assumed that the crosslink effect lies in the configurational entropy of the unfolded chain, and that the presence of the crosslink in the folded protein presents no conformational strain or other constraints in the native form. It has been argued by Doig and Williams (1991) that the presence of disulphide crosslinks in the unfolded polypeptide leads to strain and other additional effects in the unfolded proteins that override the entropic effects, however work done by Johnson et al. (1978) rules this out.

Investigation of these various possibilities by more detailed thermodynamic measurements of specifically disulphide modified proteins (Cooper et al., 1992; Kuroki et al., 1992) resulted in divergent conclusions.

Cooper et al. (1992) showed that any difference in folding stability of the two proteins, native 4-disulphide and a specific 3-disulphide hen egg-white lysozyme (lacking the disulphide bond between cysteine residues 6 and 127) arose experimentally from entropy differences. By contrast, studies by Kuroki et al. (1992) of mutant human lysozymes lacking a disulphide bond between cysteine residues 77 and 95 indicate that the observed destabilization is enthalpic, with a smaller unfolding entropy for the mutants lacking this crosslink. In this case, the difference may be that the disulphide crosslink involves a tight loop and is buried within the protein structure rather than close to the surface. More recent studies by Vogl et al. (1995) confirm this trend that contributions to folding stability of enthalpic and entropic terms depend on loop length and positioning of the crosslink. Therefore, destabilization involving large loops tends to be purely entropic, while enthalpy effects play a greater role for shorter loops.

1.4.2 Effects of Ligand Binding on Folding Thermodynamics

Once folded, the specific conformation of the protein can provide a specific binding site for the recognition of other molecules (ligands), such as a small molecule, macro-molecule or other proteins. The factors that influence the association of the protein with these ligands are the same non-covalent interactions responsible for protein stability. In certain situations the ligand and protein can become covalently bound, however the initial recognition is driven by the non-covalent forces already described.

In cases where the ligand binds to the folded protein, it will stabilise the folded state and unfolding becomes gradually less favourable as the concentration of ligand increases. In contrast, if the ligand binds to the unfolded protein it will destabilise the fold and encourage unfolding (Sturtevant, 1987; Fukada et al., 1983; Cooper, 1992; Cooper and McAuley-Hecht, 1993).

In the case that a ligand molecule (L) binds specifically only to the native folded protein (N), then the following applies:



where $K_{L,N}$ is the dissociation constant for ligand binding to the native protein and K_0 is the unfolding equilibrium constant for the unliganded protein.

The effective unfolding equilibrium constant (K_{unf}) in the presence of ligand is given by the ratio of the total concentrations of unfolded to folded species:

$$K_{\text{unf}} = [U]/([N] + [NL]) = K_0/(1 + [L]/K_{L,N}) \approx K_0 K_{L,N}/[L]$$

where the approximate form holds at high free ligand concentrations ($[L] > K_{L,N}$). This indicates that K_{unf} decreases and the folded form becomes more stable with increasing ligand concentration.

Expressed in free energy terms:

$$\begin{aligned}\Delta G_{\text{unf}} &= -RT\ln(K_{\text{unf}}) = \Delta G_{\text{unf},0} + RT\ln(1 + [L]/K_{L,N}) \\ &\approx \Delta G_{\text{unf},0} + \Delta G^{\circ}_{\text{diss},N} + RT\ln[L] \quad (\text{for high}[L])\end{aligned}$$

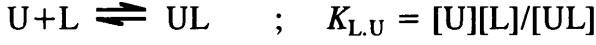
where $\Delta G_{\text{unf},0}$ is the unfolding free energy of the unliganded protein and $\Delta G^{\circ}_{\text{diss},N} = -RT\ln(K_{L,N})$ is the standard Gibbs free energy for dissociation of the ligand from its binding site on the native protein. So, the stabilizing effect of bound ligand can be thought as arising from additional free energy required to remove the ligand prior to unfolding, together with an additional contribution ($RT\ln[L]$) from the entropy of mixing of the freed ligand with the bulk solvent.

In the high ligand concentration limit the free energy can be split into enthalpy and entropy contributions:

$$\begin{aligned}\Delta H_{\text{unf}} &\approx \Delta H_{\text{unf},0} + \Delta H^{\circ}_{\text{diss},N} \\ \Delta S_{\text{unf}} &\approx \Delta S_{\text{unf},0} + \Delta S^{\circ}_{\text{diss},N} - R\ln[L]\end{aligned}$$

The enthalpy of dissociation for small ligands can be quite small compared to the enthalpy of unfolding of the protein, and can be difficult to distinguish in calorimetric unfolding studies, especially when ΔH_{unf} is in any case varying with temperature due to the effects of ΔC_p . Entropy effects, especially those occurring from the ligand mixing term ($R\ln[L]$) are much more apparent in such cases.

In cases where ligand binds only to the unfolded protein similar considerations apply (Cooper, 1992; Cooper and McAuley-Hecht, 1993):



therefore:

$$K_{\text{unf}} = ([U] + [UL])/[N] = K_0 (1 + [L]/K_{L,U}) \approx K_0 [L]/K_{L,U}$$

$$\Delta G_{\text{unf}} = -RT \ln(K_{\text{unf}}) = \Delta G_{\text{unf},0} - RT \ln(1 + [L]/K_{L,U})$$

$$\approx \Delta G_{\text{unf},0} - \Delta G_{\text{diss},U}^{\circ} - RT \ln[L] \quad (\text{for high } [L])$$

which in this situation indicates the destabilizing effect of a reduction in unfolding free energy as ligand binds to the unfolded polypeptide. Similar expressions for the enthalpy and entropy contributions may be written as above, using appropriate sign changes.

The effect of ligand binding (either N or U) on the mid-point temperature of the transition, T_m , of the protein can be generalised in the case of weakly binding ligands (Cooper and McAuley-Hecht, 1993) to give:

$$\Delta T_m/T_m = \pm(nRT_{m0}/\Delta H_{\text{unf},0}) \ln(1 + [L]/K_L)$$

where $\Delta T_m = T_m - T_{m0}$ is the shift in transition temperature and n is the number of ligand binding sites on the protein. The \pm sign relates to whether the ligand stabilizes to unfolded or fold form of the protein.

Chapter 1

For weak binding, at low ligand concentrations, this approximates to a linear form:

$$\Delta T_m/T_m = \pm nRT_{m0} [L]/(K_L \Delta H_{\text{unf},0})$$

From these expressions, the number of ligand binding sites and their average intrinsic binding constants can be estimated.

In cases of multiple ligand binding or more tightly binding ligands analysis is not as straightforward, but the same basic principles apply. For more details, refer to Sturtevant (1987) and Brandts and Lin (1990).

1.5 Microcalorimetry

The aim of this section is to provide a general understanding of basic thermodynamics and thermochemical background common to all calorimetric methods, as well as discussing various types of microcalorimeters, some of which have been used in the work reported in this thesis.

Calorimetry is the only technique available for directly measuring the basic physical forces between and within macromolecules in enough detail, so we are able to understand and manipulate biological processes at the molecular level. Calorimetry has been performed since the 1930's, however it is only the most recent designed calorimeters that are adequate for routine experiments in research laboratories. These sensitive, now commercially available instruments effectively measure small heat effects, in fact the typical microcalorimeter is sensitive enough to measure effective temperature changes of a millionth of a degree. Microcalorimetry may be used not only for determining thermodynamic data for processes such as ligand binding, conformational transition and macromolecular assembly, but also as an analytical tool to follow complex processes, such as enzyme kinetics, cellular and growth metabolism, over a range of time scales.

There are two general classes of calorimetry; (i) isothermal microcalorimetry which measures heat evolved or absorbed by a chemical or physical process, which may include titration (ITC) (Sturtevant, 1974; Cooper and Johnson, 1994a); and (ii) differential scanning calorimetry (DSC) which involves the measurement of heat uptake (heat capacity) during changes in temperature (Privalov, 1974; Sturtevant, 1974; Privalov and Potekhin, 1986; Sturtevant, 1987; Chowdhry and Cole, 1989; Cooper and Johnson, 1994b). The choice of instrumentation depends on the kind of process under investigation. Here, we focus on the use of calorimetry to study thermal stability, ligand binding and related processes.

Basic Thermodynamics

The first law of thermodynamics tells us that 'energy may be converted from one form to another but cannot be created or destroyed'. When a chemical system changes from one state to another the net transfer of energy to its surroundings must be balanced by a corresponding change in the internal energy of the system. The internal energy change (ΔU) is given by:

$$\Delta U = q + w$$

where q is the heat transferred to the system and w is the work done on the system. The term work includes all forms of work, even that arising from expansion or contraction, so called PV work. This is generally the only kind of work chemical reactions are allowed to do, so we find:

$$w = -P\Delta V$$

If a chemical system has no volume change, it can do no work, therefore ΔV is zero and the internal energy change is simply:

$$\Delta U = (q)_v \tag{1.2}$$

where the subscript v denotes constant volume.

However, if the reaction occurs at constant pressure the internal energy change is given by:

$$\Delta U = (q)_p - P\Delta V$$

which can also be written as:

$$\Delta U = U_B - U_A = (q)_p - P(V_B - V_A) \quad (1.3)$$

where the subscripts denote the states before and after the reaction has taken place. Rearrangement of equation 1.3, gives:

$$(q)_p = (U_B + PV_B) - (U_A + PV_A)$$

The enthalpy of a system is defined as:

$$H = U + PV$$

and at constant pressure:

$$\Delta H = (q)_p \quad (1.4)$$

The randomness, or the amount of disorder of a system is referred to as entropy (S). The greater the disorder in a system, the higher is its entropy. Entropy change is defined in the following way:

$$\Delta S = S_B - S_A = \int_A^B \frac{dq_{rev}}{T}$$

where q_{rev} is the heat transferred when the change is reversible i.e. at equilibrium. The absolute molar entropy of any system is given by:

$$S = k \ln w$$

where k is the Boltzmann constant and w is the number of substates of equal energy. The exponential nature of the Boltzmann probability expression:

$$p(E) = w \cdot \exp(-E/kT)$$

where $p(E)$ is the statistical probability that any molecule or system is to be found in some state and E is the energy of the system, seems to imply that low energy states are more likely and that things should tend to roll downhill to their lowest energy (enthalpy) state. However, this is generally offset by the 'w' term. The higher the energy, the more ways there are of distributing this energy in different ways to reach the same total. Therefore, a change to the system will occur in such a way as to obtain the lowest energy, however there is a larger number of ways of obtaining a higher energy, hence the system compromises these two requirements and resides in the most probable energy level.

The effects of randomness and enthalpy on a chemical reaction are such that, when possible, reactions proceed spontaneously towards a state of minimum energy and maximum disorder. The enthalpy change and the entropy change of a reaction can be combined to give the change in another state function, the free energy, G , of the system. The relationship between the free energy change, ΔG , the enthalpy change, and entropy change for a reaction is given by Gibbs-Helmholtz equation:

$$\Delta G^{\circ} = \Delta H^{\circ} - T\Delta S^{\circ} \quad (1.5)$$

where T is the absolute temperature and the superscript zeros designate changes occurring under standard state conditions. The equation can also be applied for conditions other than standard by replacing ΔG° , ΔH° and ΔS° with ΔG , ΔH and ΔS , respectively.

Chapter 1

The heat capacity of a substance is the quantity of heat which unit mass of a substance requires to raise its temperature by one degree i.e.:

$$C = \frac{dq}{dT} \quad (1.6)$$

where C is the heat capacity, q is the heat and T is the temperature. If the heat capacity is determined at constant volume, then by combining equations 1.2 and 1.6 gives:

$$C_v = \left(\frac{\partial U}{\partial T} \right)_v \quad (1.7)$$

If the heat capacity is measured at constant pressure, combination of equations 1.4 and 1.6 gives:

$$C_p = \left(\frac{\partial H}{\partial T} \right)_p \quad (1.8)$$

The following discussion of heat capacity will be limited to heat capacity at constant pressure, C_p , since it is under these conditions that most experiments are carried out. The constant pressure heat capacity differs from the constant volume heat capacity, C_v , by the work needed to change the volume of the system when pressure is held constant. For solids and liquids, C_p and C_v are usually quite similar, but for ideal gases they are significantly different. For ideal gases, the two are related as follows:

$$C_p = C_v + nR$$

where n is the number of moles of the gas and R is the gas constant.

Chapter 1

Both enthalpy and entropy are classical concepts related to the heat uptake or heat capacity of a system, and the relationships between ΔH and ΔC_p and between ΔS and ΔC_p are given by:

$$\Delta H = \int_0^T \Delta C_p(T) dT \quad (1.9)$$

$$\Delta S = \int_0^T \frac{\Delta C_p(T)}{T} dT$$

where $\Delta C_p(T)$ is the change in heat capacity at constant pressure at the temperature T (the same equation can also be used for absolute enthalpy, entropy and heat capacity, substituting H , S and C_p where appropriate). Over narrow temperature ranges, when ΔC_p stays approximately constant, the variation in enthalpy and entropy changes with temperatures is given by:

$$\Delta H(T_1) \approx \Delta H(T_0) + \Delta C_p(T_1 - T_0)$$

$$\Delta S(T_1) \approx \Delta S(T_0) + \Delta C_p(T_1 - T_0) / T_0$$

The equilibrium constant (K) of a reaction, such as where a macromolecule (M) is bound to a ligand (L) is given by:



where $[ML]$, $[M]$ and $[L]$ are the equilibrium activities of the complex, the free macromolecule and the free ligand, respectively. The inverse of the equilibrium constant is equal to the dissociation constant.

The equilibrium constant for a reaction is related to the standard free energy change in the following equation:

$$\Delta G^{\circ} = -RT\ln K \quad (1.10)$$

where R is the gas constant. Combining equations 1.1 and 1.10 gives

$$-RT\ln K = \Delta H^{\circ} - T\Delta S^{\circ} \quad (1.11)$$

rearranging equation 1.11 gives:

$$\ln K = -\frac{\Delta H^{\circ}}{RT} + \frac{\Delta S^{\circ}}{R}$$

Differentiation with respect to inverse temperature allows the van't Hoff equation to be obtained:

$$\Delta H_{vH} = \frac{-Rd(\ln K)}{d\frac{1}{T}}$$

If it is assumed that ΔH° and ΔS° do not vary with temperature (in other words assuming that ΔC_p is zero, which is often a fair assumption when considering a limited temperature range) then a plot of $\ln K$ vs. $1/T$ ("van't Hoff plot") gives a line whose slope at any point equals $-\Delta H_{vH}/R$. In simple cases, over a limited temperature range, this plot is linear, but in general the temperature dependence of ΔH will result in a curved van't Hoff plot that needs more careful analysis.

Ligand Binding

Ligand binding can be studied by a range of experimental techniques, however isothermal calorimetry has the advantage of giving both the equilibrium constant and enthalpy data simultaneously. Here, we focus on the simple single-binding site situation.

As stated earlier, the binding of a ligand molecule (L) to a single site on a macromolecule (M) may be described by the equilibrium equation:



where the binding constant, K_b , (also known as the equilibrium constant or association constant) is a measure of the strength of binding i.e. larger K_b indicating tighter binding.

The dissociation constant, K_d , is the reciprocal of K_b and has the advantage of indicating the free ligand concentration required to produce fifty percent saturation of binding sites.

When ligand and macromolecule solutions are mixed, heat energy is released (or absorbed) in proportion to the extent of binding and to the heat of binding. Hence, the heat released per mole of macromolecule (Q_r) is given by:

$$Q_r = \frac{[ML]\Delta H^o}{[M]_t}$$

where $[M]_t$ is the total concentration of macromolecule and $[ML]$ is the concentration of the complex. So, as the ligand concentration is increased, the observed cumulative enthalpy effect increases to a saturation value equal to the molar heat of binding per site. However, Q_r is also a measure of the proportion of sites occupied with a given

ligand concentration, and may be used to estimate K_b . For simple one to one binding this can be expressed as:

$$Q_r = \frac{K_b[L]\Delta H^o}{1 + K_b[L]}$$

where $[L]$ is the free ligand concentration. This can then be rearranged to give:

$$\frac{1}{Q_r} = \frac{1}{\Delta H^o} + \frac{1}{K_b[L]\Delta H^o}$$

For analysis of weak binding situations where the free ligand concentration does not differ much from the total ligand concentration ($[L]_t$), a double reciprocal plot is convenient for analysis. A plot of $1/[Q_r]$ vs $1/[L]$ yields a straight line with an intercept of $1/\Delta H^o$ and a slope equal to $1/\Delta H^o K_b$. However, this is only appropriate for preliminary estimates and in most cases the ligand binding affinity is too strong therefore, it is not sufficient to assume $[L]=[L]_t$. A preferred method is full least squares fitting of one to one binding data to the complete hyperbolic equation 1.12:

$$Q_r = -\Delta H^o \left[n[M]_t + [L]_t + \frac{1}{K_b} \right] \frac{\left[1 - \left(1 - \frac{4n[M]_t[L]_t}{\left(n[M]_t + [L]_t + \frac{1}{K_b} \right)^2} \right)^{1/2} \right]}{2[M]_t} \quad (1.12)$$

where n is the number of binding sites.

For a system that contains multiple non-interacting binding sites, the heat effect will be:

$$Q_r = \sum_{i=1}^j \frac{n_i \Delta H_i^o [L]_t K_i}{1 + K_i [L]_t}$$

where j is the number of distinct binding sites, K_i , ΔH_i^o , and n_i are the apparent binding constant, enthalpy change and number for each set of sites, respectively.

Both the enthalpy and the binding constant can be obtained from a simple calorimetric binding curve, leading to the calculation of standard free energy (ΔG^o) and entropy changes (ΔS^o).

A range of experiments at different temperatures allows the calculation of ΔC_p from the temperature dependence of ΔH^o . An estimate of the van't Hoff enthalpy of binding, from the same experiments, can be calculated from the temperature dependence of K_b . The number of (identical) binding sites on the macromolecule in simple cases, can be obtained from a comparison of the van't Hoff enthalpy of binding and the directly measured calorimetric enthalpy in a similar way as it is to calculate the size of the cooperative unit from DSC data (see thermal transitions). However, this is rarely achieved since n is determined by fitting the titration curve.

Thermal Transitions

A typical DSC trace of a thermal transition can produce a variety of information. In simple cases, for a two state unfolding process in which equilibrium is between just two possible states, native (N) and unfolded (D):



the mid-point temperature (T_m) of a transition is the temperature at which equal numbers of molecules will be in the native (N) and unfolded (D) state, or taking a more realistic view, it is the temperature at which any molecule will spend exactly half of its time in each state. The T_m may be altered by changing experimental conditions, such as pH, denaturant concentration, the presence of ligands and so forth.

In a DSC experiment the difference in heat uptake between the sample and the reference is measured, therefore the change in heat capacities at constant pressure (C_p) is measured as a function of temperature. Remembering equation 1.9:

$$\Delta H = \int_0^T \Delta C_p(T) dT \quad (1.9)$$

shows that the calorimetric enthalpy (Δh_{cal} per gram) of the transition can be obtained by integration of the DSC trace with respect to temperature. It is normally expressed as enthalpy per mole of protein (ΔH_{cal}):

$$\Delta H_{cal} = \Delta h_{cal} M$$

where M is the molecular weight of the molecule under investigation. This estimate does not depend on any models chosen to fit the experimental data. It is an absolute measure of the extra energy supplied to the sample cell during the transition. However, the choice of baseline used for integration must be carefully selected.

The van't Hoff enthalpy for the transition can be obtained by using the calorimetric signal as a probe to measure the extent of reaction and hence the equilibrium constant as a function of temperature and employing the van't Hoff

equation:

$$\Delta H_{vH} = - \frac{Rd(\ln K)}{d(\frac{1}{T})}$$

The van't Hoff enthalpy is independent of the calorimetric enthalpy, and may be estimated even if the sample concentration or volume is unknown, but rather is calculated per mole. However, it does depend on an assumed model for the unfolding process. This is a useful aspect of the calorimetric technique, not only does it allow us to calculate the size of the cooperative unit but also supplies us with two independent measures of the enthalpy.

Molecules in a protein unfolding transition may act as dimers, trimers or much larger aggregates, therefore this results in the cooperative unit being two, three or more, respectively. In the case when monomers unfold, the cooperative unit is ideally one (a cooperative unit of less than one would tend to indicate either the existence of more than one domain in the protein with different T_m 's or that the unfolding is non-cooperative). The van't Hoff enthalpy measurements based on the calorimetric signal are per mole of cooperative unit, while the calorimetric enthalpy is calculated per mole of monomer, the cooperative unit is simply given by:

$$n = \frac{\Delta H_{vH}}{\Delta H_{cal}}$$

where n is the number of monomers in the cooperative unit.

The van't Hoff enthalpy is derived from the shape of the transition, therefore the cooperativity of the transition can be determined from the shape of the C_p versus T curve. A highly cooperative process is indicated by a sharp transition, while a less inter-molecular cooperativity is shown by a broad transition.

1.5.1 Isothermal Titration Calorimetry

Isothermal microcalorimetry is a non-destructive technique used for direct measurement of the energetics of biological processes in samples at constant temperature in situations where changes may be brought about by mixing two solutions. Of the range of isothermal calorimeters available from various manufacturers, only those originating from Thermometric (previously LKB) and, more recently, from Microcal Inc. have reasonable biophysical applications.

The LKB reaction microcalorimeters (flow and batch versions) are based on designs by Wadsö (Wadsö, 1968; Chen and Wadsö, 1982) using the “heat leak principle”. The direct successor is the Thermometric TAM and is based on the same principle but with improved temperature control and updated electronics. The microcalorimeter has sample and reference vessels (cell) contained within a relatively heavy and carefully temperature-controlled heat sink (Figure 1.4). Solid-state thermopiles are located between each vessel and the heat sink, which generate a voltage proportional to the rate of heat energy flux across them. Sample and reference thermopiles are connected back-to-back in series for differential measurements. For small temperature differences, ΔT , between any cell and the heat sink, both the heat flux across a thermopile and the potential (V) it generates are proportional to ΔT :

$$(dQ/dt) \approx k_1 \Delta T \quad \text{and} \quad V \approx k_2 \Delta T$$

Hence,

$$(dQ/dt) = kV \quad \text{and the heat of reaction} \quad Q = k \int V dt$$

where k is the calibration constant. Integration over a heat pulse or measurement of the voltage offset during a steady-state experiment yields the desired heat.

This measurement system tends to be somewhat slow to equilibrate and use, however has the advantage of simplicity and reliability. The simplicity of these instruments means that they are quite versatile and relatively easy to adapt for special purposes. A number of reaction vessels are available, such as (a) batch cell for single mixing experiments; (b) flow cell for continuous or stopped-flow mixing experiments using either peristaltic pumps, or precision syringe pumps for delivery of samples; (c) titration cell for *in situ* thermal titrations by microsyringe injection of ligand; and (d) photocalorimeter cell for light-induced reactions. Vessels may be glass or inert metals (Au, Pt, tantalum, HastelloyTM etc.) and typical cell volumes are 1 to 10 ml. Titration cells are usually fitted with motor-driven microliter syringes for delivery of ligand into fixed volumes of macromolecule solution. To minimize incorrect heat effects owing to lack of temperature equilibration of injected solutions, syringes may be mounted in the thermostat or, alternatively, incorporate a heat exchanger coil in the delivery tube.

The Omega titration microcalorimeter is a more recent development utilizing a rather more complex active feedback system for determination of reaction heats. The calorimeter consists of two lollipop shaped cells contained within an evacuable adiabatic chamber (to prevent condensation at low temperatures this chamber must be evacuated). Both cells are made of Hastelloy C and have a volume of approximately 1.4 ml (Figure 1.5). Samples are introduced into the cells through long narrow access tubes. The reference cell is only a blank, unstirred and usually filled with water and azide (the azide is to inhibit the growth of micro-organisms). However, the sample cell is fitted with a rotating syringe that acts as both stirrer and delivery device. Injection syringes (25-250 μ l) are precision bore glass with long narrow stainless needles having a stir paddle attached to the extreme end. The injection syringe fits firmly in a low friction bearing assembly which contains an attached timing wheel. This syringe assembly is engaged into the Teflon loading barrel and the timing wheel is attached to a stirring motor. The syringe continuously rotates at 400 rpm during a titration to ensure complete mixing in the cell. The syringe plunger is connected to a stepper motor which controls the volume of sample injected.

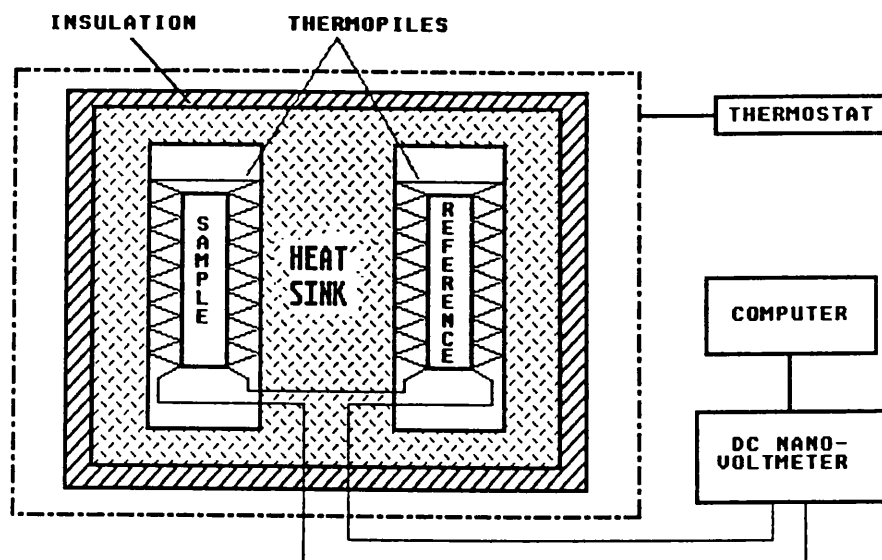


Figure 1.4 Basic layout of a typical isothermal reaction microcalorimeter using the “heat leak” principle.

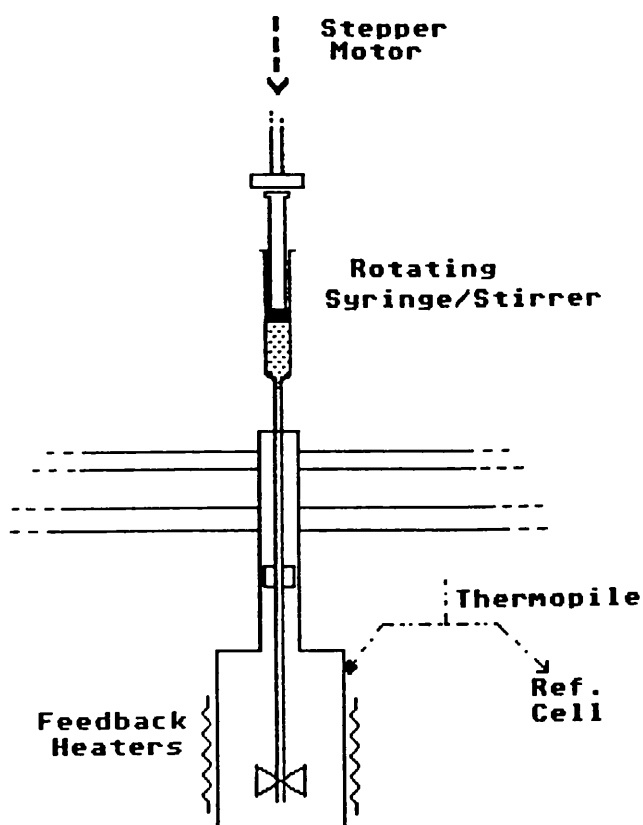


Figure 1.5 Schematic of the Microcal Omega titration calorimeter cell.

Thermopiles are mounted between the sample cell and reference cell, and between the cells and the adiabatic jacket to measure any differences in temperature. A feedback system maintains both cells and jacket at the same temperature through feedback heater currents. The difference in energy required to maintain both cells at the same temperature is a measure of the energetics of processes occurring in the sample, and it is this energy that is recorded as a function of time during an experiment. The temperature of the whole system tends to rise about 0.1°C/h or less as a result of the feedback process, however, is not a significant problem.

The microcalorimeter is PC operated with Microcal Inc. software which allows you to control the syringe stepper motor, set up an injection schedule (number of injections, volume per injection, duration of injection and the time between injections) and collection of all data (analysed by Microcal Origin package). However, choice of temperature, stirring of the syringe and the rotation speed of the syringe are all manually controlled. Comparing the Microcal Omega microcalorimeter with other reaction calorimeters (such as the Thermometric TAM), there is little difference in sensitivity, however the Microcal Omega is faster in operation, resulting in complete titrations in less than an hour.

The Omega microcalorimeter was used extensively in this thesis, therefore more details on typical experiments and models used for analysis are discussed in chapter 2.

1.5.2 Differential Scanning Calorimetry

Differential scanning calorimetry (DSC) can be used to study a range of temperature-induced transitions in biological systems. Typical examples are nucleic acid 'melting', lipid membrane phase transitions and thermal denaturation (unfolding) of proteins. Such experiments can be analysed to give information on the cooperativity/stoichiometry of the process, as well as the midpoint temperature (T_m) and energetics of a transition. The DSC measures the difference in heat uptake between a dilute sample and the solvent as temperature is increased. There are several types of DSC's, the DASM-4 (manufactured by the Bureau of Biological Instrumentation, Russian Academy of Sciences), the Microcal MC-2 (from Microcal Inc.) and a more recent ultrasensitive DSC from Microcal Inc.

The DASM-4 consists of two cells composed of gold or platinum capillary tubing, which are suspended within two adiabatic shields with a 200-junction thermopile between them. The cells have an effective volume of 0.5 ml and are filled through vertical extensions of the capillaries. Electric heaters are used to heat the cells and are in good thermal contact with them. A control circuit adjusts the power to the heaters and is activated by the output of the thermopile between the cells, which maintains them at closely equal temperatures. Thermopiles between the adiabatic shields and the cells activate control circuits, which hold the shield temperatures close to that of the cells. The instrument supplies signals that show the cell temperatures and the differential heating power to the cells. The signals may be registered on an X-Y recorder or may be fed to a computer for subsequent analysis. Each cell is equipped with a second electric heater that is used for calibration purposes. Scan rates of 0.125 to 2.0 K min⁻¹ are available, lower scan rates require modification of the heater circuits.

The DASM-4 and MC-2 are very similar in basic principle and performance, being based on earlier designs by Privalov (Privalov, 1980; Privalov and Potekhin, 1986), although the Microcal system currently offers the advantage of software for data collection and analysis and more sophisticated computer interface.

The Microcal MC-2 calorimeter contains two matched cells, the reference cell and the sample cell. Both cells are of lollipop shape and have a volume of approximately 1.3 ml. They are of a total-fill type and made from tantalum. Samples are introduced into the cells via long narrow access tubes. During an experiment the sample and reference solutions are normally under inert gas pressure to inhibit bubbles.

The cells are suspended in an adiabatic chamber (Figure 1.6) supplied with thermopiles and heaters to measure differences in temperature between the sample and reference cells and between the adiabatic jacket. The feedback control systems monitor temperature differences between cells and the jacket, and supply power to the cell heaters so that the cell temperatures follow the jacket as closely as possible. The difference in power supplied to the sample and reference cells is recorded as a function of temperature, and is directly related to the heat capacity difference between them. The calorimeter is fitted with a circulating water bath for rapid cooling after completion of the scan. The DSC instrument is PC controlled, and both instrument control and data collection (analysed by Microcal Origin package) are from Microcal Inc. software.

The MC-2 calorimeter was used in this thesis to study the thermal unfolding of proteins, therefore more information on performing a typical experiment as well as details on data analysis are discussed in chapter 2.

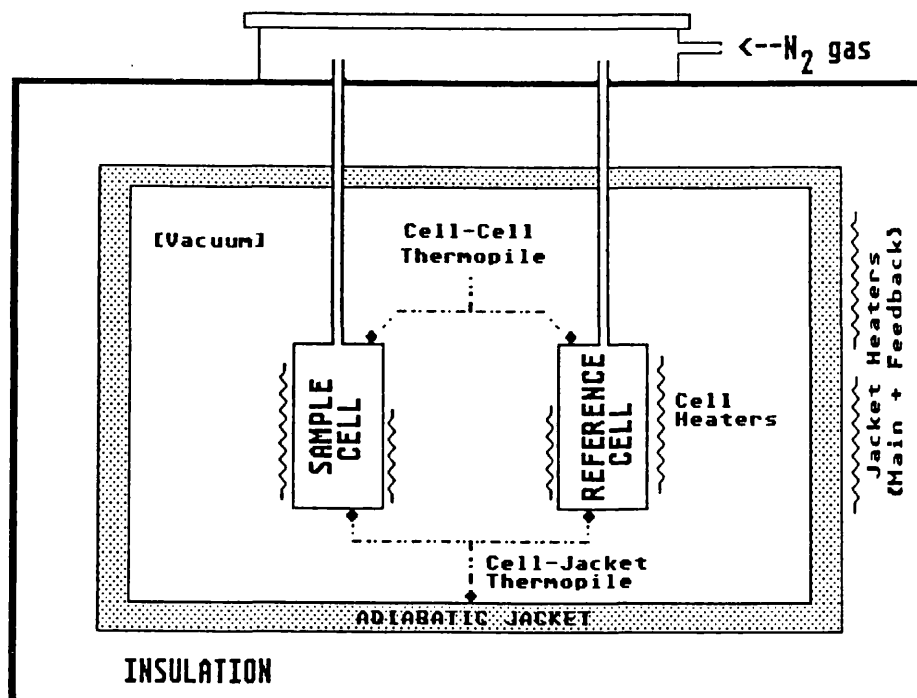


Figure 1.6 Schematic view of the Microcal MC-2 differential scanning calorimeter.

Lastly, the new ultrasensitive DSC from Microcal has a higher sensitivity than the previous MC-2 and its enhanced performance results not only from details of the calorimetric hardware itself, but also from a greater level of involvement of software various aspects of instrument operation and control. In addition, the noise and baseline repeatability are an order of magnitude better than published raw data from other instruments so that high quality results can be obtained on protein solutions, for example, using as little as 50 micrograms of protein in the sample cell (Plotnikov et al., in preparation).

CHAPTER 2

MATERIALS AND METHODS

2.1 Reagents

Dithiothreitol (DTT), D(-) 3-phosphoglyceric acid (3-PG; disodium salt), ethylenediaminetetracetic acid (EDTA; disodium salt), adenosine 5'-triphosphate (ATP; disodium salt) and reduced β -nicotinamide adenine dinucleotide (NADH; disodium salt) were obtained from Sigma Chemical Co.

Triethanolamine (TEA), *p*-nitrophenol and sodium dithionite were obtained from Koch-Light Laboratories, and *p*-aminobenzoic acid and N-methylacetamide (NMA) from Aldrich. All other reagents, unless otherwise stated, were of AnalaR grade, and used without further purification.

Hydroxypropyl- β -cyclodextrin (0.8 avg.subst.) and methyl- β -cyclodextrin (1.8 avg.subst.) were obtained from Aldrich, α -cyclodextrin was from Sigma Chemical Co. Cyclodextrins used for experiments in chapter 3 were dried in vacuo over phosphorous pentoxide.

Amino acids, bovine Zn-insulin (trial fplc, gel filtration and dynamic light scattering experiments indicated no significant protein contaminants in preparations), phosphoglycerate kinase (PGK; yeast, E.C 2.7.2.3), bovine serum albumin (BSA), cytochrome c (horse heart), hemoglobin (bovine blood), lysozyme (hen egg white) and glyceraldehyde-3-phosphate dehydrogenase (GAPDH; rabbit muscle EC 1.2.1.12) were obtained from Sigma Chemical Co. and used without further purification.

2.2 Isothermal Titration Calorimetry

All isothermal titration calorimetry was carried out using a PC controlled Omega titration calorimeter from Microcal Inc. The unstirred reference cell was filled with degassed distilled water containing 0.05% sodium azide, this reference is occasionally re-filled. The preparation of sample solutions was done by simply dissolving in the appropriate buffer (refer to relevant section). Prior to the experiment, sample and buffer solutions were degassed by placing the solution for two or three minutes under vacuum in a small desiccator attached to a water aspirator and mounted on a magnetic stirrer. The sample cell was filled to the top of inlet tube with sample solution, using a syringe fitted with a long narrow gauge Teflon tubing, taking care to avoid air bubbles. After loading, the sample cell was raised to the experimental temperature (usually 25°C, unless otherwise stated) and the system was allowed to reach thermal equilibrium. This could take some time, especially if the sample is substantially cooler than the calorimeter. To accelerate equilibration, the sample could be warmed to the required temperature before loading, by using the heat of the hand around the loading syringe.

The injection syringe was then rinsed and filled with the appropriate solution. Again care was taken in order to ensure that no bubbles were trapped in the syringe. The syringe was mounted in the calorimeter and stirred at a constant 400 rpm. An extra period of final equilibration was allowed (approximately 5 minutes). When a stable, noise-free baseline was obtained, details of the injection schedule (indicated where appropriate in the relevant chapter) was set up and entered into the PC. Appropriate control experiments were carried out under identical conditions. The data were stored and analysed later using the Microcal Origin software package, as described later.

Here isothermal titration calorimetry was used for two types of experiments; (i) competitive inhibition experiments - binding of amino acid enantiomers to cyclodextrins by competition with *p*-nitrophenolate or *p*-aminobenzoic acid; and (ii) dilution experiments - dissociation of insulin in the absence or presence of cyclodextrins. The following sections outline typical experiments, including controls, as well as the various models used for data analysis.

2.2.1 Competitive Inhibition Experiments

Competitive inhibition experiments were carried out at 25 °C with a 250 μ l syringe. In a typical titration, small aliquots (20 μ l) of *p*-nitrophenolate or *p*-aminobenzoic acid dissolved in buffer or buffer/amino acid mix were injected into the calorimeter reaction cell containing cyclodextrin dissolved in identical buffer mixture. In general, to obtain the heat from only the binding reaction, it was essential to carry out, at least in initial trials, a series of control experiments:

Expt.	Contents of sample cell	Contents of syringe
1	cyclodextrin	buffer
2	buffer	<i>p</i> -nitrophenolate or <i>p</i> -aminobenzoic acid
3	buffer	buffer

All calorimetric data were analysed using Origin software. The raw data obtained from a titration experiment is a record of the energy required to maintain the sample and reference cells at the same temperature as a function of time. For each experiment a set of injections was obtained (including control experiments), the peaks were then integrated and control experiments were subtracted (where required) to give corrected heat values. These heats were then plotted as a function of injection number. This data was then fitted to a one set of sites model yielding, n , K and ΔH . In situations of weak binding it was sometimes necessary to fix the number of binding

sites in order to obtain reasonable values for the enthalpy change and the binding constant, since there was insufficient data to define n uniquely.

In this thesis, dissociation constants were used for comparison, which involved taking the reciprocal of the binding constant (K). Also, further analysis was required for titrations in the presence of amino acids to give dissociation constants and enthalpies of formation for complexes of cyclodextrin with amino acids. Both types of data analysis are discussed next.

One Set of Sites Model

The Origin software package contains the following model for the fitting of binding data (Wiseman et al., 1989; Microcal, Incorporation Omega Instruction Manual). For a one to one binding reaction the binding constant (K) is given by the equation:

$$K = \frac{\Theta}{(1 - \Theta)[L]} \quad (2.1)$$

where Θ is the fraction of sites occupied by the ligand. The free ligand concentration, $[L]$, and the total ligand concentration, $[L]_t$, can be related by the equation:

$$[L] = [L]_t - n\Theta[M]_t \quad (2.2)$$

where n and $[M]_t$ are the number of binding sites and the bulk macromolecule concentration, respectively. Combining equations 2.1 and 2.2 gives:

$$\Theta^2 - \Theta \left[1 + \frac{[L]_t}{n[M]_t} + \frac{1}{nK[M]_t} \right] + \frac{[L]_t}{n[M]_t} = 0 \quad (2.3)$$

The total heat content (Q) of the solution is equal to:

$$Q = n\Theta [M]_t \Delta H V_o \quad (2.4)$$

where V_o is the active cell volume and ΔH is the enthalpy of binding. Solving the equation 2.3 for Θ and then substituting this into equation 2.4 gives:

$$Q = \frac{n[M]_t \Delta H V_o}{2} \left[1 + \frac{[L]_t}{n[M]_t} + \frac{1}{nK[M]_t} - \sqrt{\left(1 + \frac{[L]_t}{n[M]_t} + \frac{1}{nK[M]_t} \right)^2 - \frac{4[L]_t}{n[M]_t}} \right] \quad (2.5)$$

This equation can be solved for Q_i given values for n , K and ΔH at the end of the i th injection. The calorimeter measures the differences in heat between the i th and $(i-1)$ th injection:

$$\Delta Q_i = Q_i - Q_{i-1}$$

where ΔQ_i is the difference in heat, Q_i and Q_{i-1} are the heats of the i th and $(i-1)$ th injections, respectively. Initial guesses of the values of the fitting parameters (n , K and ΔH) are made and substituted into equation 2.5 to find values for ΔQ_i for each injection. These calculated ΔQ_i values are compared with the experimental values and new values of the fitting parameters are obtained using statistical methods until no further significant improvement in fit occurs with continued iteration.

Further Analysis of Competitive Inhibition Data

In the simple case of 1:1 complex formation between cyclodextrin (C) and ligand (L) where $C + L = CL$; ΔH_o , the dissociation constant is expressed as $K_o = [C][L]/[CL]$. However, in the presence of a competitive inhibitor (I) where $C + I = CI$; ΔH_I , the dissociation constant for the competing complex is $K_I = [C][I]/[CI]$.

For calorimetric titrations which involved the titration of cyclodextrin with *p*-nitrophenolate or *p*-aminobenzoic acid (ligand) in the presence of amino acid enantiomers (inhibitor) the following equations were used to calculate K_I and ΔH_I .

The apparent dissociation constant (K_{app}) for the binding of ligand in presence of a fixed concentration of inhibitor is as follows:

$$K_{app} = \frac{([C] + [CI])[L]}{[CL]} = \frac{[C][L]}{[CL]} \left(1 + \frac{[CI]}{[C]} \right) = K_o \left(1 + \frac{[I]}{K_I} \right)$$

this can be rearranged so the dissociation constant for the competing complex (K_I) equals:

$$K_I = \frac{[I]}{\frac{K_{app}}{K_o} - \frac{K_o}{K_o}} = \frac{[I]K_o}{K_{app} - K_o} \quad (2.6)$$

The apparent enthalpy of titration (ΔH_{app}) is as follows:

$$\Delta H_{app} = (1-x)\Delta H_o + x(\Delta H_o - \Delta H_I) = \Delta H_o - x \cdot \Delta H_I$$

where x is equal to the fraction of cyclodextrin present as CI complex:

$$x = \frac{[CI]}{[C] + [CI]} = \frac{1}{1 + \frac{[C]}{[CI]}} = \frac{1}{1 + \frac{K_I}{[I]}} = \frac{[I]}{[I] + K_I}$$

therefore,

$$\Delta H_{app} = \Delta H_o - \left(\frac{[I]}{[I] + K_I} \right) \Delta H_I$$

and this can be rearranged to give:

$$\Delta H_I = (\Delta H_o - \Delta H_{app}) \left(\frac{[I] + K_I}{[I]} \right) = (\Delta H_o - \Delta H_{app}) \left(1 + \frac{K_I}{[I]} \right) \quad (2.7)$$

2.2.2 Insulin Dilution Experiments

Calorimetric dilution experiments were carried over a range of temperatures with a 250 μ l injection syringe and 400 rpm stirring. In a typical dilution experiment small aliquots (10-20 μ l) of concentrated insulin, dissolved in buffer or buffer/cyclodextrin mix, were injected into the calorimeter reaction vessel containing the identical buffer mixture. Integrated heat pulse data, after correction for mixing controls done separately under identical conditions, were analysed by non-linear regression in terms of a simple monomer-dimer equilibrium model (not available in Microcal Origin). This gave the apparent equilibrium constant (K_{diss}) and enthalpy of dissociation (ΔH_{diss} per mole dimer).

Dimer Dissociation Model

Heats of dilution data for a simple monomer-dimer system were analysed as follows (McPhail and Cooper, 1997). If only monomer or dimer states of (macro)molecule I are possible:



the equilibrium concentration of monomers is given by:

$$[I] = \{(1 + 8K_{\text{dim}}C)^{1/2} - 1\}/4(K_{\text{dim}}) \quad (2.8)$$

where C is the total concentration of I, expresses as monomer:

$$C = [I] + 2[I_2] \quad (2.9)$$

In a dilution experiment the heat change (δq) is measured when a small volume (δV) of concentrated solution (concentration C_0) is injected into the calorimeter cell (volume V_0) containing initially buffer but, for later injections, more dilute solution. The heat arises from dimers present in the higher concentration solution that dissociate upon entering the lower concentration environment.

For the i th injection of a series the observed heat is given by:

$$\delta q_i = \Delta H_{\text{dim}}\{V_0([I_2]_i - [I_2]_{i-1}) - V([I_2]_0 - [I_2]_{i-1})\} \quad (2.10)$$

where $[I_2]_0$, $[I_2]_i$ and $[I_2]_{i-1}$ are the dimer concentrations in the original (syringe) solution and in the calorimeter cell after the i th and $(i-1)$ th injections: total concentrations C_0 , C_i and C_{i-1} , respectively.

Equations 2.8 to 2.10 are used in standard non-linear regression (least squares procedures to fit experimental dilution data and obtain estimates of K_{dim} and ΔH_{dim} . For insulin dissociation experiments, these values were converted into K_{diss} and ΔH_{diss} .

2.2.3 Calibration

Standard reactions can be used to calibrate the complete system including the injecting and sample volumes. Simple calibration reactions involve the addition of standardized aqueous HCl to dilute Tris or NaOH solutions. For example, using the heat of ionization data from Grenthe et al. (1970) each 5 μl injection of 0.1 M HCl into excess Tris Base or NaOH solution should give exothermic heat effects of 5.67 mcal and 6.6 mcal, respectively. However, when only the calibration of thermal sensitivity is required the standard heater resistors supplied with most instruments are sufficient.

2.3 Differential Scanning Calorimetry

2.3.1 Thermal Stability Studies

All DSC was carried out using the Microcal MC-2 ultra sensitive calorimeter, fitted with an EM Electronics N2a DC nanovoltmeter. The DSC was PC operated, which was also used for data collection. A nominal scan rate of 60 $^{\circ}\text{C}/\text{h}$ and a “filter” setting of 15 s was applied (this refers to data acquisition and averaging time e.g. a typical filter setting of 15 s will record and store averaged temperature and energy data every 15 s).

The preparation of sample solutions was done by simply dissolving 1-2 mg/ml of protein in buffer or buffer/cyclodextrin mix. Identical buffer was used for reference and baseline scans. Both sample and buffer solutions were degassed before loading (to avoid air bubble formation at higher temperatures) by placing the solution for two or three minutes under vacuum in a small desiccator attached to a water aspirator and mounted on a magnetic stirrer.

Both cells of the calorimeter were rinsed at least five times with buffer prior to filling. Filling of the cells was carried out using a small syringe fitted with a long narrow gauge Teflon tubing. It is critically important that there are no bubbles, either in the cells or in the inlet tube, therefore extreme care was taken to ensure that the syringe and tubing were free from any air bubbles. One or more buffer baseline scans were obtained by filling both sample and reference cells with the appropriate buffer and scanning in the normal manner. Multiple scans, which could be done overnight, were necessary when the machine was unused for a period of time.

The protein sample solution was then loaded into the sample cell. The small amount of buffer left in the cell prior to filling leads to a slight dilution of the sample, however this is avoided by rinsing the cell with a little of the sample and then mixing this with the rest of the sample or discarding. A little of the sample was retained for subsequent protein concentration estimation, using UV/visible spectrophotometry. During DSC a pressure head of 1-2 atm of nitrogen was maintained in order to prevent the sample boiling and to suppress bubble formation.

The procedure for obtaining a thermogram, both for the sample and the buffer baseline, was as follows. The scan parameters were selected and entered into the computer. These consist of: number of scans, initial temperature (20 °C), final temperature (100 °C, although it is possible either to stop the scan before this temperature or allow the scan to continue, up to maximum of 110 °C if necessary, at any point during the scan), scan rate, filter (as indicated above these were normally

set to 60 degrees/hour and 15s, respectively) and file name(s). Prior to starting the scan, the system was allowed to equilibrate. The time involved depends on various factors, including the temperature of the sample and buffer when loaded and the temperature at which the scan is required to start, this generally takes 10-20 minutes. The start of the active scan requires the temperature difference between cells and the adiabatic jacket to be less than 1 °C. A further, 5 minute, period of equilibration, during which the feedback system (refer to section 1.5.2) is used to finely balance the temperatures, preceded the scan.

2.3.2 Analysis of DSC Data

DSC data were analysed using Microcal Origin software package. The software collects differential thermal energy data as a function of time i.e. a typical data file will consist of the time, cell temperature and differential energy input into the cells since the last data point, at intervals determined by the filter setting. Conversion of differential heat capacity requires division by the mean scan rate at each point.

Due to variations in total heat capacity and heat losses in the instrument, the DSC scan rate varies slightly over the temperature range. This is displayed as a curvature of the DSC trace. Most of the nonlinearities and artefacts arising from instrumental problems, such as the mismatch of cell volume are eliminated by subtracting a buffer baseline.

It is usual for the data to be normalized to different excess heat capacity per mole by dividing by the total amount of sample in the cell. Origin software allows for this and has the cell volumes set as a default, the software also enables the operator to enter the sample concentration. A non-two state model based on original work by Sturtevant, Brandts, and Privalov (Sturtevant, 1974, 1987; Jackson and Brandts, 1970; Privalov and Potekhin, 1986) was fitted to this normalized experimental data

using the facility built into the software package. The model used is based upon the van't Hoff equation:

$$\left(\frac{\partial \ln K}{\partial T} \right)_p = \frac{\Delta H_{vH}}{RT^2} \quad (2.11)$$

where ΔH_{vH} is the van't Hoff heat change for the reaction which corresponds to the heat change for the cooperative unit which actually participates in the reaction.

Normally it is understood that the protein is composed of a number of structural domains A, B, C... each of which is involved independently in a transition between the folded and unfolded forms (e.g. $A=A'$, $B=B'$,...). Equilibrium constants are expressed in terms of fractions e.g.

$$K_A = \frac{f_{A'}}{f_A}$$

where K_A is the equilibrium constant for the unfolding of the A domain, $f_{A'}$ and f_A are the fractions of the unfolded and folded A, respectively. Remembering that $f_{A'}$ and f_A are simply related as follows:

$$f_A = 1 - f_{A'}$$

The total molar enthalpy for the system H is given by:

$$H = H_N + f_{A'}\Delta H_A + f_{B'}\Delta H_B + \dots \quad (2.12)$$

where H_N is the total enthalpy of the native state, to which all measurements of ΔH

are relative. The total molar heat capacity is the temperature derivative of equation 2.12:

$$C_p = C_{pN} + \left[f_{A'} \Delta C_{pA} + \Delta H_A \left(\frac{\partial f_{A'}}{\partial T} \right) \right] + \dots \quad (2.13)$$

where C_{pN} is the molar heat capacity of the totally folded state. Substituting equilibrium constants in place of fractional concentrations in equation 2.13 and then carrying through the differentiation gives:

$$\left(\frac{\partial f_{A'}}{\partial T} \right) = \left(\frac{K_A}{(1 + K_A)^2} \right) \left(\frac{\partial \ln K_A}{\partial T} \right) \quad (2.14)$$

By substituting equations 2.11 and 2.14 into equation 2.13 gives:

$$C_p = C_{pN} + \left[\frac{K_A \Delta C_{pA}}{1 + K_A} + \frac{K_A \Delta H_{vH} \Delta H_A}{(1 + K_A)^2 RT^2} \right] + \dots \quad (2.15)$$

If we assume each transition is two-state, then the van't Hoff enthalpies become equal to the calorimetric enthalpies. If we also assume that C_{pN} is a linear function of temperature then equation 2.15 gives:

$$C_p(T) = B_0 + B_1 T + \left[\frac{K_A(T) \Delta C_{pA}}{1 + K_A(T)} + \frac{K_A(T) \Delta H_A(T)^2}{(1 + K_A(T))^2 RT^2} \right] + \dots \quad (2.16)$$

where $C_p(T)$, $K_A(T)$ and $\Delta H_A(T)$ are the heat capacity, equilibrium constant and enthalpy change at temperature T , respectively. This can be expressed in terms of the T_m of the transition as follows:

$$\Delta H_A(T) = \Delta H_{mA} + \Delta C_{pA} (T - T_{mA}) \quad (2.17)$$

and then integrating the van't Hoff equation (2.11) from T_{mA} to T gives:

$$K_A(T) = \exp \left\{ \frac{-\Delta H_{mA}}{RT} \left(1 - \frac{T}{T_{mA}} \right) - \frac{\Delta C_{pA}}{RT} \left(T - T_{mA} - T \ln \frac{T}{T_{mA}} \right) \right\} \quad (2.18)$$

By substituting equations 2.17 and 2.18 into equation 2.16 this gives the model to which DSC data can be fitted. To initiate curve fitting with Origin, the operator gives initial guesses and the model fits by non linear least squares until there is no further improvement in the fit.

When all heat capacity changes are assumed to be zero, then equations 2.16-2.18 are simplified to:

$$C_p(T) = \frac{K_A(T)\Delta H_A(T)^2}{(1 + K_A(T))^2 RT^2} + \dots$$

$$K_A(T) = \exp \left\{ \frac{-\Delta H_{mA}}{RT} \left(1 - \frac{T}{T_{mA}} \right) \right\}$$

Curve fitting is again by non linear least squares.

2.3.3 Calibration: Temperature

For temperature calibration, standard samples are available from Microcal. These consist of sealed steel capillaries containing small samples of pure hydrocarbons of known melting temperature, which are inserted into water filled DSC cells. The very sharp melting transitions of these samples are readily observed and give a suitable check on temperature axis calibration ($\pm 0.1^\circ\text{C}$).

2.3.4 Calibration: Excess Heat Capacity

Occasional checks on the calibration of the excess heat capacity measurements were necessary. For this purpose, electrical calibration is satisfactory. With both cells filled with water, a small current, up to a maximum equivalent of 50 mJ/min, is passed through the calibration heater, for 4 minutes, and the amount of heat supplied by the feedback system to maintain cell temperature equilibrium is measured in the usual manner. The height and area of such calibration pulses should agree with the values entered, after subtraction of a water/water baseline.

2.4 Spectral Titration Experiment

Solutions of *p*-nitrophenolate (*ca.* 5×10^{-5} M), with and without known concentrations of phenylalanine enantiomers (inhibitor), were titrated with increasing concentrations of α -cyclodextrin (0-1.6 mM), and difference spectra over the range 330-520 nm were recorded at each addition (Shimadzu UV-160A spectrophotometer, with thermostatted cells). The maximal change in *p*-nitrophenolate absorbance occurring at 370 nm was used for computer binding parameters.

In spectral titrations the change in absorbance, ΔA , of *p*-nitrophenolate at 370 nm when bound to α -cyclodextrin was used as a probe of α -cyclodextrin-nitrophenolate complex concentration. In order to obtain dissociation constants, plots of $1/\Delta A$ versus $1/[\text{cyclodextrin}]_{\text{total}}$ in the absence and presence of a known concentration inhibitor were carried out. This gave a straight line in which the slope divided by the intercept yields K_O (absence) and K_{app} (presence). Further calculations were necessary to give dissociation constants for complexes of cyclodextrin with phenylalanine enantiomers. This was done by using equation 2.6 (as for calorimetry data).

2.5 UV Absorption of Amino Acids

Where the extinction coefficient (ϵ) is known it is possible to measure the concentration of aromatic amino acid samples by UV absorbance according to the Beer-Lambert law (other amino acid concentrations were estimated by weight). The following wavelengths and molar extinction coefficient were used (Dawson et al., 1986).

Amino acid	λ_{\max} (nm)	Molar extinction coefficient ($M^{-1} \text{ cm}^{-1}$)
Phenylalanine	257.5	195 ^s
Tyrosine	293.5	2330 [†]
Tryptophan	278.0	5550 [*]

Table 2.1 Spectroscopic properties of aromatic amino acids. ^s pH 3.5, 7.4 and 11; [†] pH 11 only; ^{*} pH 3.5 and pH 11.

2.6 UV Absorption of Proteins

Protein concentrations were confirmed by UV absorbance measurements on diluted aliquots. The protein concentration can be calculated according to the Beer-Lambert law. The following extinction coefficients and molecular weights were applied.

Protein	ϵ_{280}^{280} mg/ml	Molecular weight
Insulin	1.0 [‡]	6,000
Lysozyme	2.65 [†]	14,500
PGK	0.495 ^s	45,000

Table 2.2 Summary of extinction coefficients used. [‡] Porter, 1953; [†] McKenzie and White, 1991; ^s Bucher, 1955.

The concentration of cytochrome c (mol wt 12,384) was determined using a value of 11100 M^{-1} for the molar extinction coefficient at 530 nm (Margoliash and Frohwirt, 1959).

2.7 Measurement of *p*-Nitrophenolate and *p*-Aminobenzoic Acid Concentrations

Concentrations of *p*-nitrophenolate (mol wt 139.11) at pH 11 were verified by UV absorbance measurements on diluted aliquots, assuming a molar extinction coefficient (ϵ_{400}) of 18197 M^{-1} (Millieresi and Ruchkin, 1974). At pH 7.4, *p*-nitrophenolate concentrations were estimated by weight. Concentrations of *p*-aminobenzoic acid (mol wt 137.14) at pH 3.5 were also estimated by weight.

2.8 PGK Assay

PGK activity was measured using the coupled assay of Scopes (1975). Activity was assayed in the direction of 1,3-DPG formation by coupling the PGK reaction to the reaction catalysed by GAPDH as displayed in Figure 2.1. The rate of reaction was followed by monitoring the decrease in absorbance at 340 nm as a result of oxidation of NADH.

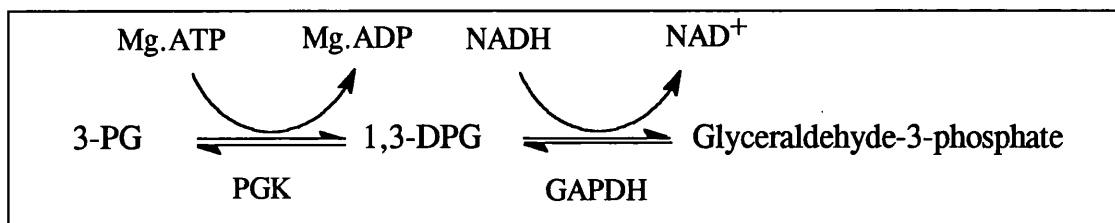


Figure 2.1 Reaction diagram for PGK assay.

The stock assay buffer comprised of 30 mmol l^{-1} (TEA), 50 mmol l^{-1} KCl, 5 mmol l^{-1} MgSO₄, 0.2 mmol l^{-1} EDTA and 10 mmol l^{-1} 3-PG, adjusted to pH 7.5 with HCl. This buffer could be stored for several weeks at 4°C .

The assay mix was prepared from the stock assay buffer by adding BSA and NADH to give concentrations of 0.2 mg ml^{-1} and 0.1 mmol l^{-1} , respectively. This mixture was prepared daily and was stable for several hours at 4°C . Solutions of ATP and GAPDH were prepared in 30 mmol l^{-1} TEA, pH 7.5 at concentrations of 50 mmol l^{-1} and 1 mg ml^{-1} , respectively. These solutions could be stored frozen at -20°C for several months. A dilute solution of PGK was prepared using 30 mmol l^{-1} TEA, pH 7.5 (containing 1 mM DTT).

The following reagents were added to a microcuvette of 1 cm path length, 0.88 ml assay mix, $40 \text{ }\mu\text{l}$ stock GAPDH solution and $80 \text{ }\mu\text{l}$ stock ATP solution. The microcuvette was placed in the thermostat block of the spectrophotometer (Shimadzu UV-160A) and allowed to reach required temperature (25°C). A baseline was measured at 340 nm to check for contaminating enzyme, then $25 \text{ }\mu\text{l}$ of a dilute PGK solution was added. The decrease in absorbance was measured as a function of time. Subsequent trials involved the measurement of dilute PGK solutions heated to 63°C for 15 minutes in the presence of various cyclodextrins, NMA, both separately and together in mixtures of various concentrations. Solutions were allowed to cool for up to 1 hour before activity was measured. PGK activity was calculated (where required) using a millimolar extinction coefficient of 6.22 cm^{-1} for NADH at 340 nm as follows:

$$\text{Number of enzyme units added to cuvette} = \Delta A_{340} / 6.22$$

where ΔA_{340} is the change in absorbance at 340 nm per minute (initial rate of reaction). One unit of activity is defined as $1 \text{ }\mu\text{mol}$ of NADH oxidised min^{-1} (Scopes, 1975). The approximate specific activity is equal to the number of enzyme unit per milligram of enzyme.

CHAPTER 3

INTERACTION OF CYCLODEXTRINS WITH AMINO ACID ENANTIOMERS

3.1 Introduction

The ability of cyclodextrins to form inclusion complexes with a variety of guest compounds has been extensively utilized in many industrial, pharmaceutical, agricultural and other related applications (Szejtli, 1982; Saenger, 1980). Cyclodextrins have also been extensively employed in separation science. They have been shown to be extremely useful as chiral selectors for the separation of enantiomers by various types of chromatography (Hinze et al., 1985; Armstrong et al., 1987; Li and Purdy, 1991; Bhushan and Joshi, 1993) and capillary electrophoresis (Okafo and Camilleri, 1993; Copper et al., 1994; Sun et al., 1994).

In many fields, the resolution of amino acid enantiomers has been considered important and widely studied because of their simplicity of structure, ease of availability and commercial significance. The industrial manufacture of chiral amino acids is of great importance to the pharmaceutical industry, the food industry, animal husbandry and poultry farms because they all require generally the L-isomer of the corresponding amino acid. In addition, to the industrial importance of amino acids, *in vitro* and *in vivo* analysis of racemic amino acids is also of great significance because racemization of amino acids may take place even at neutral pH, in the metabolically stable proteins of living mammals. As a result of racemization reaction the protein function or structure may be altered. Optically pure amino acids are also required for the synthesis of several chiral reagents, catalysts and physiologically active substances including antibiotics.

In this thesis, with a view towards possible applications in chiral separation technologies, enantiomeric discrimination in complexes between cyclodextrins and a wide range of α -amino acids was investigated using titration calorimetry.

3.2 Results

Previous researchers have used competitive spectrophotometry for studying the formation of complexes between cyclodextrins and guest compounds (Cooper and MacNicol, 1978; Horsky and Pitha, 1994). Here, competitive titration calorimetry was used to determine dissociation constants and enthalpies of complex formation for complexes of cyclodextrins with amino acid enantiomers. This strategy was adapted because, in most cases, cyclodextrin-amino acid complex formation is too weak to be determined by direct calorimetric titration. Calorimetric experiments consisted of titrations of cyclodextrin with a competing reagent in the absence and presence of a fixed amino acid concentration. The competing reagent for experiments at pH 11 was *p*-nitrophenolate because it had been previously used by Cooper and MacNicol (1978). Also, it is known to form complexes with α -cyclodextrin and β -cyclodextrin (Connors, 1987; Buvári and Barcza, 1988). For experiments at pH 3.5, *p*-aminobenzoic acid was used. Buffers used were 0.1 M Na-phosphate/NaOH pH 11 or 0.1 M Na citrate/citric acid pH 3.5. Because the buffering capacity of 0.1 M Na-phosphate/NaOH was rather low, it was necessary to readjust the pH of *p*-nitrophenolate and amino acid solutions to pH 11.

All experiments were performed at 25°C with an injection schedule usually of 12 injections of 20 μ l at 3 minute intervals. In general, injection of *p*-nitrophenolate or *p*-aminobenzoic acid into the cyclodextrin solution resulted in exothermic heat effects which decreased in size during the titration until the cyclodextrin became saturated. At this point, heat effects were still observed but these were similar to the heat effects observed on titration of buffer with *p*-nitrophenolate or *p*-aminobenzoic acid. Typical datasets for such titrations are shown in Figures 3.1 and 3.2. All controls were insignificant compared to titration experiments, as a result they were neglected. Also, initial experiments were normally repeated several times, however they appeared to be consistent. As a result, subsequent experiments showing chiral discrimination were repeated, while other experiments were carried out only the once.

Experimental data in Figure 3.1 and subsequent data in this chapter have been analysed using Origin's one set of sites model (refer to section 2.2.1). Further analysis using equations 2.6 and 2.7 was required for titrations in the presence of amino acid to yield dissociation constants (K_{diss}) and enthalpies of formation (ΔH) for complexes of cyclodextrin with amino acids.

Table 3.1 summarizes the results of complexes between *p*-nitrophenolate and α -cyclodextrin, β -cyclodextrin, methyl- β -cyclodextrin and hydroxypropyl- β -cyclodextrin. The apparent dissociation constants of these complexes are close to those reported for *p*-nitrophenol, pH 7.4 (Horsky and Pitha, 1994); this is understandable because pK_{D} values of 6.90-7.15 for the dissociation constant of *p*-nitrophenol were reported (Serjeant and Dempsey, 1979). Thus *p*-nitrophenolate should be the major species at the pH value of pH 7.4. Also, the dissociation constant for the complex between *p*-nitrophenolate and α -cyclodextrin agrees well with previous determinations (Cooper and MacNicol, 1978; Cramer et al., 1967).

Results of complexes between *p*-aminobenzoic acid and α -cyclodextrin, and β -cyclodextrin are shown in Table 3.2. The apparent dissociation constant for the complex between *p*-aminobenzoic acid and β -cyclodextrin was very weak and as a result β -cyclodextrin was unable to be used for competitive inhibition experiments at pH 3.5.

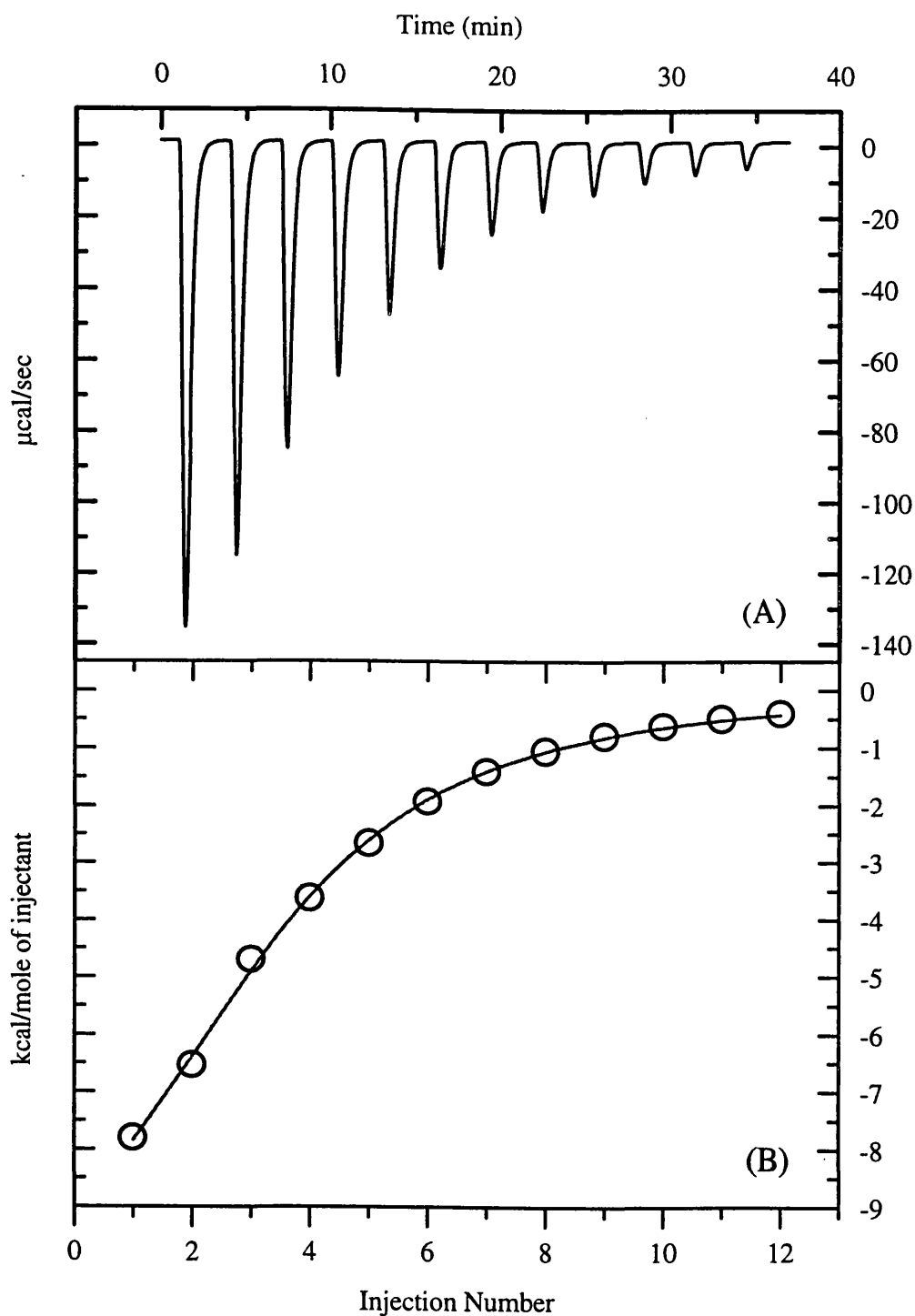


Figure 3.1 Calorimetric titration of α -cyclodextrin (1.5 mM) with *p*-nitrophenolate (31 mM), pH 11 (25°C). (A) Raw data for 12 x 20 μ l injections. (B) Integrated heat effects, $K_{\text{diss}}=0.63$ mM, $\Delta H = -51.5$ kJ/mol.

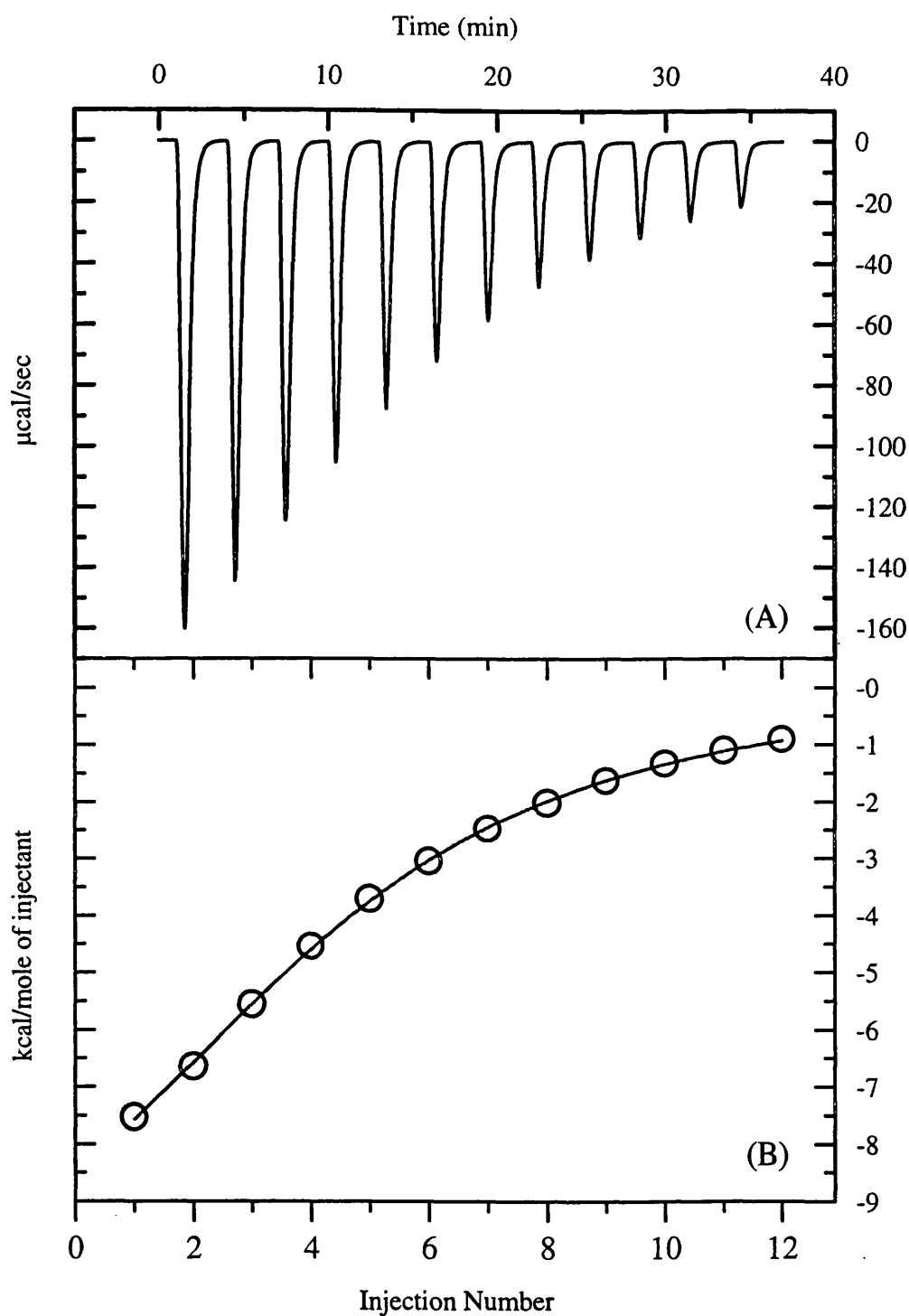


Figure 3.2 Calorimetric titration of α -cyclodextrin (3.1 mM) with *p*-aminobenzoic acid (39 mM), pH 3.5 (25°C). (A) Raw data for 12 x 20 μ l injections. (B) Integrated heat effects, $K_{\text{diss}}=1.39$, $\Delta H=-53.3$ kJ/mol.

Cyclodextrin	K_{diss}	$-\Delta H/\text{kJ}$	$-\Delta G^0/\text{kJ}$	$\Delta S^0/\text{J K}^{-1}$
	mM	mol^{-1}	mol^{-1}	mol^{-1}
α -	0.62 (0.05)	51.8 (5.5)	18.3	-112
β -	2.06 (0.22)	18.6 (1.3)	15.3	-11
methyl- β -	1.54 (0.06)	17.0 (0.3)	16.0	-3
hydroxypropyl- β -	1.92 (0.08)	17.4 (1.0)	15.5	-6

Table 3.1 Thermodynamic data for the binding of *p*-nitrophenolate to cyclodextrins, pH 11, 25°C. Standard deviations in parentheses.

Cyclodextrin	K_{diss}	$-\Delta H/\text{kJ}$	$-\Delta G^0/\text{kJ}$	$\Delta S^0/\text{J K}^{-1}$
	mM	mol^{-1}	mol^{-1}	mol^{-1}
α -	1.46 (0.1)	56.0 (4.1)	16.2	-134
β -	3.9	7.1	13.7	22

Table 3.2 Thermodynamic data for the binding of *p*-aminobenzoic acid to α -cyclodextrin and β -cyclodextrin, pH 3.5, 25°C. Standard deviations in parentheses.

3.2.1 α -Cyclodextrin

Many studies of complexes between α -cyclodextrin and aromatic amino acids under various conditions have been reported (Lewis and Hansen, 1973; Wood et al., 1977; Cooper and MacNicol, 1978; Matsuyama et al., 1987; Lipkowitz et al., 1992; Horsky and Pitha, 1994). Here, initial experiments consisted of studying all twenty naturally occurring amino acids and their corresponding enantiomer with α -cyclodextrin at high pH to investigate any enantioselective binding. However, experiments indicate that the majority of amino acids show no complexation with α -cyclodextrin or in some cases, calorimetric effects were too small to determine data accurately, such amino acids are listed below.

Alanine	Cysteine	Histidine*	Threonine
Arginine	Glutamic acid	Lysine*	Tyrosine*
Asparagine	Glutamine	Proline	Valine
Aspartic acid	Glycine	Serine	

* calorimetric effects too small to determine data accurately.

Thermodynamic data for amino acids that form inclusion complexes are summarized in Table 3.3. Also, examples of calorimetric data obtained for such experiments are shown in Figures 3.3 and 3.4. Typical concentrations used to observed such effects were: 25-50 mM for *p*-nitrophenolate, 1.5-2.3 mM for α -cyclodextrin and 30-100 mM for amino acids.

Guest	Enantiomeric form	K_{diss} mM	$-\Delta H/\text{kJ}$ mol^{-1}	$-\Delta G^{\circ}/\text{kJ}$ mol^{-1}	$\Delta S^{\circ}/\text{J K}^{-1}$ mol^{-1}
Phenylalanine	L	62.4 (1.1)	20.0 (2.8)	6.9	-44
	D	48.9 (3.2)	19.7 (3.0)	7.5	-41
Tryptophan	L	110.9	51.5	5.4	-155
	D	110.2	57.3	5.5	-174
Leucine	L	29.6	11.3	8.7	-9
	D	26.4	10.0	9.0	-3
Isoleucine	L	46.0	38.1	7.6	-102
	D	37.9	39.3	8.1	-105
Methionine	L	41.2	38.9	7.9	-104
	D	43.5	43.9	7.8	-121

Table 3.3 Thermodynamics of complexes between amino acids and α -cyclodextrin at pH 11 (25 °C) by competition with *p*-nitrophenolate. Standard deviations in parentheses.

Results appear to indicate that only enantiomers of phenylalanine show a significant difference in dissociation constants. Such chiral discrimination is also observed in spectral competitive inhibition experiments at pH 11, as shown in Figure 3.5. Dissociation constants obtained by this method are 0.54 mM, 60.8 mM and 44.8 mM, for complexes between α -cyclodextrin and *p*-nitrophenolate, D- and L-phenylalanine, respectively. These values are consistent with those published by Cooper and MacNicol (1978). Also, the dissociation constant for L-phenylalanine agrees with Horsky and Pitha (1994), even though different experimental methods and conditions were used.

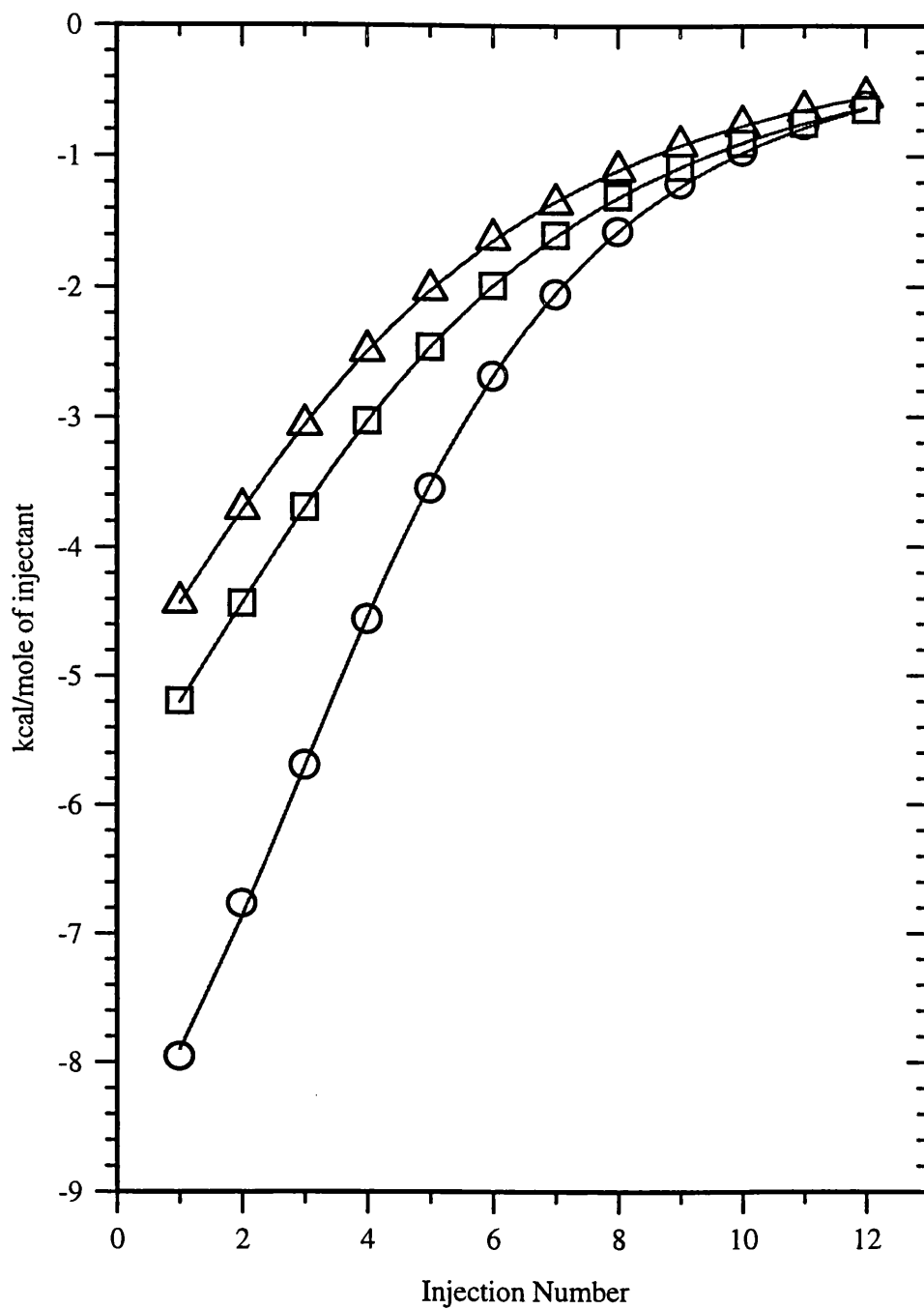


Figure 3.3 Exothermic heats effects for the titration of α -cyclodextrin with *p*-nitrophenolate in the absence (O) or presence (Δ D and \square L-phenylalanine, [50 mM]) of competing enantiomers, pH 11 (25°C).

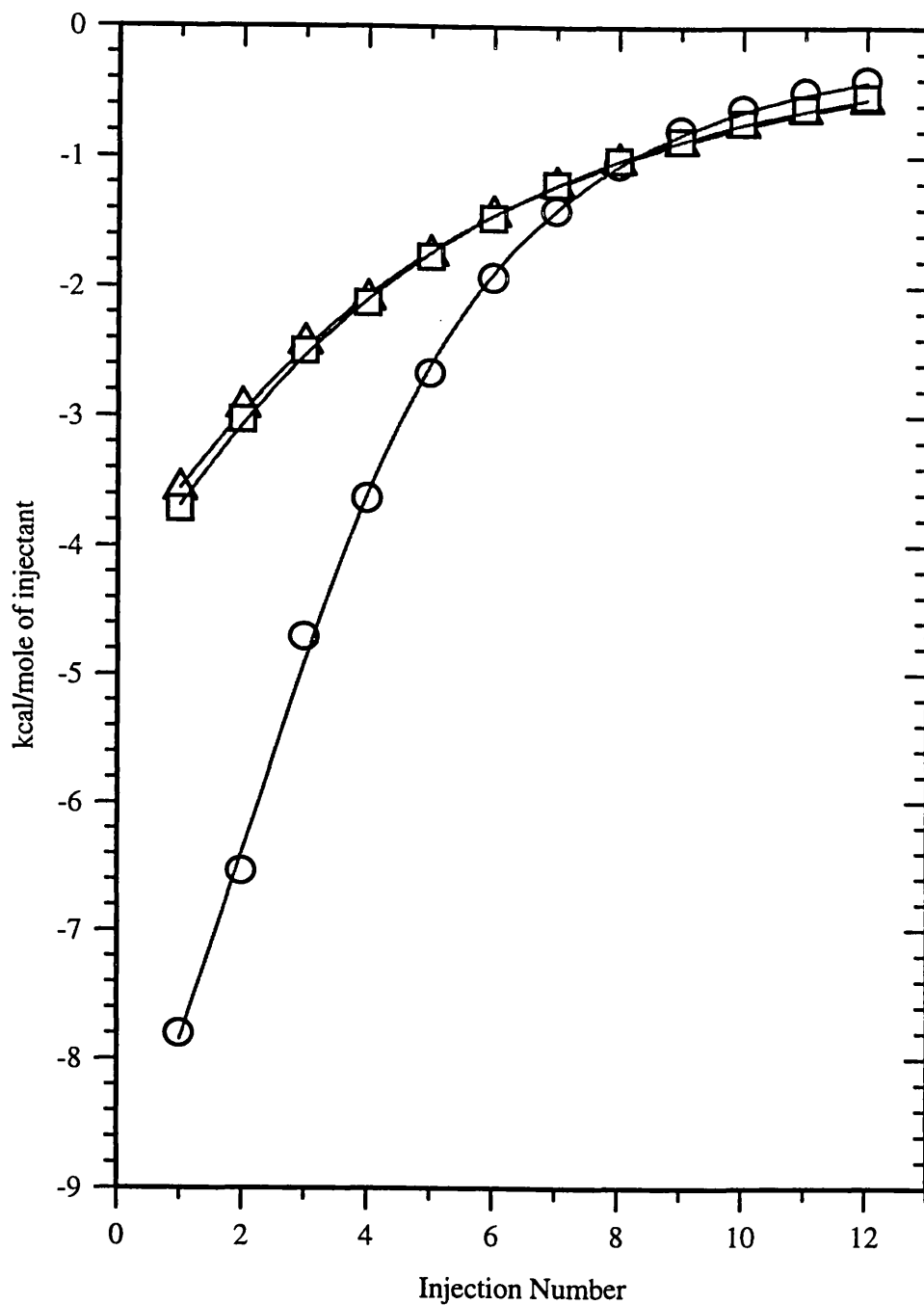


Figure 3.4 Exothermic heats effects for the titration of α -cyclodextrin with *p*-nitrophenolate in the absence (O) or presence (Δ D and \square L-leucine, [69 mM]) of competing enantiomers, pH 11 (25°C).

Amino acids that appeared to show significant inhibitory effects with α -cyclodextrin at pH 11 were further studied at pH 3.5. Thermodynamic values for the amino acids that show complexation with α -cyclodextrin at low pH are shown in Table 3.4. Amino acids, isoleucine and histidine, did not appear to form detectable complexes. Also, at low pH tyrosine was not soluble enough to obtain any result. Concentrations of reagents were: 38-40 mM for *p*-aminobenzoic acid, 3 mM for α -cyclodextrin and 40-65 mM for amino acids.

Guest	Enantiomeric form	K_{diss} mM	$-\Delta H/\text{kJ}$ mol^{-1}	$-\Delta G^0/\text{kJ}$ mol^{-1}	$\Delta S^0/\text{J K}^{-1}$ mol^{-1}
Phenylalanine	L	106.6 (6.4)	5.8 (3.0)	5.5	-1
	D	96.6 (7.9)	7.8 (1.6)	5.8	-7
Tryptophan	L	92.9 (5.5)	9.3 (0.9)	5.9	-11
	D	66.1 (2.8)	14.6 (0.6)	6.7	-27
Leucine	L	141.1	1.7	4.9	+11
	D	144.1	1.7	4.8	+10
Methionine	L	107.9	9.2	5.5	-12
	D	117.8	5.9	5.3	-2

Table 3.4 Thermodynamics of complexes between amino acids and α -cyclodextrin at pH 3.5 (25 °C) by competition with *p*-aminobenzoic acid. Standard deviations in parentheses.

At low pH, results suggest that only enantiomers of tryptophan show a significant difference in dissociation constants. In order to illustrate this chiral discrimination, calorimetric data for the titration of α -cyclodextrin with *p*-aminobenzoic acid in the absence and presence of D- and L- tryptophan are displayed in Figure 3.6. At pH 3.5 tryptophan seems to bind more strongly to α -cyclodextrin compared to pH 11 while, leucine, methionine and phenylalanine form weaker complexes at this pH.

The complexation of phenylalanine enantiomers with α -cyclodextrin were also studied at pH 7.4 (0.1 M Na-phosphate buffer) by competition with *p*-nitrophenolate. Dissociation constants and enthalpies of formation for D- and L-phenylalanine are 71.1 mM, -17.1 kJ/mol and 86.4 mM, -19.2 kJ/mol, respectively. The dissociation constant for L-phenylalanine agrees with Horsky and Pitha (1994). Also, the difference in dissociation constants for complexes of α -cyclodextrin with enantiomers of phenylalanine at pH 7.4, indicates enantioselective binding.

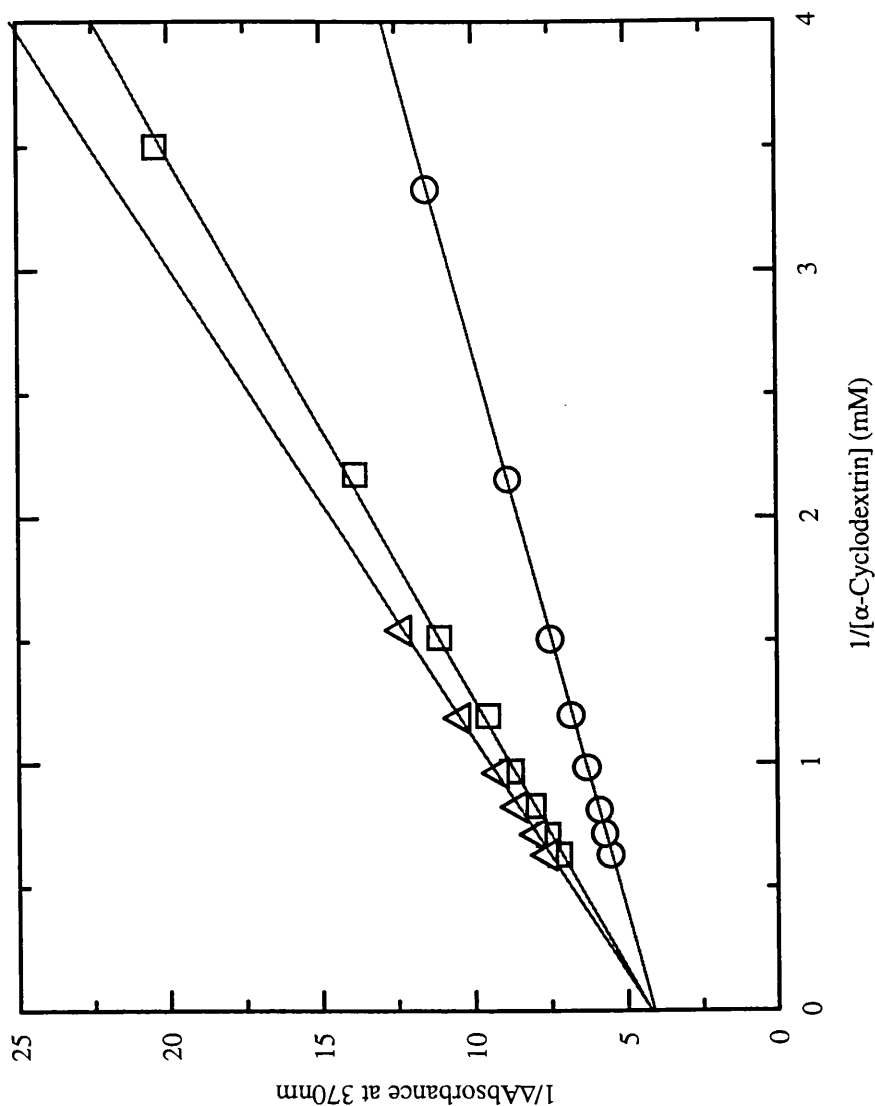


Figure 3.5 Double-reciprocal plot of the spectral titration of *p*-nitrophenolate with α -cyclodextrin, in the absence (O) or presence (Δ D and \square L-phenylalanine, [60 mM]) of competing enantiomers, pH 11 (25°C).

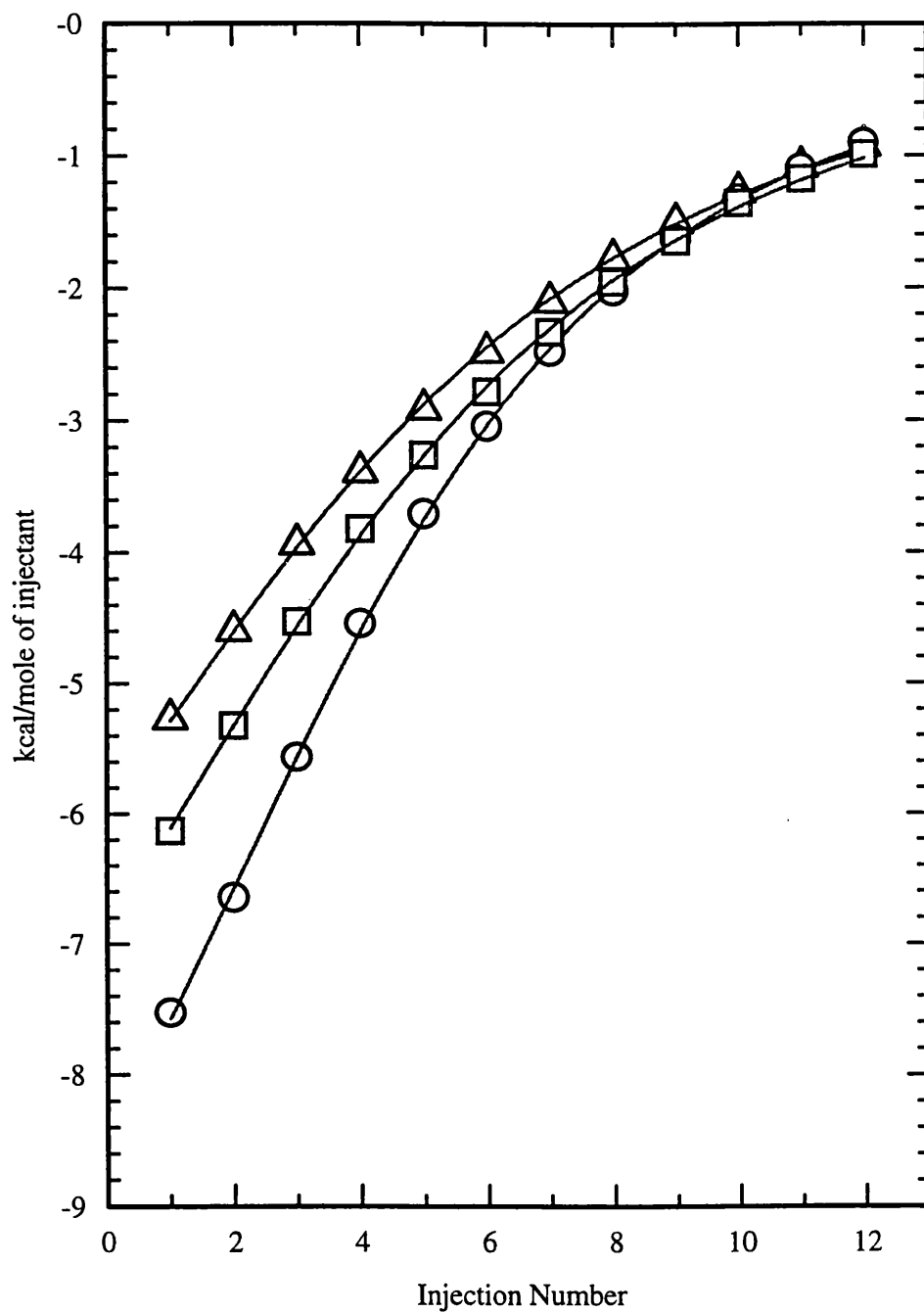


Figure 3.6 Exothermic heats effects for the titration of α -cyclodextrin with *p*-aminobenzoic acid in the absence (O) or presence (Δ D and \square L-tryptophan, [50 mM]) of competing enantiomers, pH 3.5 (25°C).

3.2.2 β -Cyclodextrin

Thermodynamics for complexes of β -cyclodextrin with aromatic amino acids at pH 11 are presented in Table 3.5. It appears that these amino acids form more stable complexes with β -cyclodextrin than for α -cyclodextrin. Nevertheless, there is no indication of any significant chiral discrimination. Other amino acids which formed complexes with α -cyclodextrin at pH 11 were also studied with β -cyclodextrin (i.e. histidine, isoleucine, leucine and methionine). However, no complexation with β -cyclodextrin was observed. Typical concentrations were: 35-50 mM for *p*-nitrophenolate, 2-3 mM for β -cyclodextrin and 7-17 mM for amino acids.

Guest	Enantiomeric form	K_{diss} mM	$-\Delta H/\text{kJ}$ mol^{-1}	$-\Delta G^{\circ}/\text{kJ}$ mol^{-1}	$\Delta S^{\circ}/\text{J K}^{-1}$ mol^{-1}
Phenylalanine	L	17.3	7.1	10.1	+10
	D	16.0	5.0	10.2	+17
Tyrosine	L	11.1	11.3	11.2	0
	D	11.0	11.7	11.2	-2
Tryptophan	L	15.9	13.4	10.3	-10
	D	17.2	16.7	10.1	-22

Table 3.5 Thermodynamics of complexes between aromatic amino acids and β -cyclodextrin at pH 11 (25 °C) by competition with *p*-nitrophenolate.

3.2.3 Methyl- β -Cyclodextrin

Thermodynamics for complexes of methyl- β -cyclodextrin with aromatic amino acids at pH 11 are presented in Table 3.6. These results indicate that methyl- β -cyclodextrin appears to bind only with enantiomers of tryptophan. Dissociation constants also indicate that methyl- β -cyclodextrin forms a weaker complex with tryptophan than β -cyclodextrin, but binds more strongly than α -cyclodextrin. Although tryptophan binds to methyl- β -cyclodextrin there is no significant difference in dissociation constants for separate enantiomers. Typical concentrations were: 44-47 mM for *p*-nitrophenolate, 2 mM for methyl- β -cyclodextrin and 26-31 mM for amino acids.

Guest	Enantiomeric form	K_{diss} mM	$-\Delta H/\text{kJ}$ mol^{-1}	$-\Delta G^0/\text{kJ}$ mol^{-1}	$\Delta S^0/\text{J K}^{-1}$ mol^{-1}
Phenylalanine	L or D	x			
Tyrosine	L or D	x			
Tryptophan	L	64.0	7.9	6.8	-4
	D	60.9	5.4	6.9	+5

Table 3.6 Thermodynamics of complexes between aromatic amino acids and methyl- β -cyclodextrin at pH 11 (25 °C) by competition with *p*-nitrophenolate. * x, not detectable.

3.2.4 Hydroxypropyl- β -Cyclodextrin

Table 3.7 presents thermodynamic data for complexes of hydroxypropyl- β -cyclodextrin with aromatic amino acids at pH 11. As is evident from Table 3.7, hydroxypropyl- β -cyclodextrin binds with enantiomers of tyrosine and tryptophan, however not with phenylalanine. Dissociation constants indicate that hydroxypropyl- β -cyclodextrin forms a weaker complex with tryptophan than β -cyclodextrin, but more strongly compared to methyl- β -cyclodextrin and α -cyclodextrin. While, the complex of hydroxypropyl- β -cyclodextrin and tyrosine is less stable than for β -cyclodextrin. Even though tyrosine and tryptophan seems to bind there are still no significant differences between individual enantiomers. Typical concentrations were: 46 mM for *p*-nitrophenolate, 2 mM for hydroxypropyl- β -cyclodextrin and 26-31 mM for amino acids.

Guest	Enantiomeric form	K_{diss} mM	$-\Delta H/\text{kJ}$ mol^{-1}	$-\Delta G^{\circ}/\text{kJ}$ mol^{-1}	$\Delta S^{\circ}/\text{J K}^{-1}$ mol^{-1}
Phenylalanine	L or D	x			
Tyrosine	L	46.7	12.1	7.6	-15
	D	50.1	14.2	7.4	-23
Tryptophan	L	28.6	10.5	8.8	-6
	D	31.0	11.7	8.6	-10

Table 3.7 Thermodynamics of complexes between aromatic amino acids and hydroxypropyl- β -cyclodextrin at pH 11 (25 °C) by competition with *p*-nitrophenolate.

* x, not detectable.

3.3 Discussion

Although various cyclodextrins and conditions were used, the majority of amino acids showed no complexation with cyclodextrins. In addition, out of all the amino acids which formed complexes with cyclodextrin only two showed distinct differences in the dissociation constants for their separate enantiomers; (i) phenylalanine with α -cyclodextrin at pH 7.4 and pH 11, and (ii) tryptophan with α -cyclodextrin at pH 3.5. Even though chiral discrimination was observed, the effect is quite small, the differences amounting to only about 0.8 kJ mol^{-1} in free energy of complex formation. In the case of phenylalanine, similar results were reported by Cooper and MacNicol (1978). Cyclodextrins also formed complexes with enantiomers of tyrosine, leucine, isoleucine and methionine under various pH, but no chiral discrimination was observed.

It is clear that amino acids which formed complexes, even in some cases relatively weak complexes, all have some hydrophobic character. In the case of aromatic amino acids, it is known from earlier studies of cyclodextrin inclusion complexes the most likely mode of binding is the insertion of the aromatic ring into the hydrophobic cavity of cyclodextrin (Wood et al., 1977; Lipkowitz et al., 1992). However, it has been previously suggested that the interactions which determine chiral discrimination are that of the unidirectional 2- and 3-hydroxyl groups located at the mouth of the cyclodextrin cavity (Armstrong et al., 1986; Lipkowitz et al., 1992). In the chiral discrimination cases observed here, presumably the amino acid group of enantiomers of phenylalanine and tryptophan have different interactions with the cyclodextrin rim. These rim interactions, if any, may also be affected differently when the charge alters with pH. This may explain why tryptophan shows chiral discrimination with α -cyclodextrin at low pH and not at high, and vice versa for phenylalanine. In addition, D- enantiomers may fit into the cyclodextrin cavity in such a way that more hydrogen bonds are formed which results in a more stable complex. In the cases of leucine, isoleucine and methionine the mode of binding is not known.

Table 3.8 shows a comparison of L-aromatic amino acids with various cyclodextrins at pH 11.0. L-tryptophan forms detectable inclusion complexes with all cyclodextrins studied. Noticeably lower dissociation constants were found for β -cyclodextrin and hydroxypropyl- β -cyclodextrin. The dissociation constant for L-phenylalanine was found to be considerably lower for β -cyclodextrin than for α -cyclodextrin (17 mM vs. 62 mM). This observation was also noted by Horsky and Pitha (1994) at pH 7.4. The complex of α -cyclodextrin and L-tyrosine was too weak to determine accurately. However, data for complexes of L-tyrosine and α -cyclodextrin have been previously reported (Matsuyama et al., 1987; Lewis and Hansen, 1973).

Guest	K_{diss} (mM)			
	α -CD	β -CD	methyl- β -CD	hydroxypropyl- β -CD
L-phenylalanine	62	17	x	x
L-tyrosine	x	11	x	47
L-tryptophan	111	16	64	29

Table 3.8 Dissociation constants, K_{diss} , of complexes between cyclodextrins and L-aromatic amino acids at pH 11, measured by competition with *p*-nitrophenolate.

* x, not detectable or too weak to determine accurately.

In the case of β -cyclodextrin, the dissociation constants were similar for all three amino acids. They also appear to form stronger complexes with β -cyclodextrin than for any other cyclodextrin. This may indicate that the cavity diameter of β -cyclodextrin (6.0-6.5 Å) suits the sizes and shape of these amino acids under these particular conditions.

In summary, although several cases of chiral discrimination were observed there were not enough examples to further study the separation of amino acid enantiomers with cyclodextrins using specific separation methods such as capillary electrophoresis. Nevertheless, thermodynamic data obtained are consistent with previous observations of interaction between cyclodextrins in solution and aromatic amino acid side chains and similar groups (Cooper and MacNicol, 1978; Cooper 1992; Horsky and Pitha 1994; Lovatt et al., 1996). Also, results support previous observations that cyclodextrins specifically recognize unfolded proteins by binding to exposed hydrophobic side chains on the polypeptide chain (Cooper, 1992; Cooper and McAuley-Hecht, 1993). Furthermore, results support suggestions that aromatic amino acid residues are primarily responsible for the interaction of protein/peptides with cyclodextrins (Cooper, 1992; Matsuyama et al., 1987).

CHAPTER 4

ENERGETICS OF PROTEIN-CYCLODEXTRIN INTERACTIONS

4.1 Introduction

The interaction of cyclodextrins with amino acid groups on proteins can have several consequences. In the course of this work we predicted that interactions with groups on oligomeric folded proteins might lead to dissociation of these protein aggregates, especially if the complexations occurs at sites in the protein-protein interface (Lovatt et al., 1996). In order to test this hypothesis, we have examined the dissociation of insulin in absence and presence of cyclodextrins under various conditions. Additionally, binding of cyclodextrins to exposed side-chains on unfolded polypeptides will destabilize the native folded form of the protein and lead to denaturation at lower temperature (Cooper, 1992; Cooper and McAuley-Hecht, 1993). Combining these effects cyclodextrin interactions with unfolded proteins may enhance the solubility of denatured proteins by masking the exposed hydrophobic residues, thereby possibly assisting the refolding of the polypeptide. In this way cyclodextrins might act as small chaperone mimics in protein folding process in cases where refolding is inhibited by poorly-reversible aggregation or entanglement. The energetics of these processes have been examined by microcalorimetry yielding information on the thermodynamics of protein-cyclodextrin interactions. The effects of cyclodextrins on regain of enzyme activity following thermal denaturation are described in chapter 5.

4.2 Cyclodextrin-Induced Dissociation of Insulin

4.2.1 Introduction

Insulin is a hormone secreted by the pancreas and its role is to promote the uptake of glucose by body cells and thereby control its concentration in the blood, which ensures that it circulates and brings about its biological effects as a monomer (Blundell et al., 1972). The insulin monomer contains two polypeptide chains, A and B, containing 21 and 30 residues, respectively, with a molecular weight of approximately 5,800. The A chain contains a disulphide bridge at A6-A11, and is linked to the B chain by two disulphide bridges, at A7-B7 and A20 and B19 (Figure 4.1).

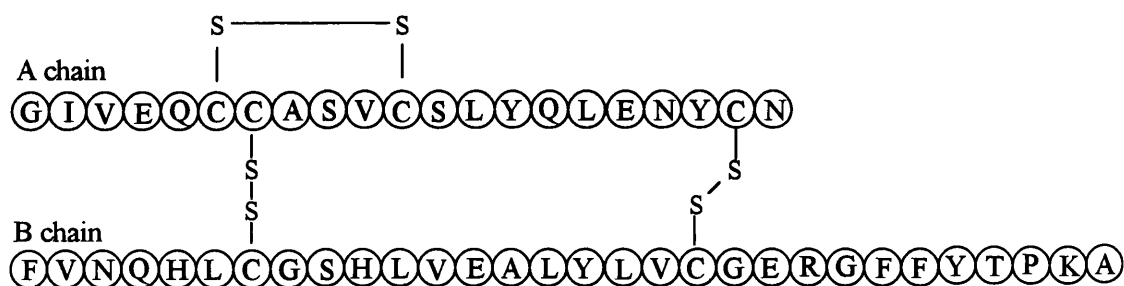


Figure 4.1 Amino acid sequence of bovine insulin.

Insulin's three-dimensional structure was determined by X-ray analysis of a 2Zn insulin hexamer (Adams et al., 1969). It was seen that the molecule's A and B chains were arranged compactly around a non-polar core made up of the central B-chain helix B9-B19 and the inner directed residues from the two short, adjacent and anti-parallel A-chain helices A2-A8 and A13-A20. There prove to be two non-polar surfaces on the molecule, one involved in dimer assembly, the other in hexamer assembly. The dimer is constructed from two-fold related molecules whose association is stabilized by the burial of two equivalent non-polar and mostly aromatic surfaces. At one edge of these surfaces is the B-chain C-terminal segment of some 10 residues. These run anti-parallel and come together between B24 and B26 to form a

β -sheet hydrogen bonded structure which adds further compactness and specificity to the dimer forming interactions (Figure 4.2).

The assembly of insulin dimers to hexamers requires the co-ordination of zinc ions (or other divalent metal ions) to the B10 histidine imidazole rings. Each of the three equivalent dimers presents two B10 histidine side chains to the zinc ions which lie on the central three-fold axis. The dimers make looser contacts in the hexamer than the monomers in the dimer though like the dimer they pack together around a central non-polar region.

Insulins are known to occur in a variety of aggregation (oligomer) states in solution depending on concentration, pH, temperature, Zn^{2+} concentration and other ionic conditions (Blundell et al., 1972; Bi et al., 1984). Insulin's aggregation states can potentially affect their use in therapeutic situations, since it appears that the assembly of insulin to hexamers is associated with the hormone's slow absorption by tissue. Based on previous observations on interaction of cyclodextrins with globular proteins (Cooper, 1992; Cooper and McAuley-Hecht, 1993) it was predicted that complexation of these cyclic polysaccharides with surface protein residues might significantly affect the state of aggregation of protein in solution. The non-polar cavities of toroidal cyclodextrin molecules have a particular affinity for small non-polar groups and can both enhance the solubility and improve stability of such molecules in water. Cyclodextrins are finding increasing use as solubilizing agents and stabilizing excipients for protein drugs, including insulins (Brewster et al., 1991). We show here by calorimetric measurement of heats of dilution that the dissociation of bovine insulin in solution is significantly enhanced in the presence of various cyclodextrins. The energetics of this process are consistent with association of cyclodextrin molecules with insulin surface residues. Such a complexation might also bring about conformational changes in insulin which might contribute indirectly to the disaggregation process.

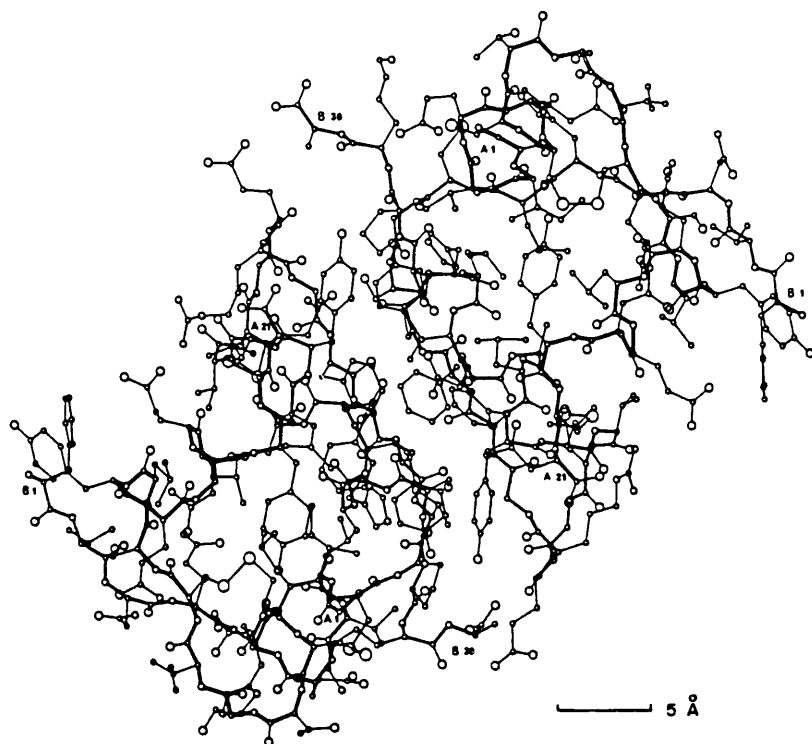


Figure 4.2a View of the insulin dimer in the direction of its two-fold axis.

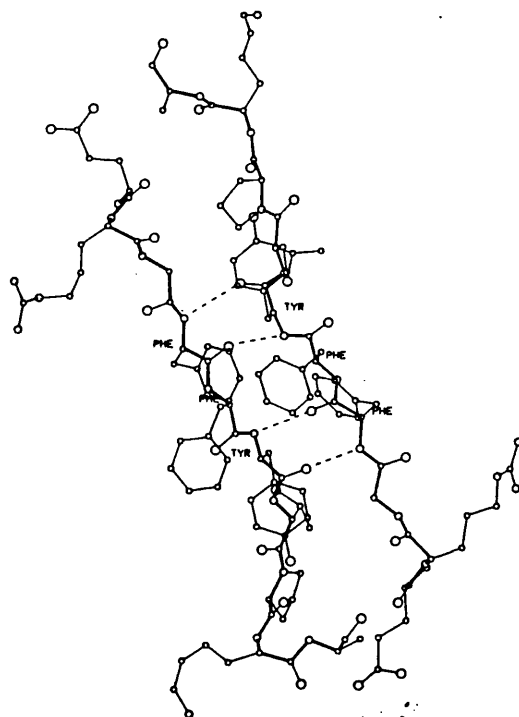


Figure 4.2b The anti-parallel pleated sheet of the C terminal residues in the insulin dimer viewed in the same direction as above. Hydrogen bonds are dotted.

4.2.2 Results and Discussion

Calorimetric dilution experiments were performed at 25 °C (unless otherwise stated) with a 250 μ l injection syringe at 400 rpm stirring. In a typical dilution experiment small aliquots (10-20 μ l) of concentrated insulin, dissolved in buffer or buffer/cyclodextrin mix, were injected into the calorimeter reaction vessel (1.4 ml volume) containing the identical buffer mixture. Dilution of a series of small aliquots of insulin into a larger volume of buffer gives a sequence of endothermic heat pulses characteristic of molecular dissociation (Figure 4.3A). With successive injections, as protein concentration in the calorimeter cell increases, the magnitude of the heat uptake diminishes, presumably because the extent of dissociation decreases at the higher insulin concentrations. This gives rise to a typical heat of dilution curve (Figure 4.3B), which after being corrected for control heats can be fit in terms of a monomer-dimer equilibrium model (refer to section 2.2.2) yielding K_{diss} and ΔH_{diss} .

Thermodynamic data obtained in this manner for calorimetric dilution experiments in the absence and presence of cyclodextrins are given in Table 4.1. Qualitatively similar effects are seen both at pH 2.5 (0.1 M glycine/HCl), where the insulin concentrations in the injection syringe were typically 10 mg/ml, and at pH 7.4 (0.1 M Na-phosphate) where, because of the much lower solubility, insulin concentrations were only about 1 mg/ml, and dilution heats were concomitantly smaller. Consequently, only limited quantitative data are reported here for pH 7.4, though the overall trends seem similar at both pH's.

Addition of cyclodextrins (up to 200 mM) to the buffer mixture gives rise to two significant effects (Figure 4.4): (i) insulin dilution heats become more endothermic, and (ii) the dilution curves become more attenuated, indicating greater dimer dissociation in the presence of cyclodextrins. This seems to be confirmed by the

apparent thermodynamic parameters in Table 4.1, and is consistent with cyclodextrin binding to the dissociated form of the insulin molecule, thereby shifting the equilibrium in favour of dissociated protein. Previous studies have shown that, at low pH, insulin is predominantly dimeric in solution at high concentrations (Blundell et al., 1972) and, in agreement with this, our preliminary dynamic light scattering measurements (not shown) at pH 2.5, under the same conditions as used for calorimetric measurements, give an estimated molecular weight in the region of 11-12 kDa. The heat of dilution data obtained here are also consistent with a dimer dissociation model, and we use this for quantitative comparison. In the absence of cyclodextrins at pH 2.5 the insulin dimer dissociation constant (K_{diss}), obtained from non-linear regression analysis of dilution data, is around 12 μM and in agreement with previous determinations by other techniques (Blundell et al., 1972). Computer simulations of more complex oligomer models show sigmoidal dilution curves unlike anything observed so far here. At pH 7.4 the oligomeric state of insulin is less clear, and hexamers or higher oligomers almost certainly exist under the conditions used here. Nevertheless, at 25 °C the dilution data seems to fit reasonably to a dimer model, and we use this for empirical comparison purposes.

Cyclodextrins appear to have similar effects at various temperatures at pH 2.5 and in some cases at pH 7.4, as shown in Figures 4.5 and 4.6. However, at these particular temperatures thermodynamic data were only obtained for dilution data at pH 2.5 (Table 4.2). This may be the result of the presence of other oligomeric states at pH 7.4, resulting in the inaccurate fitting of data to the dimer model.

As a result of calorimetric measurements over a range of temperatures, ΔC_p values were calculated for pH 2.5 data from the gradients of best-fit straight lines through the experimental data of the variation of ΔH_{diss} with temperature, as shown in Figure 4.7. This sort of ΔC_p effect is frequently seen in biomolecular interactions. It

is usually associated with changes in exposed non-polar surface areas (ΔA_{np}) during the process. The positive ΔC_p observed here is consistent with an increase in exposed molecular surface area on dissociation of the dimers, as would be expected. Using the empirical procedure of Spolar and Record (1994), together with the estimated heat capacity changes in Table 4.2, the estimated exposed non-polar surface area for insulin (approximately 50 Å) was larger than expected. This discrepancy may be due to the fact that the empirical basis for the ΔA_{np} - ΔC_p correlation has yet to be tested for relatively small molecular complexes, and major discrepancies have recently been found in much larger systems (Xu et al., 1997).

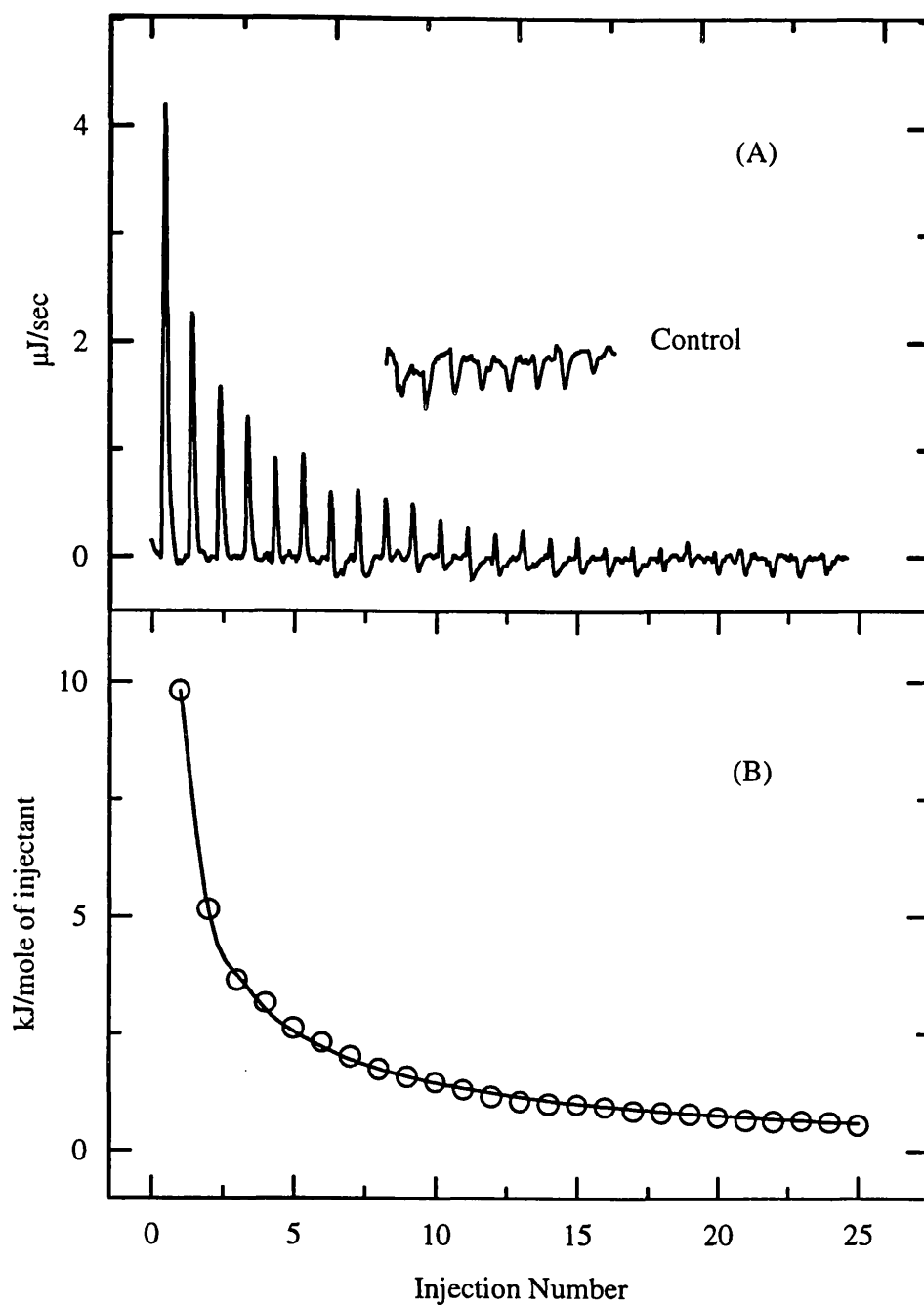


Figure 4.3 Calorimetric data for the endothermic dissociation of insulin dimers at pH 2.5; (A) Raw data for injection of insulin, 1.53 mM (8.8 mg/ml), $25 \times 10 \mu\text{l}$ injections, into buffer at 25°C , with control data showing the calorimetric response for blank buffer injections on this very sensitive scale; (B) Integrated injection heats, corrected for control heats and fit (solid line) to a dimer dissociation model with $K_{\text{diss}} = 12\mu\text{M}$ and $\Delta H_{\text{diss}} = 41 \text{ kJ mol}^{-1}$.

pH	Cyclodextrin	[CD] mM	K_{diss} μM	ΔH_{diss} kJ mol^{-1}	$\Delta G^{\text{O}}_{\text{diss}}$ kJ mol^{-1}	$\Delta S^{\text{O}}_{\text{diss}}$ $\text{J K}^{-1} \text{mol}^{-1}$
2.5	None	-	12 (1)	41.0 (3.5)	28.1	43
2.5	Methyl- β -	30	51 (13)	59.8 (3.9)	24.5	118
		50	88 (17)	64.7 (1.2)	23.1	139
		74	184 (19)	67.8 (5.1)	21.3	156
		99	284 (56)	72.5 (0.9)	20.2	175
		141	690 (99)	75.0 (0.9)	18.0	191
		199	1690 (21)	79.1 (2.1)	15.8	212
2.5	Hydroxypropyl- β -	29	25 (12)	47.3 (6.2)	26.3	71
		50	24 (6)	54.7 (4.7)	26.4	95
		79	64 (24)	47.7 (4.7)	23.9	80
		120	70 (3)	53.1 (1.9)	23.7	99
		139	78 (4)	52.7 (1.9)	23.4	98
		209	152 (45)	58.3 (4.3)	21.8	123
2.5	α -	25	17 (3)	38.3 (0.8)	27.2	37
		48	41 (2)	34.0 (0.8)	25.0	30
		75	68 (8)	33.1 (1.2)	23.8	31
		97	67 (8)	29.4 (2.1)	23.8	19
7.4	None	-	nd*	nd	nd	nd
7.4	Methyl- β -	50	20	60	26.8	110
		100	57	65	24.2	138
		150	190	88	21.2	224
7.4	Hydroxypropyl- β -	100	47	52	24.7	91
7.4	α -	100	221	31	20.9	35

Table 4.1 Thermodynamic data for the dissociation of insulin dimers at 25°C, determined from calorimetric dilution data in the presence or absence of cyclodextrins. Each experiment was normally repeated three times to give the mean values of apparent dissociation constants and enthalpies (K_{diss} , ΔH_{diss}), with standard deviations in parentheses. * nd, calorimetric effects too small to determine accurately.

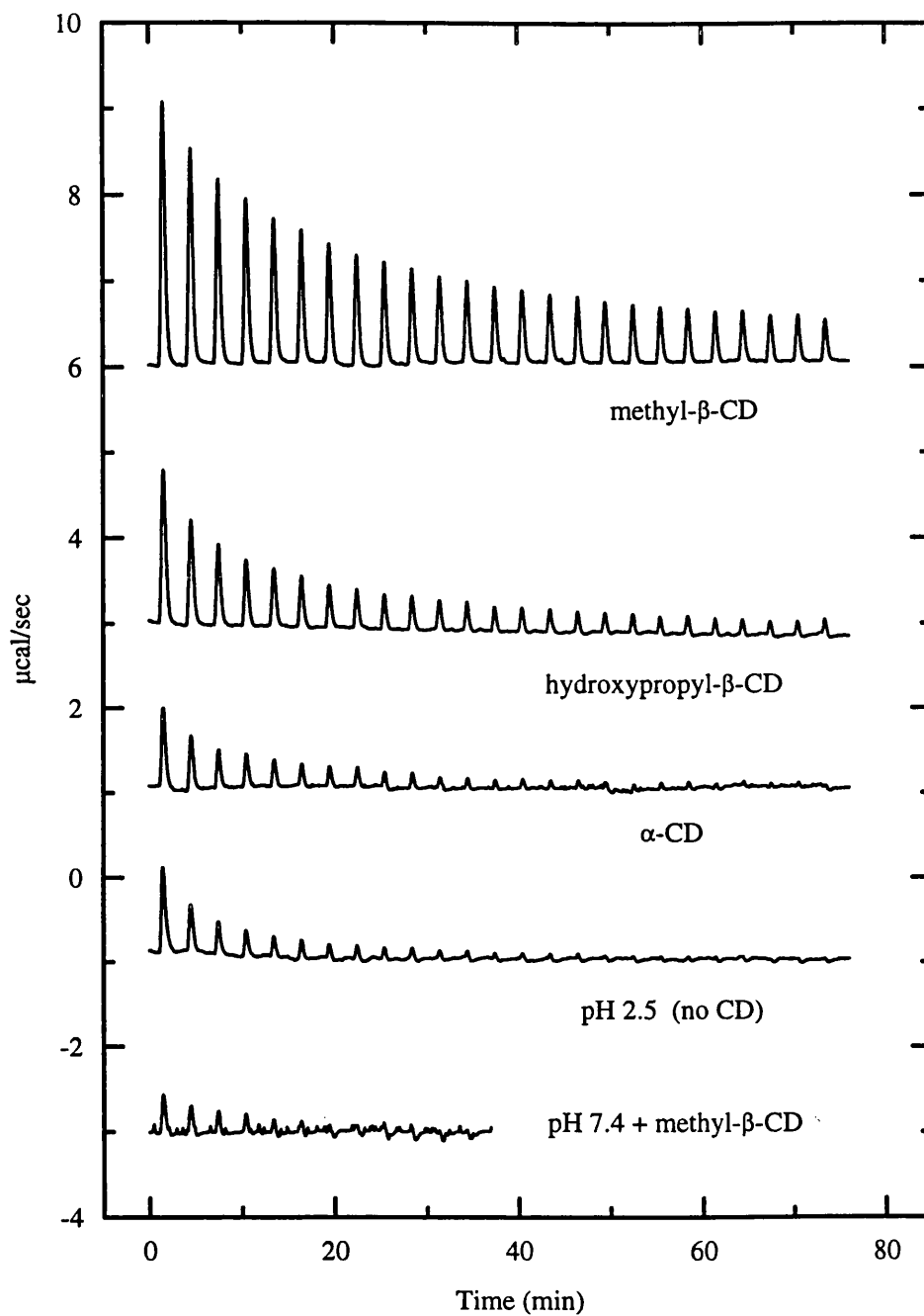


Figure 4.4 Examples of raw calorimetric dilution data showing the effects of different cyclodextrins on insulin dissociation, all at pH 2.5 except where indicated. For comparison, cyclodextrin concentrations (when present) are all approximately 100 mM in this case.

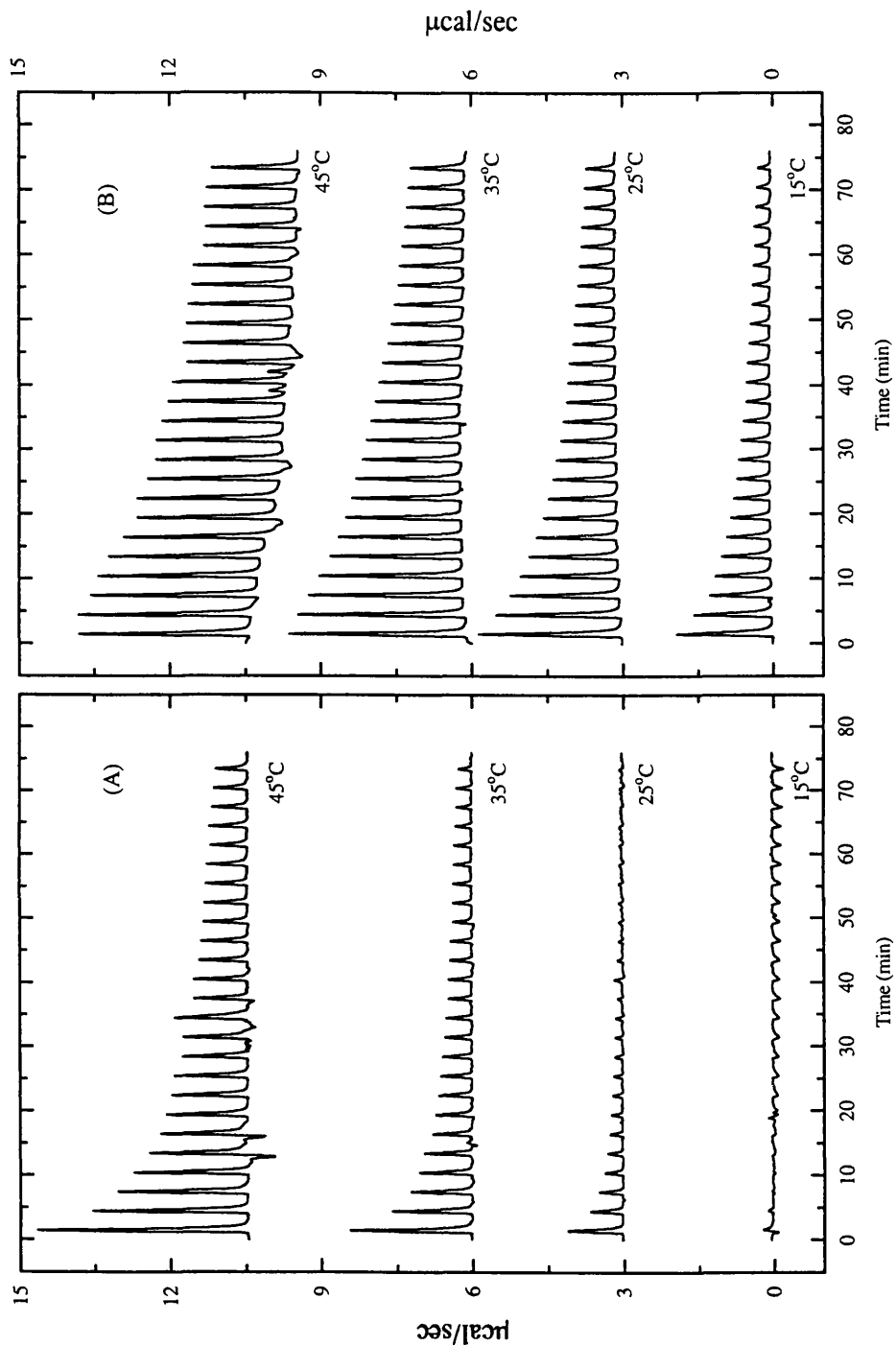


Figure 4.5 Examples of raw calorimetric dilution data of dissociation of insulin at various temperatures, pH 2.5. (A) in the absence of cyclodextrin. (B) in the presence of methyl- β -cyclodextrin (100 mM).

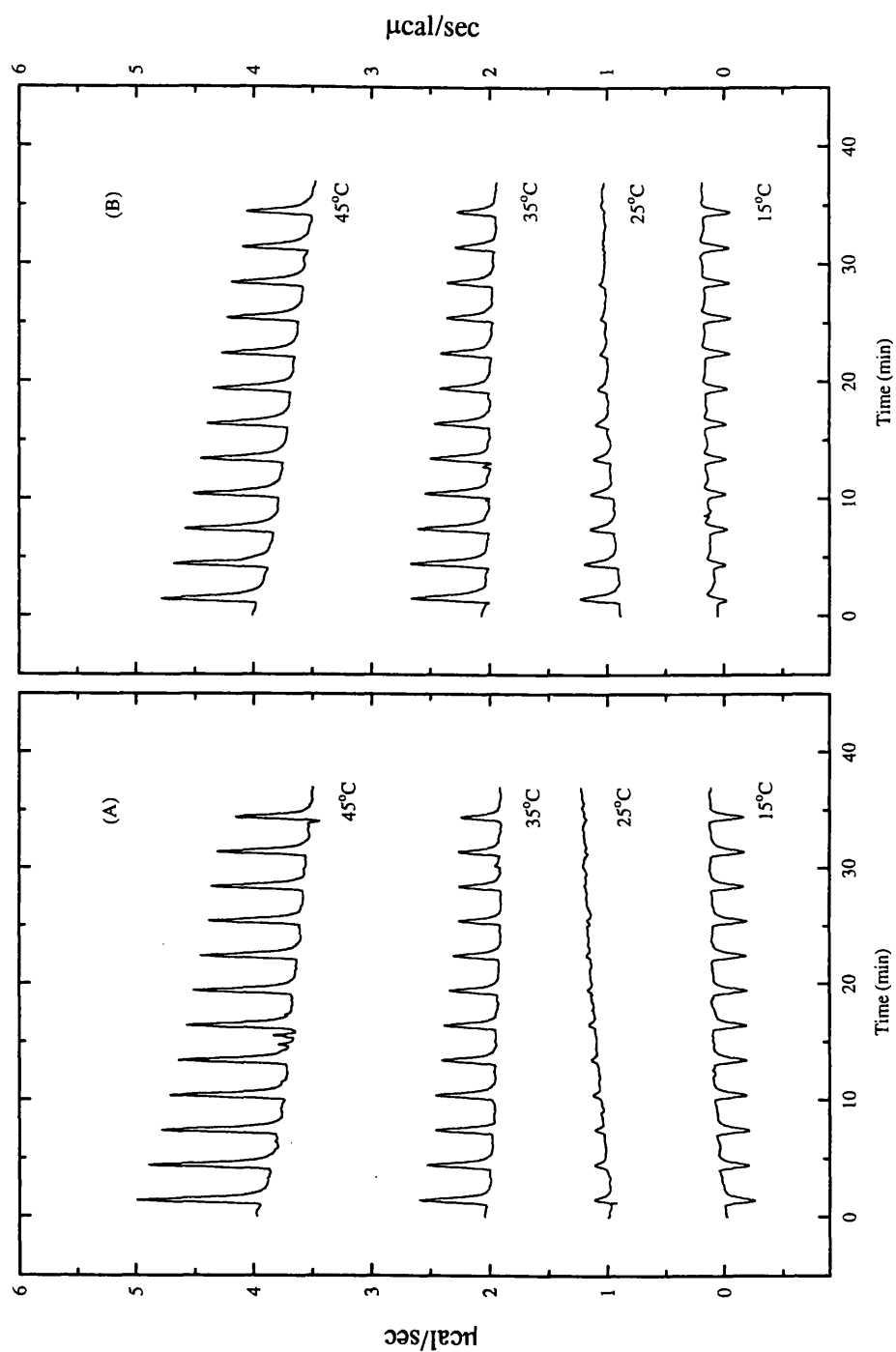


Figure 4.6 Examples of raw calorimetric dilution data of dissociation insulin at various temperatures, pH 7.4. (A) in the absence of cyclodextrin. (B) in the presence of hydroxypropyl- β -cyclodextrin (100 mM).

Temp. (°C)	Cyclodextrin	K_{diss} μM	ΔH_{diss} kJ mol^{-1}	$\Delta G^{\circ}_{\text{diss}}$ kJ mol^{-1}	$\Delta S^{\circ}_{\text{diss}}$ $\text{J K}^{-1} \text{mol}^{-1}$	ΔC_p $\text{kJ mol}^{-1} \text{K}^{-1}$
15	None	nd*	nd	nd	nd	
25		12 (1)	41.0	28.1	43	3.6 (0.59)
35		49.5 (9.9)	66.3 (5.3)	24.6	140	
45		110 (5.7)	112 (3.8)	22.6	300	
15	Methyl- β - [100 mM]	183	52.5	21.3	105	
25		355	72.4	19.7	177	3.2 (0.49)
35		900	100.4	17.4	279	
45		3650	150.6	13.9	459	
15	Hydroxypropyl- β - [100 mM]	nd	nd	nd	nd	
25		69	46.4	23.7	76	3.9 (0.31)
35		122	79.5	22.3	196	
45		334	123.4	19.8	348	
15	α - [100 mM]	nd	nd	nd	nd	
25		63	26.4	24.0	8	4.9 (0.50)
35		154	66.9	21.7	152	
45		525	124.7	18.7	356	
15	Methyl- β - [201 mM]	927 (175)	58.8 (2.1)	17.3	140	4.5 (0.66)
25		1872 (227)	79.1 (0.6)	15.6	213	
35		6588 (1236)	132 (18.7)	12.4	401	
45		13514	192.5	10.7	611	

Table 4.2 Thermodynamic data for the dissociation of insulin dimers (pH 2.5) at different temperatures determined from calorimetric dilution data in the presence or absence of cyclodextrins. The mean values of apparent dissociation constants and enthalpies (K_{diss} , ΔH_{diss}), with standard deviations in parentheses, were normally repeated three times. * nd, calorimetric effects too small to determine accurately.

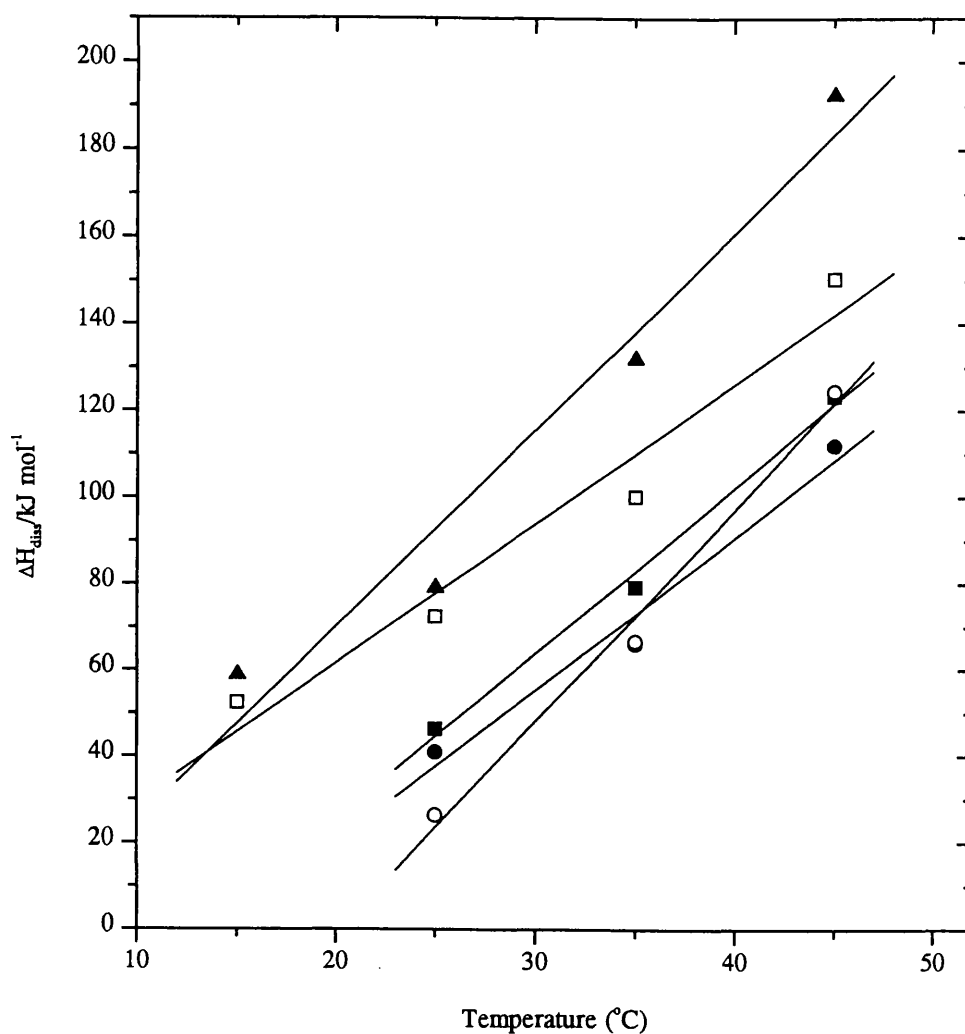
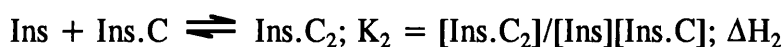
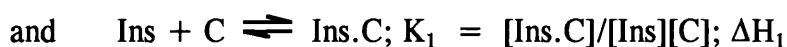
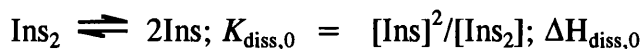


Figure 4.7 Variation with temperature of the enthalpy of dissociation of insulin alone (filled circles) or in the presence of various cyclodextrins. Cyclodextrin concentrations are all approximately 100 mM, except with where indicated. (open circles) α -cyclodextrin, (filled squares) hydroxypropyl- β -cyclodextrin, (open squares) methyl- β -cyclodextrin and (filled triangle) methyl- β -cyclodextrin (200 mM).

The variation in apparent dissociation constant with cyclodextrin concentrations can be simulated, at least in part, by a simple (but probably unrealistic) model involving sequential binding of cyclodextrins to sites on the dissociated insulin. Assuming:



..... and so on for sequential binding steps.

where C represents the cyclodextrin, the apparent dissociation constant may be written:

$$K_{\text{diss}} = [\text{Ins}_{\text{tot}}]^2/[\text{Ins}_2] = K_{\text{diss},0}(1 + K_1[\text{C}] + K_1K_2[\text{C}]^2 + \dots)^2$$

Despite uncertainties regarding the number of potential binding sites and their binding affinities, this polynomial expression does form a reasonable basis for empirical modelling of the observed effects of cyclodextrins on insulin dissociation thermodynamics. Non-linear regression analysis of experimental data (pH 2.5, 25°C) for the variation of apparent dimer dissociation constant with cyclodextrin concentration (Figure 4.8) indicates that two sequential binding sites are adequate for describing the data satisfactorily over the accessible concentration range. The numerical values obtained for the site-binding constants (K_1 , K_2) are consistent with the relatively weak affinities expected on the basis of previous observations of interaction between cyclodextrins in solution and aromatic amino acid side chains and similar groups (Cooper, 1992; Cooper and MacNicol, 1978; Horsky and Pitha, 1994).

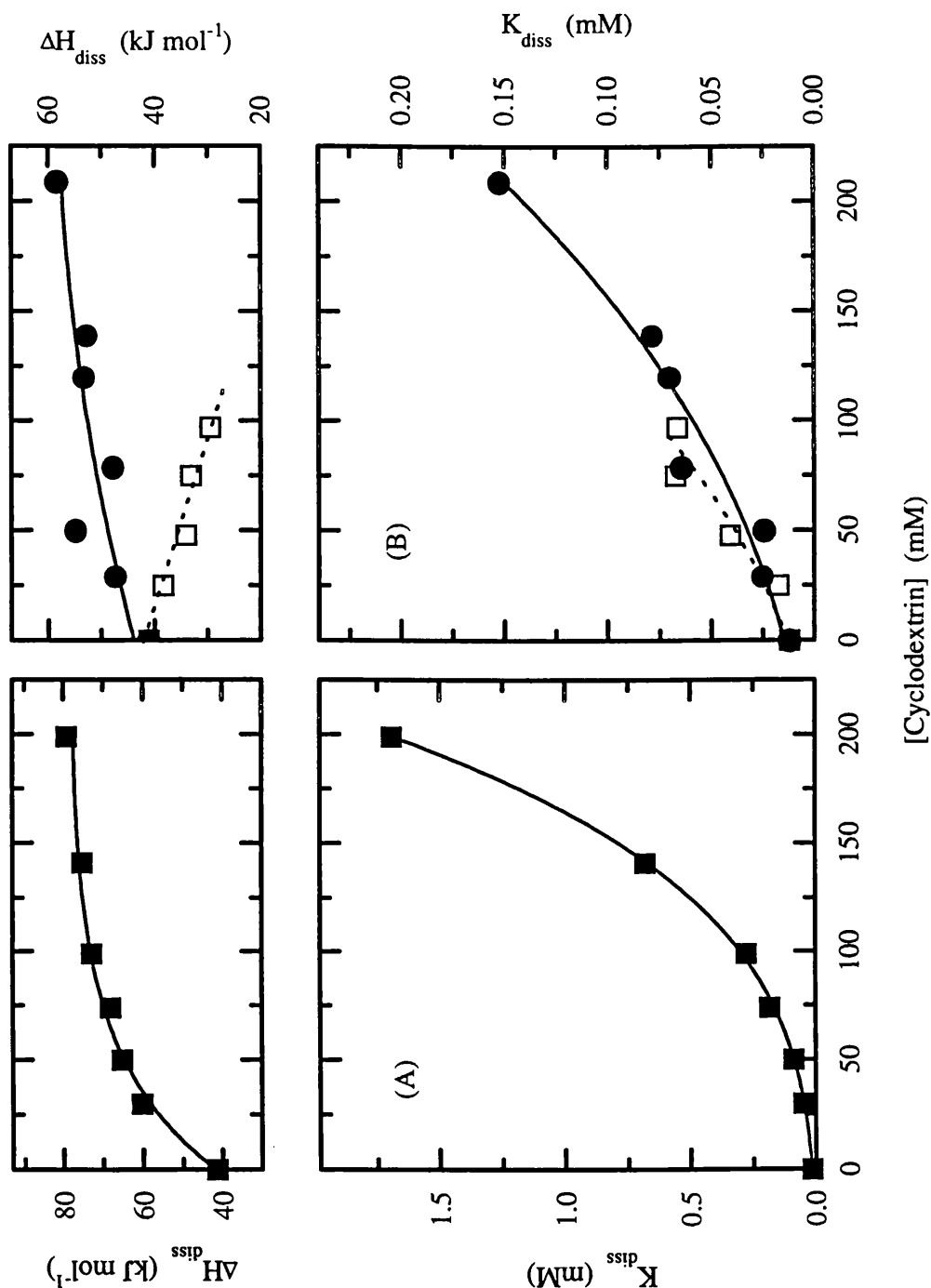


Figure 4.8 Change in apparent dissociation constants (K_{diss} , lower panels) and enthalpies of dissociation of insulin (ΔH_{diss} , upper panels) at pH 2.5 (25 °C) with increasing cyclodextrin concentrations. In the lower panels the curves show the theoretical fits to a simple sequential binding model, using the parameters given in the text. (A) Methyl- β -cyclodextrin (filled squares). (B) Hydroxypropyl- β -cyclodextrin (filled circles) and α -cyclodextrin (open squares).

For methyl- β -cyclodextrin, which shows the biggest effect, K_1 and K_2 are estimated to be about 20 and 6.5 M^{-1} , respectively. For the other cyclodextrins $K_1 \approx 10\text{--}15 \text{ M}^{-1}$, with $K_2 < 5 \text{ M}^{-1}$.

The enthalpies also show interesting variations (Figure 4.8). In the absence of cyclodextrins the dissociation of insulin oligomers is endothermic. Addition of α -cyclodextrin, in addition to encouraging oligomer dissociation, also makes this dissociation less endothermic in a manner consistent with the exothermic binding of α -cyclodextrins to exposed groups on insulin monomers after dissociation. In contrast, although methyl- and hydroxypropyl- β -cyclodextrins similarly induce oligomer dissociation, this dissociation is observed to be more endothermic. This suggests that the binding of these modified β -cyclodextrins to exposed insulin residues, although thermodynamically favourable, is endothermic and consequently entropy-driven. The nett effect is to increase the apparent insulin dissociation constant, whilst making the overall dissociation process more endothermic. The concomitant increase in dissociation entropy ($\Delta S_{\text{diss}}^{\circ}$, Table 4.1) may arise from displacement of solvent/ solvation layers from the insulin surface when the bulky modified β -cyclodextrins bind. It may also suggest an additional hydrophobic contribution to the cyclodextrin interaction arising from the methyl- and hydroxypropyl- substituent groups on the cyclodextrin ring. Such interactions may not be seen in model experiments involving just simple amino acids or analogues that lack the bulk/surface effects to be expected with side chains on the insulin molecule.

Since, it seems likely that cyclodextrins might have similar effects on the dissociation of other oligomeric systems, preliminary investigations were carried out on hemoglobin. Hemoglobin is a tetrameric protein and when saturated with ligands such as O_2 or CO_2 , it has been suggested that it more easily dissociates into dimers. Therefore, trial experiments involved: (i) binding CO to hemoglobin dissolved in buffer or buffer/cyclodextrin mix; and then (ii) injecting this solution into the calorimeter reaction cell containing identical buffer mixture. However, after

numerous attempts such experiments did not produce a typical dilution curve. Hence, the effect of cyclodextrins on hemoglobin dissociation were not studied.

Finally, since insulin's amino acid sequence contains 4 tyrosine residues that have fluorescent side chains, fluorescence spectroscopy was used to investigate the binding of cyclodextrins to these hydrophobic residues. However, in trial experiments it was found that cyclodextrins contained an impurity that also fluoresced, thereby possibly hiding any effect that cyclodextrins had on insulin.

4.3 Effect of Cyclodextrins on the Thermal Stability of Cytochrome c and Lysozyme

4.3.1 Introduction

Cyclodextrins can bind to a wide range of non-polar molecules in water, usually by complexation within the relatively hydrophobic cavity of the toroidal molecule (Bender and Komiyama, 1978; Saenger, 1980; Szejtli, 1982). Since, the unfolding of globular proteins normally involves exposure of buried hydrophobic side chains (Kauzmann, 1959; Privalov and Gill, 1988), the binding of cyclodextrins to these exposed residues should destabilize native conformations by shifting the equilibrium in favour of the unfolded polypeptide chain. Cooper (1992) found that this was indeed the case, where DSC measurements of a range of proteins showed that α -cyclodextrin promotes unfolding and that increasing cyclodextrin concentrations reduces the thermal stability of the proteins in a manner consistent with weak non-covalent attachment of α -cyclodextrin molecules onto the unfolded chain. Examples of thermal transitions from these experiments are shown in Figure 4.9. Cooper and McAuley-Hecht (1993) also found similar results for lysozyme with various concentrations of hydroxypropyl- β -cyclodextrin. Here, as part of a general study, the effect of various cyclodextrins on the thermal stability of cytochrome c and lysozyme were studied.

Cytochrome c and lysozyme were chosen for these studies because thermodynamic studies indicate that the folding/unfolding transitions follow a two-state mechanism i.e., no thermodynamically stable partially folded states are significantly populated during the folding/unfolding process (Privalov, 1979). In addition, lysozyme had been previously used for similar microcalorimetric studies (Cooper, 1992; Cooper and McAuley-Hecht, 1993). Finally, all lysozyme data presented here were carried out in collaboration with Margaret Nutley.

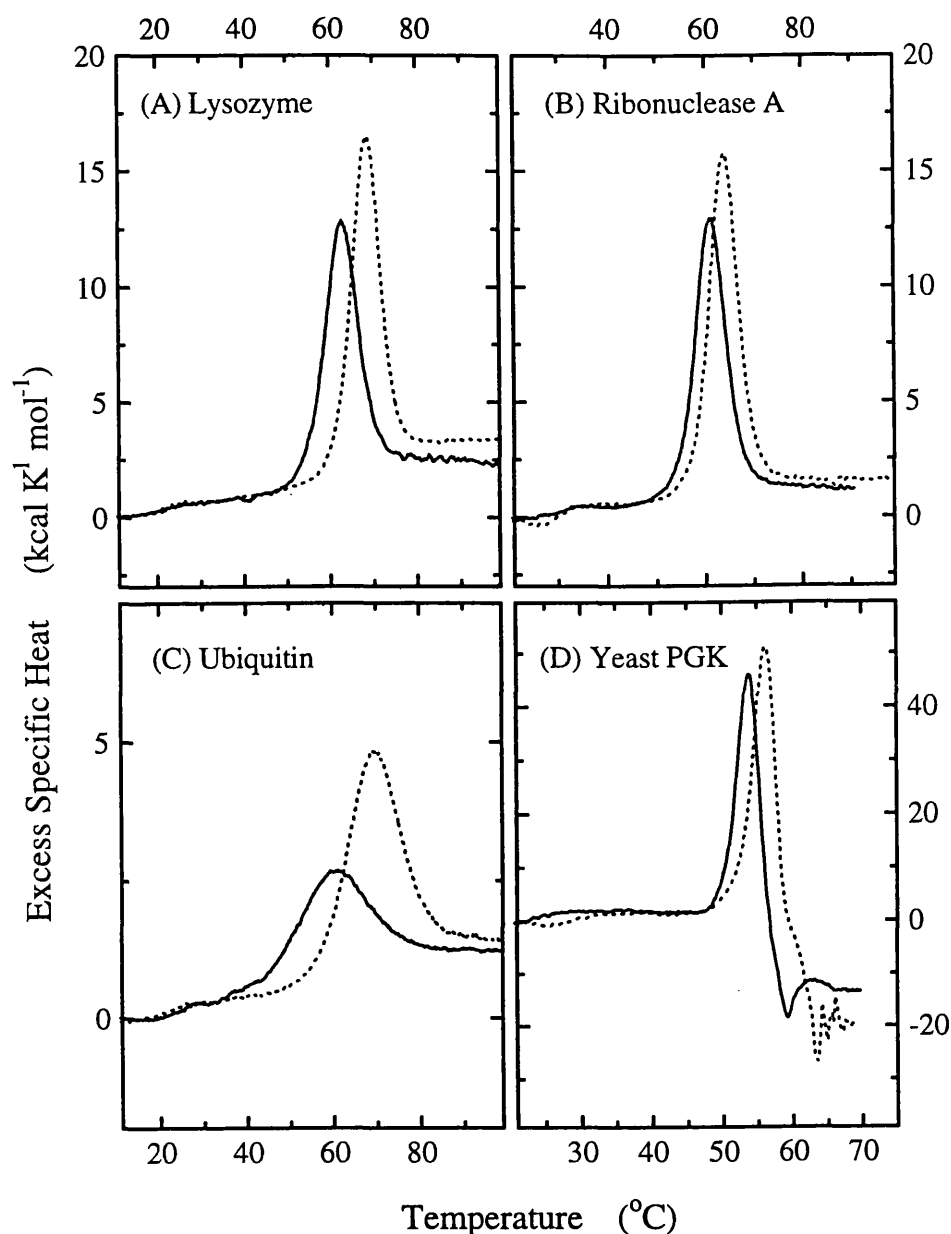


Figure 4.9 Effects of cyclodextrins of the thermal unfolding of proteins in the presence (solid) and absence (dotted lines) of α -cyclodextrin, after baseline subtraction and concentration normalization. (A) Hen egg white lysozyme in 40 mM glycine hydrochloride, pH 3.0, [α -CD]=138 mM. (B) Ribonuclease in 0.1 M sodium citrate, pH 4.5. [α -CD]=139 mM. (C) Ubiquitin in 40 mM glycine hydrochloride, pH 3.0, [α -CD]=137 mM. (D) Yeast phosphoglycerate kinase in 50 mM Pipes, 0.1 mM dithiothreitol, pH 7.0, [α -CD]=69 mM (Cooper, 1992).

4.3.2 Results

Cytochrome c

Table 4.3 summarizes the T_m 's for the thermal unfolding of cytochrome c in the absence and presence of α -cyclodextrin, hydroxypropyl- β -cyclodextrin and methyl- β -cyclodextrin at pH 5.0. Figures 4.10 and 4.11 gives examples of DSC traces showing the endothermic unfolding transitions of cytochrome c with and without α -cyclodextrin and hydroxypropyl- β -cyclodextrin. While, the effects of various concentrations of methyl- β -cyclodextrin on the thermal stability of cytochrome c are shown in Figure 4.12. It is evident from these DSC traces that unfolding transitions possess a rather noisy appearance, therefore T_m is estimated where necessary.

Cyclodextrins	[CD] mM	T_m (°C)
None	0	76.6
α -	120	73.2
Hydroxypropyl- β -	120	73.3
Methyl- β -	120	69.4
	200	67.3

Table 4.3 Summary of the effects of cyclodextrins on reducing the T_m of cytochrome c, pH 5.0 (0.1 M Na-citrate/citric acid).

Studies were also carried out at pH 3.0 (0.1 M glycine/HCl) and pH 7.0 (0.1 M Na-phosphate). However, at pH 3.0 cytochrome c appeared to unfold between 35-40 °C which presented problems in the presence of cyclodextrin. For instance, in the presence of 120 mM methyl- β -cyclodextrin cytochrome c had already started to unfold at the beginning of the DSC scan. Also, at pH 7.0 thermal unfolding curves were strongly affected by exothermic aggregation concomitant with the unfolding transition of the protein. This lead to artificial sharpening of the transition, resulting

in difficulties when estimating the T_m . Consequently, studies were not carried out at these pH's.

Lysozyme

Table 4.4 summarizes results of the effects of α -cyclodextrin, hydroxypropyl- β -cyclodextrin and methyl- β -cyclodextrin at various concentrations on reducing the thermal stability of lysozyme at pH 4.0. Examples of DSC traces showing unfolding transitions of lysozyme in the absence and presence of increasing α -cyclodextrin and methyl- β -cyclodextrin concentrations are shown in Figures 4.13 and 4.14. Also, Figure 4.15 shows the decrease in T_m for lysozyme as a result of increasing cyclodextrin concentration.

Cyclodextrins	% CD (w/v)	T_m ($^{\circ}$ C)
None	0	76.6
α -	5	75.3
	10	74.1
Hydroxypropyl- β -	5	75.5
	10	74.9
	15	74.1
Methyl- β -	5	73.8
	10	71.7
	15	70.2

Table 4.4 Summary of the effects of cyclodextrins on reducing the T_m of lysozyme, pH 4.0 (0.1 M Na-acetate/acetic acid). Data for α -cyclodextrin was limited by low solubility.

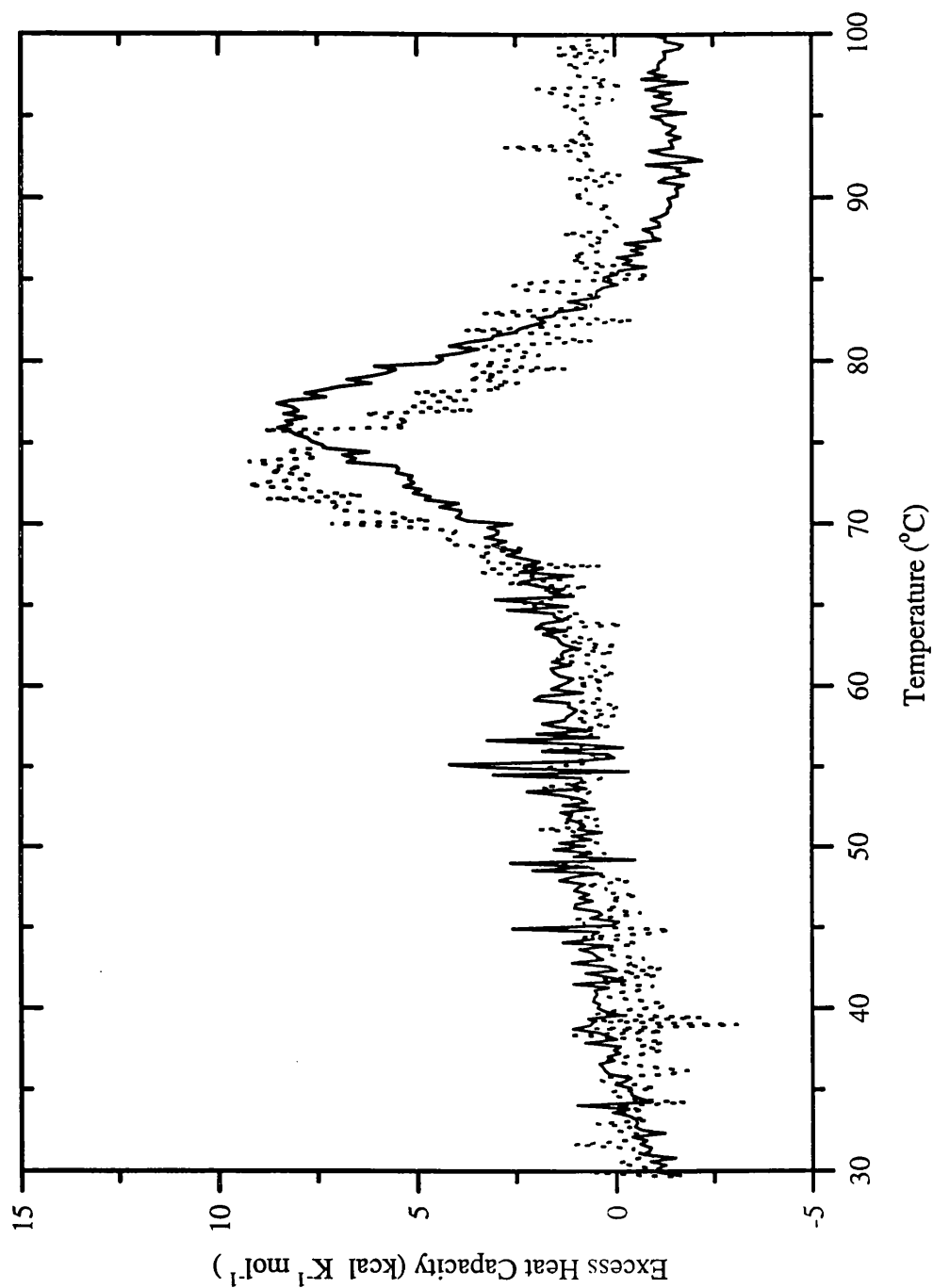


Figure 4.10 DSC of thermal unfolding of cytochrome c (1 mg/ml) at pH 5.0 (0.1 M Na-citrate/citric acid) in the absence (solid lines) and presence (dotted lines) of α -cyclodextrin (ca.120 mM), after baseline subtraction and concentration normalization.

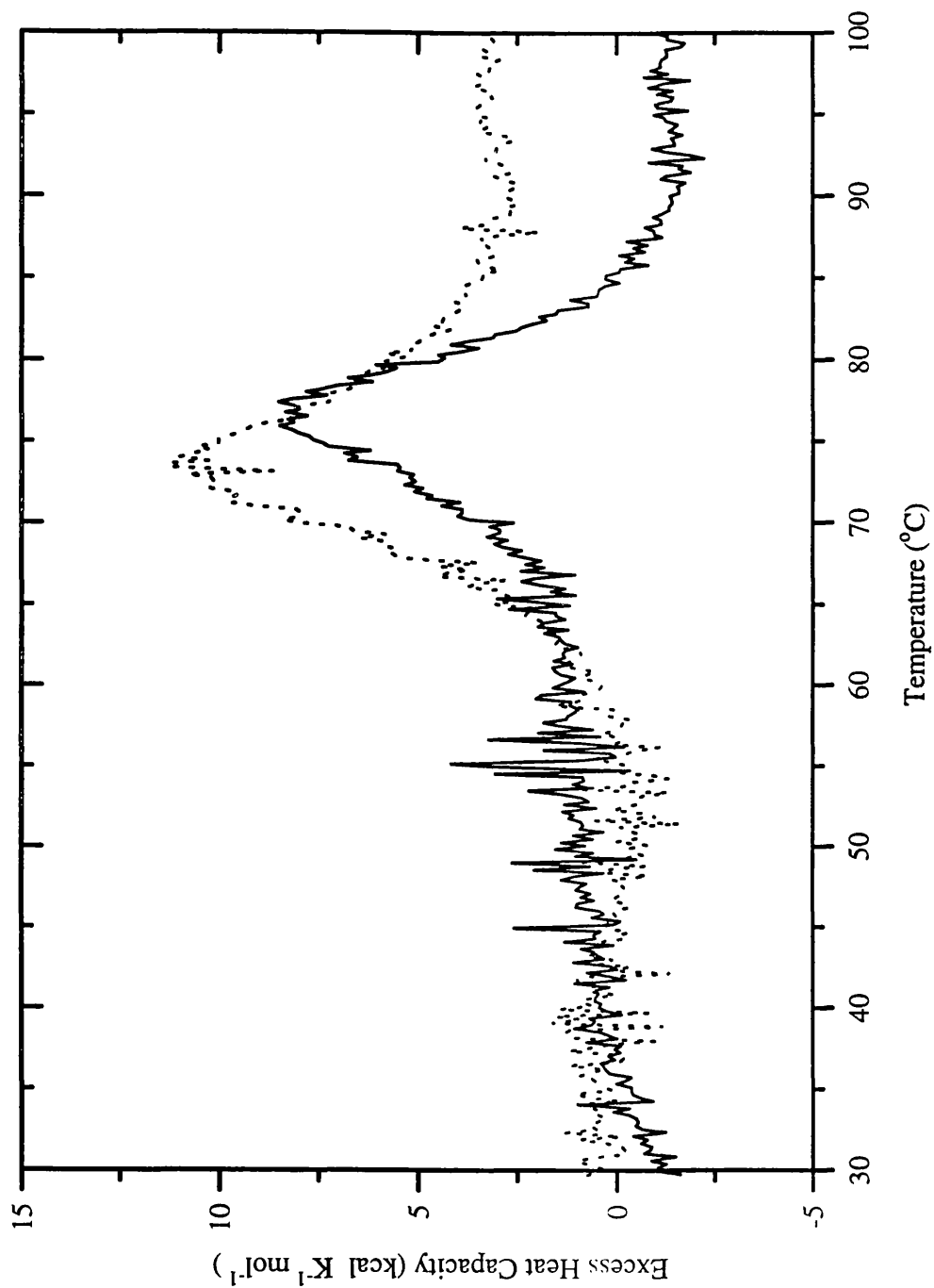


Figure 4.11 DSC of thermal unfolding of cytochrome c (1 mg/ml) at pH 5.0 (0.1 M Na-citrate/citric acid) in the absence (solid lines) and presence (dotted lines) of hydroxypropyl-β-cyclodextrin (*ca.* 120mM), after baseline subtraction and concentration normalization.

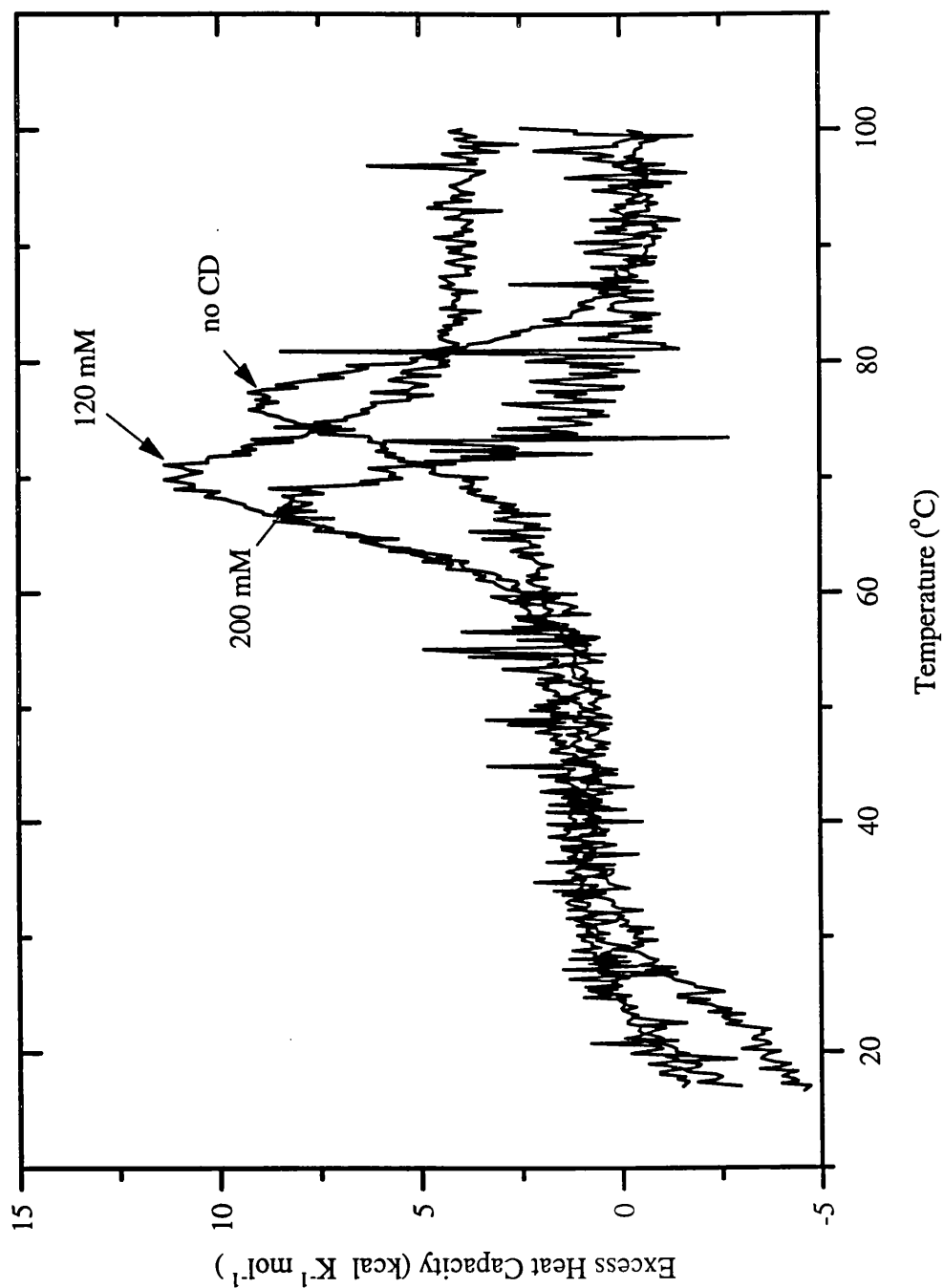


Figure 4.12 Effects of increasing methyl- β -cyclodextrin concentration on the thermal unfolding of cytochrome c (1 mg/ml) at pH 5.0 (Na-citrate/citric acid), after baseline subtraction and concentration normalization.

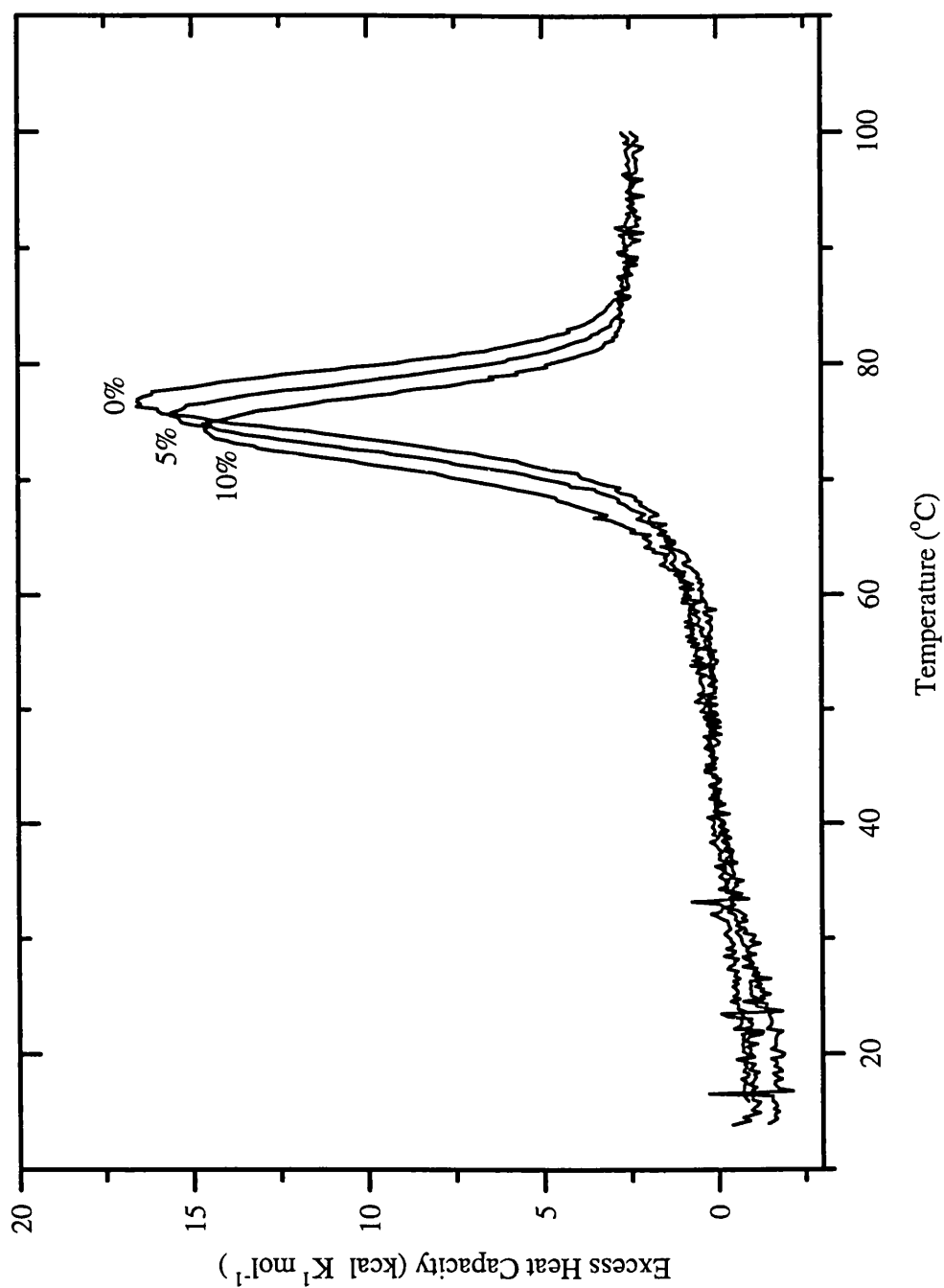


Figure 4.13 Effects of increasing α -cyclodextrin concentration on the thermal unfolding of lysozyme (1-2 mg/ml) at pH 4.0 (Na-acetate/acetic acid), after baseline subtraction and concentration normalization.

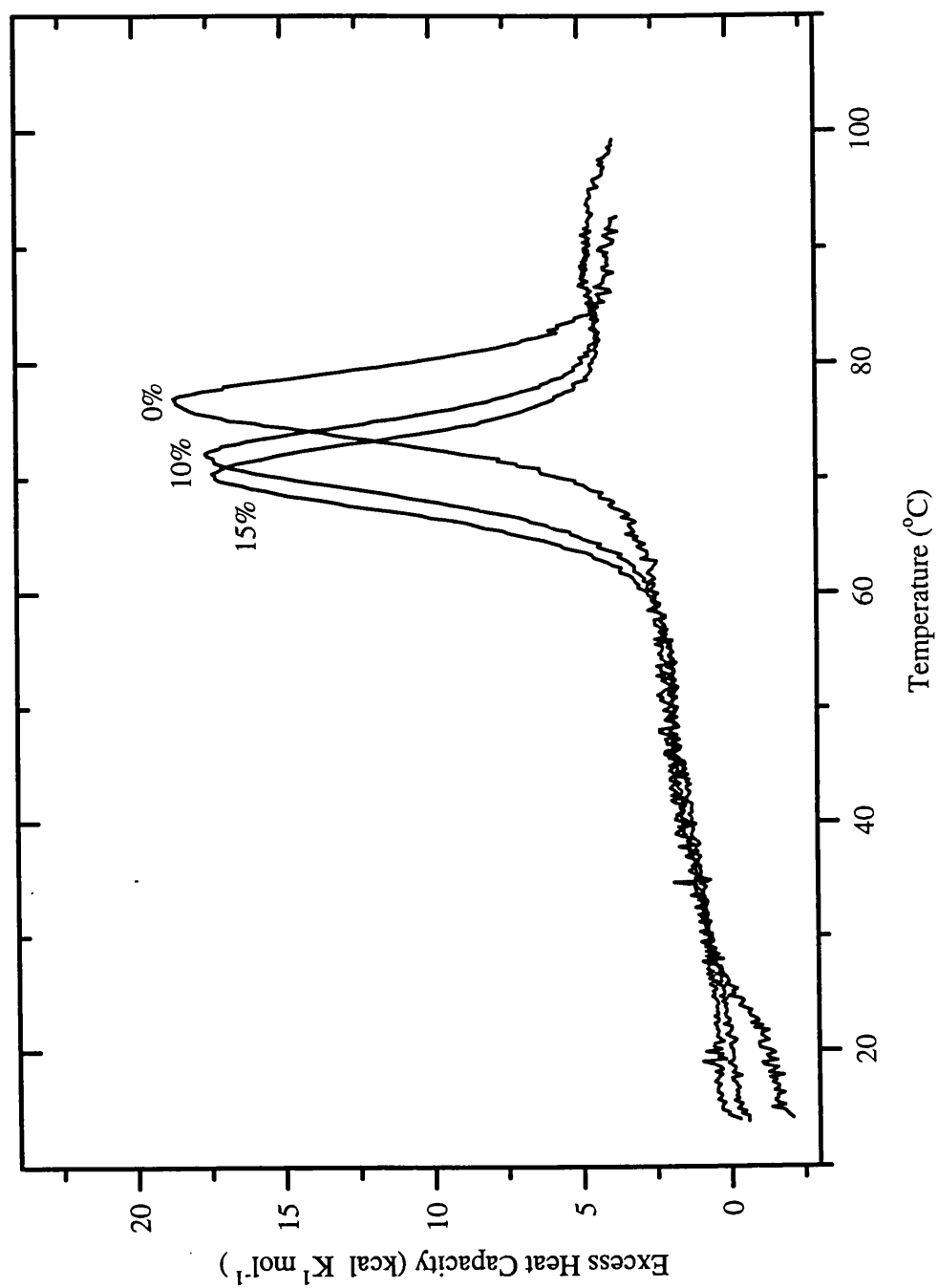


Figure 4.14 Effects of increasing methyl-β-cyclodextrin concentration on the thermal unfolding of lysozyme (1-2 mg/ml) at pH 4.0 (Na-acetate/acetic acid), after baseline subtraction and concentration normalization.

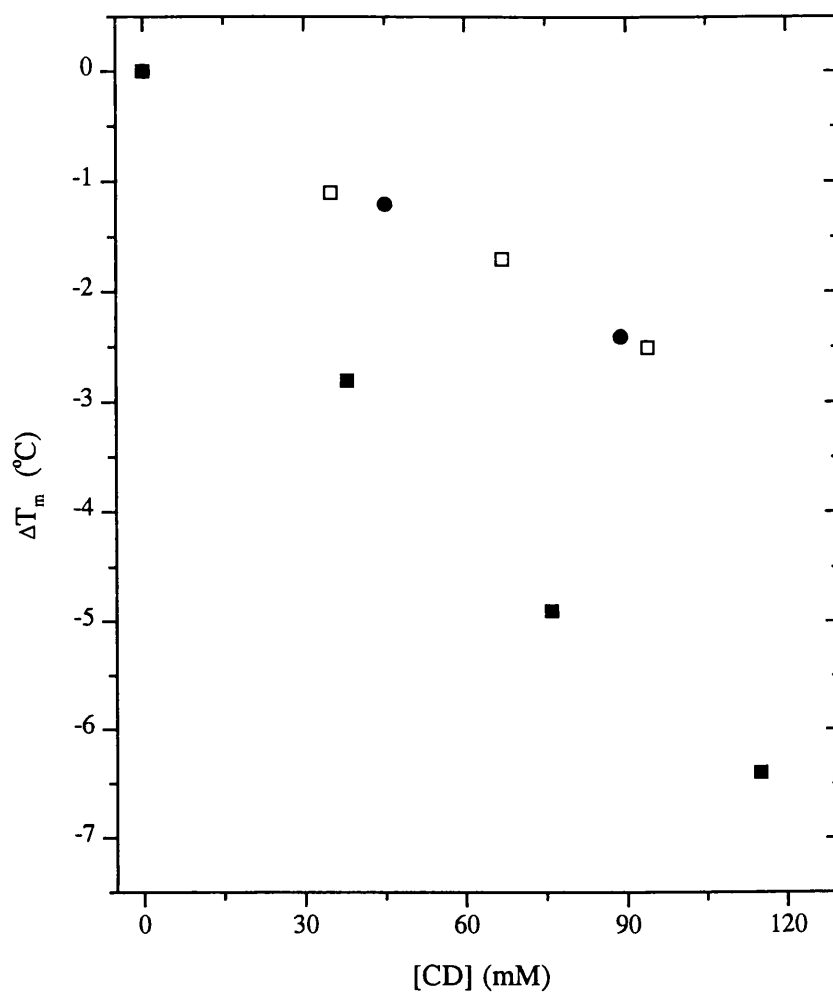


Figure 4.15 Decrease (ΔT_m) in transition temperature of lysozyme at pH 4 as a result of increasing concentrations of α -cyclodextrin (filled circles), hydroxypropyl- β -cyclodextrin (open squares) and methyl- β -cyclodextrin (filled squares).

4.3.3 Discussion

DSC experiments for cytochrome c and lysozyme showed that the thermal stability of both proteins was reduced in the presence of α -cyclodextrin, hydroxypropyl- β -cyclodextrin and methyl- β -cyclodextrin. In addition, it was also found that methyl- β -cyclodextrin appeared to be more effective in reducing the T_m than for any other cyclodextrin studied. For example, in the presence of 120 mM methyl- β -cyclodextrin the T_m of cytochrome c was reduced by 7.2 °C when compared to 3.4 °C for α -cyclodextrin.

For cytochrome c experiments, thermodynamic parameters were not able to be obtained accurately due to instrumental problems at that time, as indicated by the noisy baseline. However, it can be clearly seen from DSC transitions that cyclodextrins show a similar trend in reducing the T_m of cytochrome c as for lysozyme and other examples shown in Figure 4.9.

In lysozyme experiments where various cyclodextrin concentrations were studied, results appear to indicate that the reduction in T_m is approximately linear with cyclodextrin concentrations up to 15% (w/v), as shown in Figure 4.15. Alongside this reduction in T_m there was a decrease the transition enthalpy (ΔH_m) with increasing cyclodextrin concentration. In some cases, the observed enthalpies were consistently lower in the presence of cyclodextrin by up to about 13 kcal mol⁻¹.

In summary, most of the effects observed here, with the exception of a reduction in ΔC_p values, are consistent with that reported by Cooper (1992) and Cooper and McAuley-Hecht (1993). Also, it appears that DSC experiments show that the energetics of this process are consistent with the binding of cyclodextrin molecules to hydrophobic sites exposed on the unfolded form of the protein. Heats of complex formation between cyclodextrins with aromatic groups on the unfolded polypeptide are small but exothermic (typically -1 to -4 kcal mol⁻¹); Lewis and Hansen, 1973;

Cooper and MacNicol, 1978) and complex formation with such groups would reduce the overall transition enthalpy, by burying these groups within the cyclodextrin cavity.

Finally, in addition to these experiments the thermal stability of insulin was also investigated under various conditions, however after numerous attempts we were unsuccessful in obtaining a typical unfolding transition for insulin. As a result, the effect of cyclodextrins on insulin was not studied.

CHAPTER 5

CYCLODEXTRINS AS CHAPERONE MIMICS

5.1 Introduction

Another predicted function of cyclodextrins is the possibility of them assisting in protein refolding. Protein folding *in vivo* and *in vitro* is often inhibited by aggregation, insolubility or partial refolding of the unfolded polypeptide. This is a particular problem with larger globular proteins and is a significant technical drawback in many biotechnology applications involving expression of proteins and their use at high concentrations. Although proline isomerization, sulphydryl oxidation, and other covalent changes may also play a part, the inherent stickiness of unfolded proteins means that aggregation and precipitation of the unfolded polypeptide chain present a kinetic barrier to correct folding of the protein. This stickiness arises from the hydrogen bonding, hydrophobic interactions, and other intermolecular non-covalent forces of the kind that are also responsible for the intramolecular interactions that stabilize the specific folded conformation. *In vivo* this problem is overcome, at least in part, by a range of macromolecular chaperones and related molecules, whose function seems to be to bind to unfolded proteins and prevent their aggregation or entanglement with others, while allowing time for them to fold (Ellis, 1991). This process frequently, though not always, involves ATP binding and hydrolysis (Jaenicke and Creighton, 1993). An essential part of the definition of a molecular chaperone is that it does not form part of the final structure whose formation it has assisted.

Industrial application of these biological chaperones may be impractical or uneconomic, and it would be of some advantage to develop cheaper, more stable, lower molecular weight alternatives that mimic at least some of the functions. No single molecule is likely to incorporate all the required features of a synthetic chaperone. Consequently the aim was to develop a cocktail of small, water soluble molecules that might bind to exposed groups on unfolded proteins, thereby blocking potential aggregation/association with other proteins (or surfaces), but binding sufficiently weakly so as to allow formation of the thermodynamically more stable fold under the right conditions.

There were two components selected for such a chaperone cocktail (i) cyclodextrins, since it has been shown that they specifically recognize unfolded proteins by binding to exposed non-polar residues on the polypeptide chain (Cooper, 1992; Cooper and McAuley-Hecht, 1993); and (ii) N-methylacetamide (NMA) as it appears to destabilize proteins in a manner consistent with weak binding to exposed hydrogen-bonding peptide groups (Cooper and Nutley, unpublished). Typical experiments involved the thermal denaturation of phosphoglycerate kinase (PGK) in the presence and absence of cyclodextrins, NMA, both separately and together in mixtures of various concentrations. PGK was the chosen target protein because it is commercially available, readily assayed and particularly difficult to refold after thermal denaturation (Johnson et al., 1991).

5.2 Phosphoglycerate Kinase

Phosphoglycerate kinase is one of two enzymes required for ATP generation in glycolysis. All phosphoglycerate kinases, whether glycolytic, gluconeogenic, or 'photosynthetic' (carbon fixation) are monomers with molecular weights close to 45,000 (Scopes, 1973). The glycolytic reaction catalysed by phosphoglycerate kinase (PGK) is that of the transfer of a phosphoryl group from the acyl phosphate of 1,3-diphosphoglycerate (1,3-DPG) to ADP thus forming ATP and 3-phosphoglycerate (3-PGA).

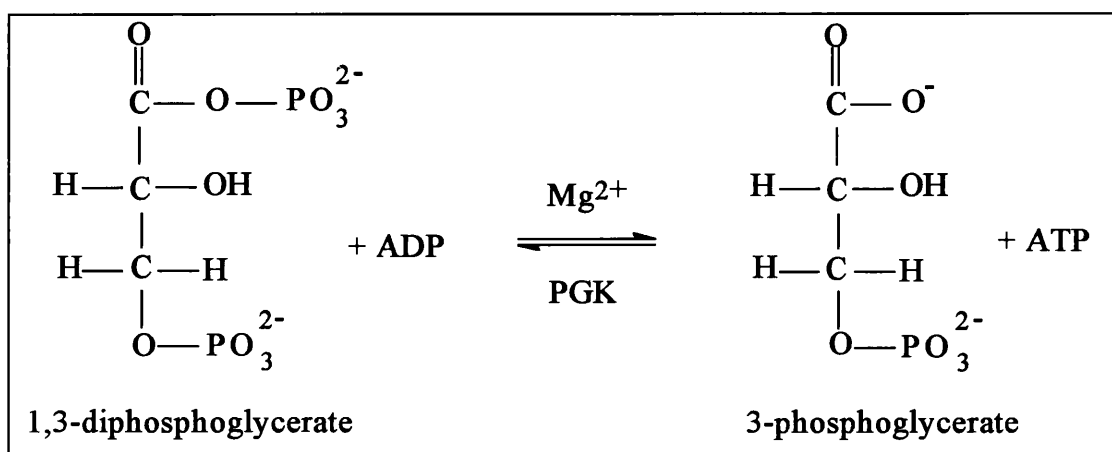


Figure 5.1 The reaction catalysed by PGK in the glycolytic pathway

X-ray studies of the horse muscle (Banks et al., 1979) and yeast (Watson et al., 1982) enzymes have shown a high degree of structural homology and a strong sequence homology. The principal structural feature being the occurrence of two distinct domains of almost equal size, referred to as the N- and C- domains. The protein folds into a bilobal structure in which the two domains are connected by a narrow waist region through which the chain passes twice (Figure 5.2). Each domain consists of a core of six parallel strands of β -pleated sheet surrounded by helices which are connected with the β -sheet strands by β -turns and sections of irregular structure. The connections between sheet strands in each domain are different, the

order of the strands in the N-domain is CDBAEF, and in the C-domain IHGLMN. This arrangement found in the C-domain is common in nucleotide binding enzymes and is known as the Rossmann Fold (Rossmann, 1974).

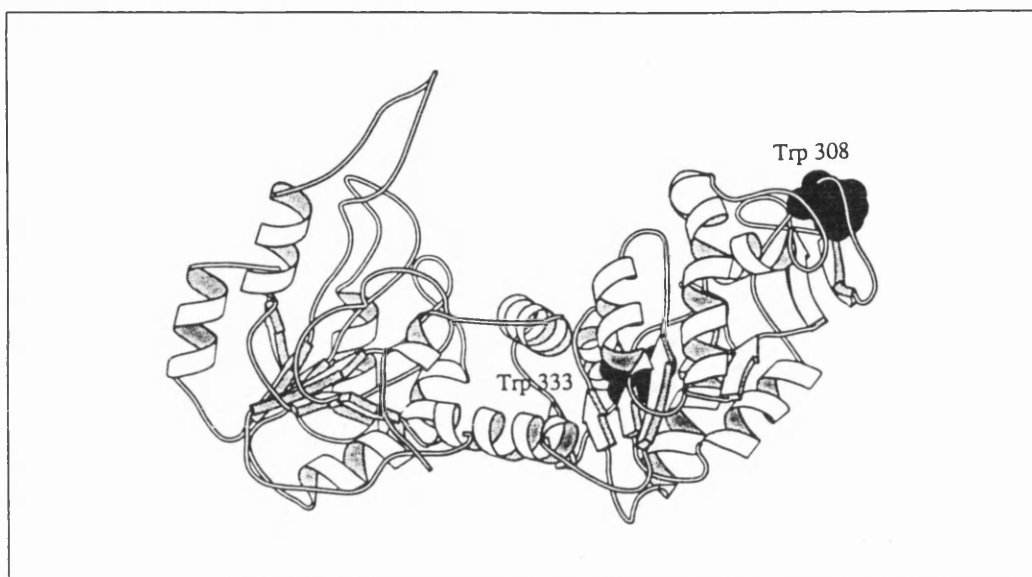


Figure 5.2 Structure of yeast PGK showing the localization of tryptophan residues (Garcia et al., 1982).

Crystal soaking experiments (Banks et al., 1979) showed that Mg-ATP and Mg-ADP molecules bind competitively in a shallow depression on the C domain, facing the N-domain. The adenine ring of ATP is almost completely buried in a deep, hydrophobic slot in the enzyme and the ribose portion is located in a shallow depression above the pyrrolidine ring of Pro 338. The α -phosphate group interacts with Lys 219 and the β - and γ -phosphates of ATP are located about 5 Å from the amino-terminus of helix 13. MgADP binds in a similar way, although the magnesium ion is positioned differently. In MgADP binding, the magnesium ion is located about 4 Å from both the α - and β -phosphates and close to the carboxylate of Asp 374, whereas, in ATP binding, it is believed to interact with either the β - or γ -phosphate or both.

The 3-PGA molecule could not be located in the density map following crystal soaking, however the authors proposed that the most probable position would be on the N-domain at a region of basic residues.

Crystal soaking experiments were also carried out with yeast PGK crystals and the binding site of an analogue of ATP, Mn-adenylyl β,γ -imidodi-phosphate, was revealed (Watson et al., 1982). The binding site of the nucleotide substrates is similar to that of horse muscle PGK. The γ -phosphate of ATP makes hydrogen bonds with the main chain nitrogen atoms of residue 372 and probably 371. The metal ion is placed 3 Å from the γ -phosphate and 5 Å from both the α - and β -phosphates. In this position the metal ion is linked with the hydroxyl of the ribose by hydrogen bonds through the carboxyl group of Asp 372. Difference Fourier maps between crystals grown in ammonium sulphate and then transferred to ammonium selenate indicated the presence of a selenate ion in the position of the γ -phosphate of ATP.

There was no evidence of 3-PGA binding to yeast PGK from X-ray studies. However, an unexplained electron density peak was assigned to the 3-PGA binding site. This site is located in the interdomain region of PGK, with the substrate in a suitable position for phosphoryl transfer.

The ambiguity of the precise location of the phosphoglycerate and diphosphoglycerate binding site was resolved by studies of the pig muscle PGK (Harlos et al., 1992) which confirmed that 3-PGA binds in a very basic site on the N-domain. In view of the distance between these binding sites, a hinge-bending model has been proposed for PGK in which movement around the waist region (or hinge) between the two domains expels water and brings the substrates into an orientation and proximity which facilitates phosphoryl transfer.

5.3 Thermal Denaturation of PGK

PGK solutions (pH 7.5, 1 mM DTT) were denatured at 63°C for 10 or 15 minutes in the presence and absence of various cyclodextrins, NMA, both separately and together in mixtures of various concentrations. Solutions were then cooled to room temperature for up to 1 hour prior to enzyme assay (section 2.8). This specific enzyme assay allowed for the monitoring of any regain of activity of the thermally denatured enzyme.

Typical results for the regain in PGK activity in the presence of 0-12% (w/v) α -cyclodextrin are shown in Figure 5.3A. It appears that α -cyclodextrin recovers up to 14% of enzyme activity, however it is clear that the percentage of recovery does not increase with increasing cyclodextrin concentration. This inconsistency was found for subsequent trials. Similarly, the presence of 0-16% (w/v) hydroxypropyl- β -cyclodextrin (Figure 5.3B) appears recover up to 18% of enzyme activity.

Figure 5.4A shows that the presence of 0-15% (w/v) methyl- β -cyclodextrin recovers up to 47% enzyme activity. Also, Figure 5.4B indicates that about 46% recovery is achieved in the presence of 0-18% (v/v) NMA. However, when both methyl- β -cyclodextrin and NMA (Figure 5.4C) are present there is only about 43% recovery.

Trial experiments were carried out to investigate whether similar effects were observed on the addition of methyl- β -cyclodextrin after thermal denaturation. However, results showed that there was only an increase of 3.6% in enzyme recovery (data not shown). This may suggest that cyclodextrins can prevent aggregation when present during denaturation, but cannot aid in refolding once aggregation has occurred.

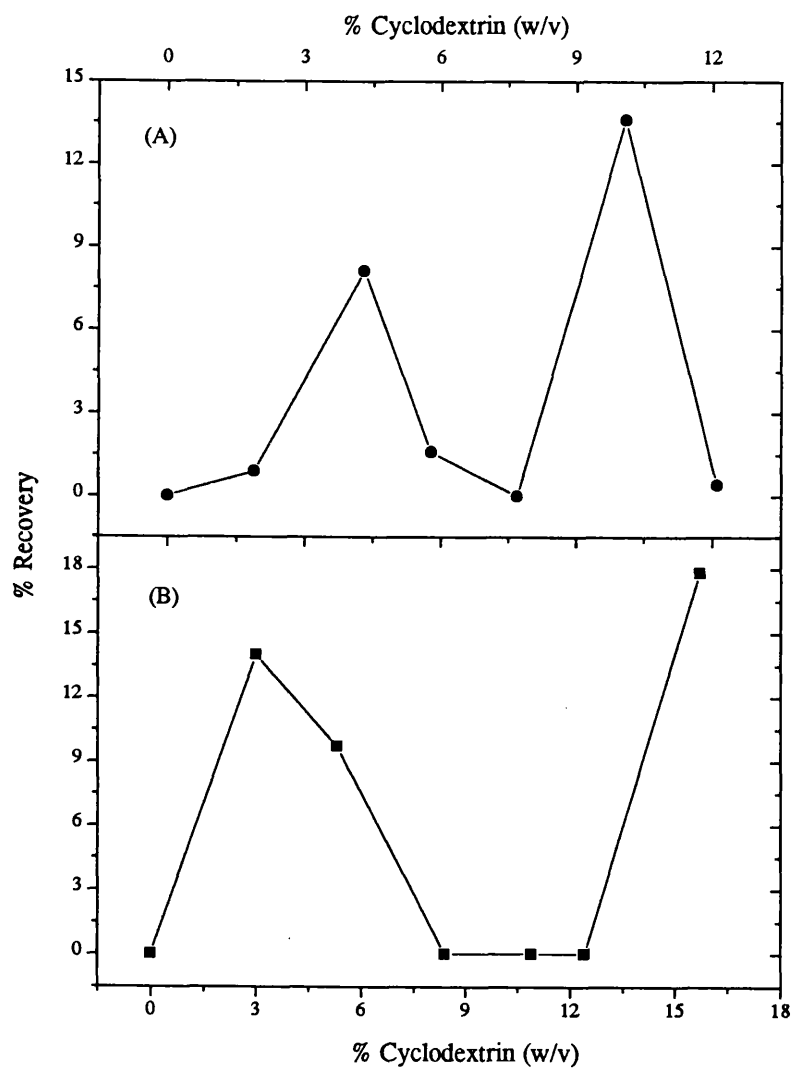


Figure 5.3 Thermal denaturation of PGK in the presence of (A) α -cyclodextrin; and (B) hydroxypropyl- β -cyclodextrin, pH 7.5 (1 mM DTT).

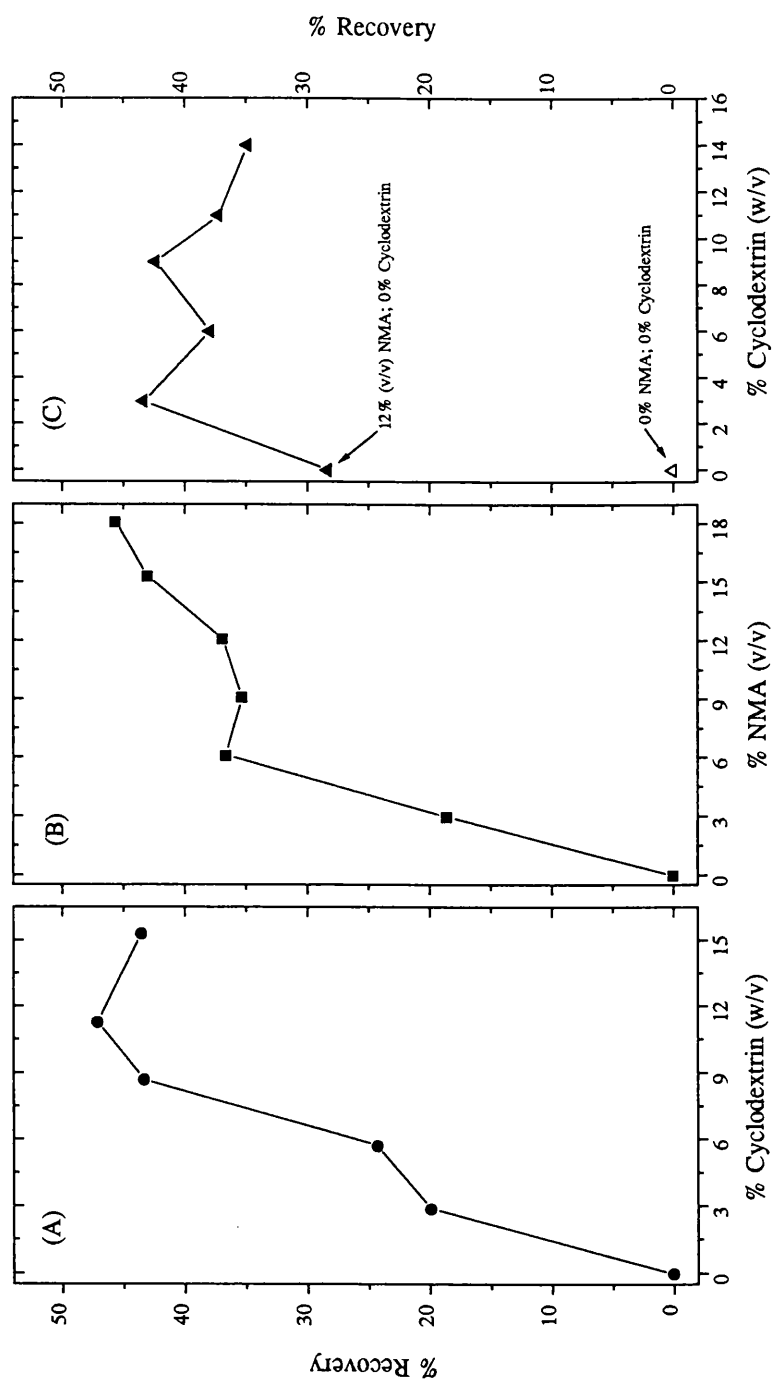


Figure 5.4 Thermal denaturation of PGK in the presence of (A) methyl- β -cyclodextrin; (B) NMA; and (C) methyl- β -cyclodextrin and 12% (v/v) NMA, pH 7.5 (1 mM DTT).

5.4 Discussion

It is well known that cyclodextrins are capable of forming inclusion complexes with hydrophobic guest molecules of appropriate dimensions. With respect to proteins, aromatic amino acids such as tryptophan and phenylalanine, are known to form weak inclusion complexes with cyclodextrins (Wood et al., 1977; Cooper and MacNicol, 1978; Lipkowitz et al., 1992; Horsky and Pitha, 1994). Previous work on PGK (Johnson et al., 1991) indicates that PGK normally forms entangled aggregates or precipitates when thermally unfolded. Therefore, the complexation of cyclodextrins with exposed groups on the unfolded protein may enhance solubility and encourage refolding rather than non-specific aggregation.

As is evident from the results the presence of methyl- β -cyclodextrin or NMA during denaturation significantly enhanced the refolding and regain of activity of thermally denatured PGK by up to a 4-fold increase compared to controls in the absence. However, the presence of α -cyclodextrin or hydroxypropyl- β -cyclodextrin during denaturation appeared to demonstrate an inconsistent increase in enzyme activity with increasing cyclodextrin concentration. These observations for cyclodextrins were also found by a colleague (Margaret Nutley), except she found similar results regardless of whether cyclodextrins were added before or after the denaturation step.

The recovery of active enzyme for experiments involving the presence of both methyl- β -cyclodextrin and NMA during denaturation was far less than predicted. It was thought that both components together would give an increase in enzyme activity of greater than 50%, however results show that this was not the case. The reason why this was not observed is not fully understood.

In summary, results appear to indicate that methyl- β -cyclodextrin may mimic naturally occurring chaperone molecules that perform similar functions *in vivo*. In

addition, methyl- β -cyclodextrin seems to be more effective in recovering enzyme activity than any other cyclodextrin studied. This may be due to methyl- β -cyclodextrin forming stronger inclusion complexes with exposed hydrophobic residues such as aromatic amino acids present in the unfolded form of the protein. Also, the outcome of these preliminary experiments may suggest we have demonstrated a novel strategy for protein reactivation by using a water soluble, low molecular weight binding agent that forms weak, non-covalent complexes with hydrophobic sites present in protein folding intermediate(s). In addition, the percentage of enzyme activity recovered in the presence of cyclodextrins may indicate that cyclodextrins can inhibit aggregation without interfering with protein refolding.

Although encouraging results have been obtained, it is clear that in order to create the perfect chaperone cocktail further work would be necessary. Studies could involve the use of DSC, UV, circular dichroism and fluorescence spectroscopy, together with specific enzyme assay to monitor regain of functional integrity. Experiments could also include addition of putative chaperone mimics to insoluble aggregates of denatured protein, produced by thermal or chemical denaturation at high concentrations, to evaluate the effects of these additives on solubilization rates as well as regain of activity.

Finally, annealing is possibly another method to recover thermally denatured enzyme. This would involve gradually heating the denatured enzyme in the presence of cyclodextrin, holding it at a particular temperature and then allow to cool slowly. In a trial annealing experiment, no recovery in enzyme activity was found for thermally denatured PGK (with cyclodextrin). However, for future work this approach may be worth another attempt.

CHAPTER 6

CONCLUSIONS

Conclusions

The aim of the work reported in this thesis was to study the interaction of cyclodextrins with amino acids, both free and in proteins, using a range of biophysical techniques centred mainly on the use of sensitive microcalorimetry. General conclusions from these studies, as well as some suggestions on future work are discussed here.

For the interaction of cyclodextrins with naturally occurring α -amino acids and their corresponding enantiomers it was found that the majority of them showed no complexation with cyclodextrins. However, out of the amino acids which formed complexes, phenylalanine and tryptophan showed enantiomeric discrimination when complexed with α -cyclodextrin. It was also found that amino acids which showed complexation, including the aromatic amino acids, all had some hydrophobic character. These observations may prove useful for the separation of phenylalanine and tryptophan enantiomers using separation methods.

The interaction of cyclodextrins with amino acid groups on proteins has several consequences. Firstly, cyclodextrins significantly increase dissociation of insulin oligomers in a manner consistent with their interaction with protein side chains. Similar effects were also found at various pH and temperature conditions. Additionally, studies of the thermal stability of cytochrome c and lysozyme showed that cyclodextrins reduce the thermal unfolding temperature in a manner consistent with the binding of cyclodextrin molecules to exposed side chains on the unfolded form of the protein. Thirdly, enzyme assays of the thermally denatured PGK showed that cyclodextrins significantly enhanced the regain of enzyme activity. Complexation of cyclodextrins with exposed groups on the unfolded protein may enhance solubility and encourage refolding rather than non-specific aggregation. In this way, cyclodextrins may mimic naturally occurring chaperones that perform similar functions *in vivo*.

Conclusions

It appears that the effects observed here support previous suggestions that aromatic amino acids are primarily responsible for the interaction of cyclodextrins with proteins. In addition, dissociation constants for the binding of cyclodextrins to sites on the dissociated insulin are not only consistent with previous observations of interaction between cyclodextrins in solution and aromatic amino acid side chains and similar groups, but also agree with the values presented here for cyclodextrins and free amino acids.

For future work, it may be of interest to study complexes of cyclodextrin with oligopeptides containing various amino acids, since simple amino acids lack the stereochemical constraints arising from the bulky surface of a peptide backbone. These studies may show whether the formation of inclusion complexes is prevented through steric hindrance. In the case of cyclodextrin-protein interactions it may be worth studying the effects of cyclodextrins on the dissociation of other oligomeric systems. Also, studies involving the use of cyclodextrins as chaperone mimics show potential for interesting further studies. Future work in this area could involve studying other enzymes, for example rhodanese which has been a chosen target for biological chaperone studies by other investigators (Martin et al., 1991; Mendoza et al., 1991; Makino et al., 1993). Also, the use of a range of biophysical techniques including fluorescence spectroscopy, DSC, and circular dichroism could be use to monitor any regain of functional integrity.

Finally, the work presented here has shown how using microcalorimetry to measure weak interactions between cyclodextrins and protein groups provides a useful probe of protein folding and subunit interactions, with potentially important biotechnology applications.

REFERENCES

References

- Adams, M.J., Blundell, T.L., Dodson, E.J., Dodson, G.G., Vijayar, M., Baker, E.N., Harding, M.M., Hodgkin, D.G., Rimmer, B. and Sheat, S. (1969) *Nature (London)*, **224**, 491.
- Anfinsen, C.B., Haber, E., Sela, M. and White, F.H. (1961) *Proc. Nat. Acad. Sci.*, **47**, 1309.
- Armstrong, D.W., Alak, A., DeMond, W., Hinze, W.L. and Riehl, T.E. (1985b) *J. Liq. Chromatogr.*, **8**, 261.
- Armstrong, D.W. and DeMond, W. (1984) *J. Chromatogr. Sci.*, **22**, 411.
- Armstrong, D.W., DeMond, W., Alak, A., Hinze, W.L., Riehl, T.E. and Bui, K.H. (1985a) *Anal. Chem.*, **57**, 234.
- Armstrong, D.W., Li, W., Stalcup, A.M., Secor, H.V., Izac, R.R. and Seeman, J.L. (1990) *Anal. Chim. Acta*, **234**, 365.
- Armstrong, D.W., Ward, T.J., Armstrong, R.D. and Beesley, T.E. (1986) *Science*, **232**, 1132.
- Armstrong, D.W., Yang, X., Han, S.M. and Menges, R.A. (1987) *Anal. Chem.*, **59**, 2594.
- Aronow, R.H. and Witten, L. (1960) *J. Phys. Chem.*, **64**, 1643.
- Baeyens, W., Lin, B. and Corbisier, V. (1990) *Analyst*, **115**, 359.
- Banks, R.D., Blake, C.C.F., Evans, P.R., Haser, R., Rice, D.W., Hardy, G.W., Merrett, M. and Phillips, A.W. (1979) *Nature (London)*, **279**, 773.

References

- Bender, M.L. and Komiyama, M. (1978) *Reactivity and Structure Concepts in Organic Chemistry* 6, Springer-Verlag: New York.
- Bersier, P.M., Bersier, J. and Klingert, B. (1991) *Electroanalysis*, **3**, 443.
- Bhushan, R. and Joshi, S. (1993) *Biomedical Chromatogr.*, **7**, 235.
- Bi, R.C., Dauter, Z., Dodson, E., Dodson, G., Giordano, F. and Reynolds, C. (1984) *Biopolymers*, **23**, 391.
- Blundell, T.L., Dodson, G., Hodgson, D. and Mercola, D. (1972) *Adv. Prot. Chem.*, **26**, 279.
- Brandts, J.F. and Lin, L.-N. (1990) *Biochemistry*, **29**, 6927.
- Breslow, R (1991) *Host Guest Molecular Interactions: From Chemistry to Biology*. Wiley, Chicester (Ciba Foundation Symposium), **158**, 115.
- Brewster, M.E., Hora, M.S., Simpkins, J.W. and Bodor, N. (1991) *Pharm. Res.*, **8**, 792.
- Büch, H.P., Omlor, G. and Knabe, J. (1990) *J. Drug Res.*, **40**, 32.
- Bucher, T. (1955) *Methods Enzymol.*, **1**, 415.
- Buser, H., Muller, M.D. and Rappe, C. (1992) *Environ. Sci. Technol.*, **26**, 1533.
- Buvari, A. and Barcza, L. (1988) *J. Chem. Soc., Perkin Trans. 2*, 543.
- Camilleri, P., Haskins, N.J. and Howlett, D.R. (1994) *FEBS Lett.*, **341**, 256.

References

- Chen, A. and Wadsö, I. (1982) *J. Biochem. Biophys. Meth.*, **6**, 307.
- Chowdhry, B.Z. and Cole, S.C. (1989) *TIBTECH*, **7**, 11.
- Cohn, E.J., McMeekin, T.I., Edsall, J.T. and Blanchard, M.H. (1933) *J. Biol. Chem.*, **100**, xxviii.
- Connors, K.A. (1987) *Binding Constants: The Measurement of Molecular Complex Stability*. John Wiley, New York.
- Cooper, A. (1992) *J. Am. Chem. Soc.*, **114**, 9208.
- Cooper, A. (1997) In: Allen, G. (ed) *Protein: A Comprehensive Treatise*, JAI Press Inc. In press.
- Cooper, A., Eyles, S.J., Radford, S.E. and Dobson, C.M. (1992) *J. Mol. Biol.*, **225**, 930.
- Cooper, A. and Johnson, C.M. (1994a) Isothermal Titration Microcalorimetry. In: Jones, C., Mulloy, B., and Thomas, A.H., (eds) *Methods in Molecular Biology: Microscopy, Optical Spectroscopy, and Macroscopic Techniques*, Humana Press, Totowa, N.J., Vol. **22**, 137.
- Cooper, A. and Johnson, C.M. (1994b) Differential Scanning Calorimetry. In: Jones, C., Mulloy, B., and Thomas, A.H., (eds) *Methods in Molecular Biology: Microscopy, Optical Spectroscopy, and Macroscopic Techniques*, Humana Press, Totowa, N.J., Vol. **22**, 125.

References

- Cooper, A., Lovatt, M. and Nutley, M.A. (1996) *J. Incl. Phenom. and Mol. Recog.*, **25**, 85.
- Cooper, A. and MacNicol, D.D. (1978) *J. Chem. Soc. Perkin Trans. II*, 760.
- Cooper, A. and McAuley-Hecht, K.E. (1993) *Phil. Trans. R. Soc. Lond. A*, **345**, 23.
- Copper, C.L., Davis, J.B., Cole, R.O. and Sepaniak, M.J. (1994) *Electrophoresis*, **15**, 785.
- Cramer, F., Saenger, W. and Spatz, H.-Ch. (1967) *J. Am. Chem. Soc.*, **89**, 14.
- Creighton, T.E. (1988) *Bioessays*, **8**, 2, 57-63.
- Creighton, T.E. (1991) *Curr. Opin. Struct. Biol.*, **1**, 5.
- Dalla Bella, M. and Szejtli, J. (1983) *Drugs of the Future*, **8**, 391.
- Dawson, R.M.C., Elliott, D.C., Elliott W.H. and Jones, K.M. (1986) *Data for Biochemical Research*, Clarendon Press, Oxford, 3rd Ed.
- Dill, K.A. (1990) *Biochemistry*, **29**, 7133.
- Doig, A.J. and Williams, D.H. (1991) *J. Mol. Biol.*, **217**, 389.
- Du, Y., Nakamura, A. and Toda, F. (1991) *J. Incl. Phenom. Mol. Rec.*, **10**, 443.
- Eastburn, S.D. and Tao, B.Y. (1994) *Biotech. Adv.*, **12**, 325.
- Ellis, R.J. (1994) *Curr. Op. Struct. Biol.*, **4**, 117.

References

- Ellis, R.J. and van der Vies, S.M. (1991) *Annu. Rev. Biochem.*, **60**, 321.
- Eriksson, T., Björkman, S., Roth, B., Fyge, A. and Höglund, P. (1995) *Chirality*, **7**, 44.
- Flory, P.J. (1956) *J. Am. Chem. Soc.*, **78**, 5222.
- Frank, H.S. and Evans, M.W. (1945) *J. Chem. Phys.*, **13**, 507.
- Frankewich, R.P., Thimmaiach. K.N. and Hinze. W.L. (1991) *Anal. Chem.*, **63**, 2924.
- Fukada, H., Sturtevant, J.M. and Quioco, F.A. (1983) *J. Biol. Chem.*, **258**, 13193.
- Fujita, K., Veda, T., Imoto, T., Tabushi, I., Toh, N. and Koga, T. (1982) *Bioorg. Chem.*, **11**, 72.
- Garcia, P., Desmadril, M., Minard, P. and Yon, J.M. (1995) *Biochemistry*, **34**, 397.
- Gelb, R.I., Schwartz, L.M., Cardelino, B., Fuhrman, H.S., Johnson, R.F. and Laufer, D.A. (1981) *J. Am. Chem. Soc.*, **103**, 1750.
- Gill, S.C. and Hippel, P.H. von (1989) *Analyt. Biochem.* **182**, 319.
- Goto, Y., Takahaski, N., and Fink, A.L. (1990) *Biochemistry*, **29**, 3480.
- Grenthe, I., Ots, H., Ginstrup, O. (1970) *Acta. Chem. Scand.*, **24**, 1067.
- Haggin, J. (1992) *Chem. Engr. News*, **70**, 25.

References

- Harlos, K., Vas, M. and Blake, C.F. (1992) *Proteins: Struct., Funct., Genet.* **12**, 133.
- Hermans, J. and Scheraga, H.A. (1961) *J. Am. Chem. Soc.*, **83**, 3283.
- Hinze, L.W., Riehl, T.E., Armstrong, D.W., DeMond, W., Alak, A. and Ward, T. (1985) *Anal. Chem.*, **57**, 237.
- Horsky, J. and Pitha, J. (1994) *J. Incl. Phenom. and Mol. Recog.*, **18**, 291.
- Howarth, O.W. (1975) *J. Chem. Soc. Faraday Trans. 1*, **71**, 2303.
- Inoue, Y., Hoshi, H., Sakurai, M., and Chujo, R. (1985) *J. Am. Chem. Soc.*, **107**, 2319.
- Inoue, Y., Liu, Y., Tong, L.H., Shen, B.J. and Jin, D.S. (1993) *J. Am. Chem. Soc.*, **115**, 10637.
- Jackson, W.M. and Brandts, J.F. (1970) *Biochemistry*, **9**, 2294.
- Jaenicke, R. and Creighton, T.E. (1993) *Curr. Biol.*, **3**, 234.
- Johnson, C.M., Cooper, A. and Brown, A.J.P. (1991) *FEBS*, **202**, 1157.
- Johnson, R.E., Adams, P. and Rupley, J.A. (1978) *Biochemistry*, **17**, 1479.
- Karuppiyah, N. and Sharma, A. (1995) *Biochemical and Biophysical Research Communications*, **211**, 60.
- Kauzmann, W. (1959) *Adv. Protein Chem.*, **14**, 1.

References

- Keilin, D. and Slater, E.C. (1953) *Brit. Med. Bull.*, **9**, 89.
- Konig, W.A., Icheln, D., Runge, T., Pfaffenberger, B., Lugwig, P. and Huhnerfuss, H. (1991) *J. High Resolut. Chromatogr.*, **14**, 530.
- Kuroki, R., Inaka, K., Taniyama, Y., Kidokoro, S., Matsushima, M., Kikuchi, M. and Yutani, K. (1992) *Biochemistry*, **31**, 8323.
- Lewis, E.A. and Hansen, L.D. (1973) *J. Chem. Soc., Perkin Trans. 2*, 2081.
- Li, S and Purdy, W.C. (1991) *J. Chromatogr.*, **543**, 105.
- Li, S. and Purdy, W.C. (1992) *Chemical Reviews*, **92**, 1457.
- Lipkowitz, K.B., Raghothama, S. and Yang, J. (1992) *J. Am. Chem. Soc.*, **114**, 1554.
- Loftsson, T., Fridriksdottir, H. and Olafsdottir, G.O. (1991) *Acta. Pharm. Nord.*, **3**, 215.
- Lovatt, M., Cooper, A. and Camilleri, P. (1996) *Eur. Biophys. J.*, **24**, 354.
- Lovatt, M., Cooper, A. and Camilleri, P. (1996) *J. Incl. Phenom. and Mol. Recog.*, **25**, 169.
- McKenzie, H.A. and White, F.H. (1991) *Adv. Protein Chem.*, **41**, 173.
- McPhail, D. and Cooper, A. (1997) *J. Chem. Soc., Faraday Trans.*, **93**, 2283.
- Makino, Y., Taguchi, H. and Yoshida, M. (1993) *FEBS Lett.*, **336**, 363.

References

- Martin, J., Langer, T., Boteva, R., Schramel, A., Horwich, A.L and Hartl, F.U. (1991) *Nature*, **352**, 36.
- Margoliash, E. and Frohwirt, N. (1959) *Biochem. J.*, **71**, 570.
- Matsue, T., Osa, T. and Evans, D.H. (1984) *J. Incl. Phenom.*, **2**, 547.
- Matsuyama, K., El-Gizawy, S. and Perrin, J.H. (1987) *Drug Devel. Indust. Pharm.*, **13**, 2687.
- Mendoza, J.A., Rogers, E., Lorimer, G.H. and Horowitz, P.M. (1991) *J. Biol. Chem.*, **266**, 13044.
- Meot-Ner, M. and Sieck, L.W. (1986) *J. Am. Chem. Soc.*, **108**, 7525.
- Milliaresi, E.E. and Ruchkin, V.E. (1974) In: *Organic Electronic Spectral Data (40)*, Vol. XVI, 30.
- Minato, S., Osa, T., Morita, M., Nakamura, A., Ikeda, H., Toda, F. and Ueno, A. (1991) *Photochem. Photobio.*, **54**, 593.
- Mirsky, A.E. and Pauling, L. (1936) *Proc. Natl. Acad. Sci USA*, **22**, 439.
- Okafo, G.N. and Camilleri, P. (1993) *J. Microcol. Sep.*, **5**, 149.
- Osa, T., Matsue, T. and Fujihira, M. (1977) *Heterocycles*, **6**, 1833.
- Pace. C.N., Grimsley, G.R., Thomson, J.A. and Barnett, B.J. (1988) *J. Biol. Chem.*, **263**, 11820.

References

- Pauling, L. (1939) *The Nature of the Chemical Bond*. Ithaca, NY: Cornell Univ. Press.
- Persson, K.M. and Gekas, V. (1994) *Process Biochem.*, **29**, 89.
- Pitha, J., Hoshino, T., Torres-Labandeira, J. and Irie, T. (1992) *Int. J. Pharm.*, **80**, 253.
- Pitha, J., Milecki, J., Fales, H., Pannell, L. and Uekama, K. (1986) *Int. J. Pharm.*, **29**, 73.
- Plotnikov, V., Brandts, J.M., Lin, L.N. and Brandts, J.F. -in preparation.
- Poland, D.C. and Scheraga, H.A. (1965) *Biopolymers*, **3**, 379.
- Porter, R.R. (1953) *Biochem. J.*, **53**, 320.
- Potekhin, S. and Pfeil, N. (1989) *Biophys. Chem.*, **23**, 55.
- Privalov, P.L. (1974) *FEBS Lett.*, **40**, S140.
- Privalov, P.L. (1979) *Adv. Protein Chem.*, **33**, 167.
- Privalov, P.L. (1980) *Pure Appl. Chem.*, **52**, 479.
- Privalov, P.L. (1982) *Adv. Protein Chem.*, **35**, 1.
- Privalov, P.L. and Gill, S.J. (1988) *Adv. Protein Chem.*, **39**, 191.
- Privalov, P.L. and Potekhin, S.A. (1986) *Methods Enzymol.*, **131**, 4.

References

- Rekharsky, M.V., Goldberg, R.N., Schwarz, F.P., Tewari, Y.B., Ross, P.D., Yamashoji, Y. and Inoue, Y. (1995) *J. Am. Chem. Soc.*, **117**, 8830.
- Richards, F.M. (1977) *Annu. Rev. Biophys. Bioeng.*, **6**, 151.
- Rose, G.D. and Wofenden, R. (1993) *Annu. Rev. Biophys. Biomol. Struct.*, **22**, 381.
- Rossman, M.G. (1974) *Nature*, **250**, 194.
- Ryle, A.P., Sanger, F., Smith, L.F. and Kitai, R (1955) *Biochem. J.*, **60**, 541.
- Rymden, R., Carifors, J. and Stilbs, P. (1984) *J. Incl. Phenom.*, **1**, 159.
- Saenger, W. (1980) *Angew. Chem. Int. Ed. Engl.*, **19**, 344.
- Schardinger, F. and Unters, Z. (1903) *Nahrungs-Genussmittel Gebrauchsgegenstande*, **6**, 865.
- Schellman, J.A. (1955) *C.R. Trav. Lab. Carlsber Ser. Chim.* **29**, 230.
- Scopes, R.K. (1973) In: Boyer, P (ed.), *The Enzymes*, 3rd Ed., Academic Press, NY, Vol. **8**, 335.
- Scopes, R.K. (1975) *Methods Enzymol.*, **42**, 127.
- Scott, D.A. (1934) *Biochem. J.*, **28**, 1592.
- Serjeant, E.P. and Dempsey, B. (1979) *Ionisation Constants of Organic Acids in Aqueous Solution*. Pergamon, Oxford.

References

- Spolar, R.S. and Record, M.T. (1994) *Science*, **263**, 777.
- Sturtevant, J.M. (1974) *Annu. Rev. Biophys. Bioeng.*, **3**, 35.
- Sturtevant, J.M. (1987) *Annu. Rev. Phys. Chem.*, **38**, 463.
- Su, C. and Yang. C. (1991) *J. Sci. Food Agric.*, **54**, 635.
- Sun, P., Barker, G.E., Mariano, G.J. and Hartwick, R.A. (1993) *J. Chromatogr.*, **648**, 475.
- Sun, P., Barker, G.E., Mariano, G.J. and Hartwick, R.A. (1994) *Electrophoresis*, **15**, 793.
- Szejtli, J. (1982) *Akademiai Kiado, Budapest*, 59.
- Szejtli, J. (1994) *Medicinal Research Reviews*, **14**, 353.
- Tabushi, I. (1984) In: Atwood JL, Davies JED, MacNicol DD (Eds). *Inclusion Compounds*, Academic Press, London, Vol. **3**, 445.
- Tanaka, M., Kawaguchi, Y., NaKae, M., Mizobucki, Y. and Shono, T. (1984) *J. Chromatogr.*, **299**, 341.
- Taneja, S. and Ahmad. F. (1994) *Biochem. J.*, **303**, 147.
- Tanford, C. (1968) *Adv. Protein Chem.*, **23**, 121.
- Thakkar, A.L. and Demarco, P.V. *J. Pharm. Sci.*, **60**, 652.

References

- Thuanud, N., Seville, B., Deratani, A. and Lelievre, G. (1991) *J. Chromatogr.*, **555**, 53.
- Ueno, A., Kuwabara, T., Nakamura, A. and Toda, F. (1992) *Nature*, **356**, 136.
- VanEtten, R.L., Sebastian, J.F., Clowes, G.A., and Bender, M.L. (1967) *J. Am. Chem. Soc.*, **89**, 3242.
- Van Osdol, W.W., Mayorga, O.L. and Freire, E. (1991) *Biophys. J.*, **59**, 48.
- Villiers, A.C.R. (1891) *Acad. Sci. Paris*, **112**, 536.
- Vogl, T., Brenegelmann, R., Hinz, H-J., Scharf, M., Lötzbeyer, M. and Engels, J.W. (1995) *J. Mol. Biol.*, **254**, 481.
- Wadsö, I. (1968) *Acta Chem. Scanda.*, **22**, 927.
- Watson, H.C., Walker, N.P.C., Shaw, P.J., Bryant, T.N., Wendell, P.L., Fothergill, L.A., Perkins, R.E., Conroy, S.C., Dobson, M.J., Tuite, M.F., Kingsman, A.J. and Kingsman, S.M. (1982) *EMBO J.*, **1**, 1635.
- Weiner, S.J., Kollman, P.A., Case, D.A., Singh, U.C., Ghio, C., Alagona, G., Profeta, S. and Weiner, P. (1984) *J. Am Chem. Soc.*, **106**, 765.
- Wilson, A.G., Brooke, O.G., Lloyd, H.J. and Robinson, B.F. (1969) *Br. Med. J.*, **4**, 399.
- Wiseman, T., Williston. S., Brandts J.F. and Lin, L.-N. (1989) *Anal. Biochem.*, **179**, 131.

References

Wnendt, S. and Zwingenberger, K. (1997) *New Scientist*, **385**, 303.

Wood, D.J., Hruska, F.E. and Saenger, W. (1977) *J. Am. Chem. Soc.*, **99**, 1735.

Wuster, M., Schulz, R. and Herz, A. (1981) *Biochem. Pharmacol.*, **30**, 1883.

Xu, D., Lin, S.L. and Nussinov, R. (1997) *J. Mol. Biol.*, **265**, 68.

Yang, A.S. and Honig, B. (1993) *J Mol. Biol.*, **231**, 459.

